MODELLING RETENTION TIME

IN A CLEARWELL

A Thesis

Submitted to the College of Graduate Studies and Research

in Partial Fulfillment of the Requirements

for the

Degree of Master of Science

in the

Department of Civil and Geological Engineering

University of Saskatchewan

Saskatoon

By

XIAOLI YU

PERMISSION TO USE

In presenting this thesis in partial fulfilment of the requirements for a postgraduate degree from the University of Saskatchewan, I agree that the Libraries of this University may make it freely available for inspection. I further agree that permission for copying of this thesis in any manner, in whole or in part, for scholarly purposes may be granted by the professor or professors who supervised my thesis work or, in their absence, by the Head of the Department or the Dean of the College in which my thesis work was done. It is understood that any copying or publication or use of this thesis or parts thereof for financial gain shall not be allowed without my written permission. It is also understood that due recognition shall be given to me and to the University of Saskatchewan in any scholarly use which may be made of any material in my thesis.

Requests for permission to copy or to make other use of material in this thesis in whole or part should be addressed to:

Head of the Department of Civil and Geological Engineering
University of Saskatchewan
57 Campus Drive
Saskatoon, Saskatchewan
Canada, S7N 5A9

ABSTRACT

Clearwells are large water reservoirs often used at the end of the water treatment process as chlorine contact chambers. Contact time required for microbe destruction is provided by residence time within the clearwell. The residence time distribution can be determined from tracer tests and is the one of the key factors in assessing the hydraulic behaviour and efficiency of these reservoirs. This work provides an evaluation of whether the two-dimensional, depth-averaged, finite element model, River2DMix can adequately simulate the flow pattern and residence time distribution in clearwells. One question in carrying out this modelling is whether or not the structural columns in the reservoir need to be included, as inclusion of the columns increases the computational effort required.

In this project, the residence time distribution predicted by River2DMix was compared to results of tracer tests in a scale model of the Calgary Glenmore water treatment plant northeast clearwell. Results from tracer tests in this clearwell were available. The clearwell has a serpentine baffle system and 122 square structural columns distributed throughout the flow. A comparison of the flow patterns in the hydraulic and computational models was also made. The hydraulic model tests were carried out with and without columns in the clearwell.

The 1:19 scale hydraulic model was developed on the basis of Froude number similarity and the maintenance of minimum Reynolds numbers in the flow through the serpentine system and the baffle wall at the entrance to the clearwell. Fluorescent tracer slug injection tests were used to measure the residence time distribution in the clearwell. Measurements of tracer concentration were taken at the clearwell outlet using a continuous flow-through fluorometer system. Flow visualization was also carried out using dye to identify and assess the dead zones in the flow. It was found that it was necessary to ensure the flow in the scale model was fully developed before starting the tracer tests, and determining the required flow development time to ensure steady state results from the tracer tests became an additional objective of the work. Tests were

carried out at scale model flows of 0.85, 2.06, and 2.87 L/s to reproduce the 115, 280, and 390 ML/day flows seen in the prototype tracer tests.

Scale model results of the residence time distribution matched the prototype tracer test data well. However, approximately 10.5 hours was required for flow development at the lowest flow rate tested (0.85 L/s) before steady state conditions were reached and baffle factor results matched prototype values. At the intermediate flow, baffle factor results between the scale model and prototype matched well after only 1 h of flow development time, with improvements only in the Morril dispersion index towards prototype values with increased flow development time (at 5 h). Similar results were seen at the highest flow tested. For fully developed flow, there was little change in the baffle factor and dispersion index results in the scale model with varied flow rate.

With the addition of columns to the scale model, there was no significant change in the baffle factor compared to the case compared to without the columns, but up to a 13.9 % increase in dispersion index as compared to the tests in the scale model without columns for fully developed flow. Further, the residence time distribution results from the scale model tests without columns matched the entire residence time distribution found in the prototype tests. However, for the model with columns, the residence time distribution matched the prototype curve well at early times, but departed significantly from it at times later in the tests. It appears the major effect of the addition of columns within a model clearwell is to increase the dispersion index and increase the proportion of the clearwell which operates as a mixed reactor.

The results also showed there was good agreement between the physical model tests and River2DMix simulations of the scale model tests for both the flow pattern and residence time distributions. This indicates that a two-dimensional depth-averaged computer model such as River2DMix can provide representative simulation results in the case where the inlet flow is expected to be quickly mixed throughout the depth of flow in the clearwell.

ACKNOWLEDGMENTS

I express my sincere appreciation and gratitude to my respected supervisors, Dr. Kerry Mazurek and Dr. Gordon Putz, for their priceless guidance, endless help and encouragement throughout the course of my M.Sc. program. Their comments, criticisms, and suggestions played a major role on the milestone achievement of this thesis.

I owe a debt of gratitude to my advisory committee members, Dr. Jim Kells and Mr. Cory Albers, for their instructive comments, suggestions and feedback. I would also like to appreciate the time and support of my advisory committee chair, Dr. Lee Barbour.

I would also like to thank technicians Mr. Dale Pavier and Mr. Brennan Pokoyoway for their help in constructing and maintaining the hydraulic model. Thanks are also extended to environmental technician Mr. Doug Fisher for help in preparation of the tracer solutions and setup of the fluorometer.

Gratitude is also expressed to the Natural Sciences and Engineering Research Council of Canada (NSERC), which provided financial support to my supervisors in the form of Discovery Grants.

Last, but not least, I express my thankfulness to my husband, David Ke, and my daughter, Jessica Ke, for their support and encouragement in the course of my M.Sc. program.

DEDICATION

This thesis is dedicated to my parents, Peiyun Han and Taiyuan Yu; and my two sisters, Lili Yu and Nili Yu.

TABLE OF CONTENTS

LIST OF TABLES

LIST OF FIGURES

LIST OF SYMBOLS

A	cross-sectional area of the flow;
C	residual concentration of the disinfectant;
C_i	initial concentration of Rhodamine WT;
C_n	new concentration of Rhodamine WT after each dilution step;
C_s	non-dimensional Chezy coefficient;
d	dead space fraction (%);
D	the diameter of one of the holes in perforated baffle wall at the entrance to the reservoir;
D_c	the diameter of the cylinder;
$E(t)$	flow-through curve;
$F(t)$	cumulative residence time distribution curve;
H	height of cylinder;
K_s	the effective roughness height;
L	length scale for the flow;
Lr	length ratio between model and prototype;
m	mixing volume portion;
N	the number of data points for RMSE;
ΔN	the mass of tracer leaving the reservoir in a time period Δt;
N_0	total mass of tracer inputted into the reservoir;
O_i	physical model values of F(t) at time i;
p	degree of plug flow (%);
P	wetted perimeter of the flow;
P_i	the computational values of F(t) from the River2DMix at time i;
q_x	the discharge intensities in the x direction;
q_y	the discharge intensities in the y direction;
Q	flow rate;
Re	Reynolds number based on the width of the rectangular columns;
Re_D	Reynolds number based on the cylinder diameter;
R_i	jet Reynolds number;

R_h	hydraulic radius;
R_r	Reynolds number of the flow in the reservoir;
S_{0x}	the bed slopes in the x directions;
S_{0y}	the bed slopes in the y directions;
S_{fx}	the friction slopes in the x directions;
S_{fy}	the friction slopes in the y directions;
SG	specific gravity;
t	time;
Δt	time interval;
T_d	theoretical detention time;
T_{10}	time required for 10% of the mass of tracer entering a clearwell to exit the clearwell;
T_{50}	time required for 50% of the mass of tracer entering a clearwell to exit the clearwell;
T_{90}	time required for 90% of the mass of tracer entering a clearwell to exit the clearwell;
T_{99}	time required for 99% of the mass of tracer entering a clearwell to exit the clearwell;
U	the average flow velocity (Chapter 2);
U_i	the average velocity of flow through the holes of the perforated baffle wall;
V	the average velocity of flow in the clearwell;
$\forall$	total volume of reactor;
V_w	volume of the added dilutents;
V_d	pipetted volume of the dye solution;
ε_1	constant (default value 0);
ε_2	bed shear generated term;
ε_3	transverse shear generated term;
μ	free-stream dynamic viscosity;
v	kinematic viscosity of the fluid;
v_t	turbulent kinematic viscosity;
ρ	the free-stream density;

κ	Von Karman's constant;
σ^2	dispersion index; and
τ_{xy}	transverse turbulent shear stress in the hydrodynamic model and mixing model ($\tau_{xy} = \tau_{yx}$).

CHAPTER 1: INTRODUCTION

1.1 Background

Adequate treatment of drinking water is a significant issue for society. There were 200 documented incidents of contamination of drinking water systems with waterborne pathogenic microorganisms between 1974 and 1996 in Canada (Edge et al. 2003). There are three main types of microorganisms that can be found in drinking water: bacteria, viruses, and protozoa. One of the main goals of drinking water treatment is to remove or kill these organisms to reduce the risk of illness (Health Canada 2006). In the United States, the United States Environmental Protection Agency introduced the Surface Water Treatment Rule (SWTR) under the Safe Drinking Water Act Amendments of 1989 to improve regulation of drinking water. Similarly, in Canada, the regulations governing water supplies are becoming more stringent. These regulations require that all public water is to be supplied without microbial contamination, with particular emphasis placed on protozoa (such as *Giardia* and *Cryptosporidium*), since these microorganisms are more resistant to destruction by chemical oxidizing agents such as chlorine. Water utilities are also required to provide continuous chemical oxidation of the drinking water entering the distribution system and to maintain a detectable chlorine residual level within the distribution system (USEPA 1989).

To specify the required level of treatment by chlorine, the CT concept has long been used. The "CT" value is the residual concentration C of chlorine in milligrams per litre (mg/L) multiplied by the contact time T in minutes (USEPA 1989). The contact time is the time it takes the water to move from the input point of a reactor to the outlet point where the residual concentration is measured. The CT product required to reduce the count for a specific microorganism under defined conditions is a way of comparing the effectiveness of different oxidizing agents, and for specifying the resistance of a variety of pathogens. The USEPA specifies CT values for free chlorine as standard indices to control pathogens in water treatment. Some of these are listed in Crittenden et al. (2005).

Although chlorination effectively destroys pathogenic microorganisms there are heath concerns related to consumption of chlorination by-products. Therefore, rules have been established to address these health risks. For example, trihalomethanes are by-products of chlorination of natural waters containing dissolved organic compounds. A minimum residual concentration of 0.1 mg/L has to be maintained to prevent contamination of the water before it reaches customers (Alberta Environmental Protection 1988). Therefore, the goal of water treatment facilities is to ensure destruction of pathogenic microorganisms while trying to avoid the formation of chlorination by-products in the water supply.

Water reservoirs in water distribution systems are used to ensure consistent water quality and adequate pressure for fire, domestic and industrial users (Clark et al. 1996). In the water treatment process, large reservoirs are also often used both as water storage tanks and chlorine contact chambers (sometimes also called “clearwells”). These reservoirs can be very large. For example, the clearwell at the Glenmore Water Treatment plant in Calgary, Alberta is approximately 123 m long, 112 m wide and 5 to 6 m deep. Due to the large size of the reservoirs and their often square geometry, reservoirs commonly have dead zones in the flow pattern through the reservoir. Within the dead zones the water tends to stagnate. Conversely, the flow can also short-circuit through the reservoir. This means the flow moves directly from the inlet to the outlet of the reservoir. Both flow behaviours have negative impacts on the disinfection performance in clearwells. Short-circuiting results in a short contact time and hence less reaction time for the disinfectant with the water. The chlorine residual in the water can drop to below required levels in dead zones, which can allow the growth of microorganisms. Generally, the two cases are related in that the higher percentage of dead zones in water storage systems, the more short-circuiting that exists. Serpentine baffle walls are frequently installed within reservoirs to produce conditions to prevent the occurrence of short circuiting and dead zones.

The flow behaviour in reservoirs is typically evaluated using tracer tests (Marske and Boyle 1973; Hart and Vogiatzis 1982; Teefy and Singer 1990; Boulous et al. 1996;

Maksymetz 1998; Grayman et al. 2004). Although tests in the full-scale reservoir give the most reliable results, it is very expensive to run these tests and only a few variables can be tested. It can also be difficult to schedule such testing. As an alternative to field tests, tracer studies in scale models have been widely used to assess reservoirs, as they are an economical means to assess the flow behaviour and potential changes to the flow due to reservoir modifications (Rebhun and Argaman 1965; Kothandaraman and Evans 1972; Hart and Gupta 1978; Hart 1979; Roy et al. 2002; McCorquodale and Machina 2002). More recently, both two and three-dimensional computational fluid dynamics models have been used to assess flow in reservoirs (Grayman et al. 1996; Wang and Falconer 1998a; Hannoun et al. 1997; Templeton et al. 2006).

Whether the tracer test is carried out in the actual reservoir or a physical or numerical model, a conservative tracer chemical is injected into the flow either continuously or as a slug in the test. In the continuous feed method, the tracer is injected at a constant dosage until the concentration at the reservoir outlet reaches a steady-state level. In a slug test, a controlled amount of tracer is instantaneously added to the inlet flow and samples are taken at the exit of the reservoir over time as the tracer passes through the reservoir. Analysis of both types of tests can define the residence time distribution of the fluid particles in the reservoir.

In theory, the residence time distribution in a reservoir is determined by the percentage of “plug flow”, “dead zone” and “mixing zone” regions in the reservoir (Crittenden et al. 2005). Plug flow is called piston-like flow, where every fluid particle spends an identical length of time in the reservoir (Levenspiel 1972). The flow of fluid through the reservoir is orderly, with no element of fluid overtaking or mixing with any other element ahead or behind. It is also assumed that the concentration is uniform through the cross-sectional area of the flow. This is because the flow is quickly mixed in the transverse and vertical directions since the depth and width of the flow is very much smaller than its length. For the situation termed “complete mixing”, it is assumed that the tracer is fully mixed with all the flow in the reservoir before leaving the reservoir. For

real flows in reservoirs, usually the flow patterns consist of some portion of plug flow, with some mixed flow and dead zones.

To assess the performance of reservoirs used as chlorine contact chambers, the USEPA (1989) sets out requirements for chlorine contact with the fluid moving through the reservoir based on the residence time distribution for the reservoir. The time it takes for 10 % of the mass of a tracer injected at the inlet to pass through the reservoir, defined as "T_{10}", is one of the most important parameters. The T_{10} gives the time for which 90 % of the mass of tracer is retained within the reservoir, while 10% of the mass has passed through the reservoir outlet. The ratio of T_{10}/T_d is called the "baffle factor" for the reservoir, where the theoretical detention time T_d is the volume of fluid in the reservoir divided by the flow rate. Several other indices to describe the flow in reservoirs based on the residence time distribution curve are also utilized such as the Morril dispersion index T_{90}/T_{10}.

1.2 Motivation for the Work

The motivation for the work discussed herein was to better understand whether the computational, two-dimensional, depth-averaged, open channel flow mixing software such as River2Dmix is an appropriate tool for modeling water reservoirs (used for both storage and as chlorine contact chambers) in water treatment and distribution systems. As a first step in this evaluation, it was decided to assess the performance of River2DMix in modeling the residence time distribution and flow pattern of a clearwell where full-scale residence time distribution data was available. It was also decided to model a reservoir that might have approximately a two-dimensional flow (depth averaged and open channel flow) based on its geometry. The results were also to be compared to tracer studies and flow pattern visualization in a scale hydraulic model of the same clearwell. Full-scale tracer study results were available from the City of Calgary for their Glenmore Water Treatment Plant northeast clearwell (Maksymetz 1998, 2003). The Glenmore reservoir northeast cell is the main focus of the current research; in this reservoir there are 122 - 400 mm × 400 mm square structural columns.

One of the issues for both the computational and hydraulic modeling of the reservoir (and reservoirs in general) was whether or not the structural columns need to be modeled. Modeling the columns takes a considerable computational effort compared to the no-column case because there are more elements in model for the with columns case. It is also an additional burden to construct in hydraulic model study. In some early work with River2DMix in modeling the Glenmore reservoir, Albers and Maksymetz (2004) and Albers et al. (2005a and 2005b) found that the simulation of the columns had a pronounced effect on the residence time distribution produced by the model. It was uncertain whether this was a numerical or physical effect.

1.3 Objectives

The objectives of this thesis are as follows:

- To assess the effect of flow rate on flow behaviour within the Calgary Glenmore NE Clearwell and the resulting residence time distribution curves using tracer studies and flow visualization in a physical scale model;
- To evaluate the influence of columns on flow behaviour within the clearwell of the physical scale model and on the resulting residence time distribution curves using tracer studies and flow visualization in a physical scale model; and
- To evaluate (most significant) whether a 2-dimensional depth averaged computational fluid dynamics model such as River2DMix can simulate the flow behaviour and residence time distribution curves seen in the scale physical model with and without columns over a range of flows by comparing the simulation results to the measured results.

1.4 Organization of Thesis

This thesis includes five chapters. The second chapter includes a review of the literature on physical and computational modeling of water treatment reservoirs. It also includes an overview of the CT concept and analysis techniques used for evaluating the flow behaviour of the reservoirs. Chapter 3 gives the details of the experimental setup, testing program, and tools that were used for physical test data measurement. This is

followed by the details of the computational model. Chapter 4 describes the results of the experiments, detailed analysis of the experimental data and computational simulation results. Finally, Chapter 5 presents conclusions developed from the study and recommendations for further work.

CHAPTER 2: LITERATURE REVIEW

2.1 Introduction

In order to fully understand the flow behaviour in clearwells, a wide range of experimental and numerical studies have been carried out. These studies measure various flow parameters, including the flow pattern, residence time distribution, hydraulic efficiency (baffle factor), dispersion index, the locations of dead zones, and the percentage of dead space, plug flow, and mixing in a flow. In this chapter, previous research on the assessment of the flow behaviour and retention time in clearwells using physical and computational modelling is reviewed. Parameters for characterizing the flow and residence time distribution in clearwells are presented. The methods for performing tracer studies to determine the residence time distribution are discussed. Finally, flow dynamics around columns are described in order to help explain the effect of columns on the flow at different Reynolds numbers in modelling columns in clearwells.

2.2 Hydraulic Retention Time in Ideal and Non-Ideal Reactors

Since the main purpose of the clearwell is to provide for sufficient contact time for the water with the chlorine before it moves into the distribution system, the hydraulic retention time in a clearwell is a key parameter in assessing whether a clearwell design will meet CT requirements. The US Environmental Protection Agency guidance manual for compliance for disinfection (USEPA 1989) specifies required CT_{10} values for control of pathogens in water treatment. As noted in Chapter 1, T_{10} is the time required for 10% of the mass of a tracer (fluid element) entering a clearwell to exit it.

The use of this CT concept for clearwell design is based on theory developed for chemical reactors (Levenspiel 1972). The ideal type of flow through the reactor, or clearwell, is plug flow (Teefy and Singer 1990). In plug flow each fluid element has the same hydraulic residence time for all water passing through the reactor (Kothandaraman and Evans 1972). The plug flow hydraulic retention time is the theoretical detention time defined in Chapter 1, T_d, which is equal to the total volume of the reactor V divided by the flow rate, Q:

$$T_d = \frac{V}{Q} \tag{2.1}$$

The actual flow in clearwells is different from the ideal case of plug flow because flow through typical clearwell geometries produces non-uniform velocity fields. Many clearwell geometries result in flow separation, such as in the corners of a clearwell, which results in dead or stagnation zones in the flow. Often the outlet of the clearwell is placed near the inlet, which can result in short circuiting in the flow. Both cases result in a lower residence time than would be expected for the ideal case. Thus, they both have negative effects on chlorine contact time in a clearwell. The USEPA guidance manual (USEPA 1989) uses the T_{10} value as the criterion for clearwell design to guard against short-circuiting within a clearwell.

For real flows in clearwells, usually the flow patterns consist of some portion of plug flow, mixed flow and dead zones (Falconer and Tebbutt 1986). The difference between plug flow and mixed flow is that in plug flow there is no mixing (flow through the clearwell is orderly with no element of fluid overtaking another). In "complete mixing", it is assumed that the tracer is fully mixed with all the flow in the clearwell before leaving the clearwell. The contact time in a reservoir is therefore determined by the percentage of "plug flow", "dead zone" and "mixed flow" in the reservoir (Hart 1979).

2.3 Characterizing Hydraulic Retention Time in Clearwells

2.3.1 Estimating Retention Time

Tracer tests are specified by the USEPA in their guidance manual (USEPA 1989) and Handbook of Community Water Supplies, Water Quality and Treatment, 5th edition (AWWA 1999) as the desired method to estimate CT values. However, the T_{10} value is also often only roughly estimated based on the degree of baffling in the clearwell (Bishop et al. 1993). USEPA (1989) provides baffle factor, or T_{10}/T_d, values based on different baffle configurations in clearwells and this is summarized in Table 2.1. It is seen in Table 2.1 that the baffling condition for a clearwell is divided into five categories. For unbaffled conditions, the baffle factor is less than 0.1 and for perfect (plug flow)

conditions, the baffle factor is 1. For typical clearwell conditions, the baffle factor is in the range of 0.1 to 0.8, since the flow is composed of some plug flow, mixed flow, and dead space.

Table 2.1 Typical baffle factors (adapted from the USEPA (1989))

Baffling Condition	T_{10}/T_d	Description
Unbaffled (mixed flow)	<0.1	Non agitated basin, very low length to width ratio, high inlet and outlet flow velocities
Poor	0.3	Single or multiple unbaffled inlets and outlets, no intra-basin baffling
Average	0.5	Baffled inlet or outlet with some intra-basin baffles
Superior	0.7	Perforated inlet baffle, serpentine or perforated intra-basin baffles, outlet weir or perforated launders
Perfect (Plug flow)	1.0	Very high length to width ratio (pipeline flow), perforated inlet, outlet, and intra-basin baffles

2.3.2 Tracer Studies in Clearwells

As noted above, performing a tracer study is the desired method for characterizing the residence time distribution in a clearwell. As such, tracer studies have been widely carried out in full-scale reservoirs and hydraulic models and also simulated in computational models (Falconer and Tebbutt 1986; Joost et al. 1990; Teefy and Singer 1990; Bishop et al. 1993; Boulous et al. 1996; Maksymetz 1998; Roy et al. 2002; and Hurtig 2003). For these types of tests, firstly, a tracer must be chosen. Joost et al. (1990) suggested the tracer chemical be mass conservative, easily analyzed, inexpensive and environmentally acceptable for use. In operating clearwells, often fluoride is used as the tracer (Maksymetz 1998). Fluoride injection is turned on or off at the start of a test. However, Rhodamine–WT and Pontacyl pink (intracid Rhodamine B) are also tracer chemicals recommended for use (Wilson et al. 1986). These fluorescent dyes are used in

liquid form and are highly water soluble, detectable at very low concentrations, harmless, and reasonably stable in normal water environments (Wilson et al. 1986).

The next step is to determine how the tracer will be injected. Joost et al. (1990) investigated tracer input options, tracer selection, and background and data analysis techniques. They suggested that the conventional continuous and slug input methods were the simplest way to analyze and interpret test results when compared with the random input and cyclic input methods. Most studies in full-scale and model clearwells use either the slug input or continuous feed input of a mass conservative tracer at the clearwell input. Following the injection of the tracer, the concentration in the water is measured at desired locations in the clearwell and recorded at a specified frequency over the course of the tracer test. Finally, the measured tracer concentration versus time can be plotted for analysis.

In a slug test, a mass of tracer is instantaneously added to the water at the clearwell inlet and samples are taken at the exit over time as the tracer passes through the clearwell. The total mass of tracer material to be injected is carefully measured in advance. Samples are taken at the outlet frequently enough to define the leading edge of the concentration versus time curve, and to identify the peak tracer concentration and time of occurrence (Hudson 1975; Joost et al. 1990). After the peak concentration passes through the outlet, the frequency of sampling can be reduced. Data from the slug test are plotted as a curve of concentration versus time. Kothandaraman and Evans (1972) investigated the hydraulic characteristics of a model of a rectangular chlorine contact chamber using slug tests. Teefy and Singer (1990) applied the slug input method to three full-scale clearwells to evaluate the CT_{10}. Roy et al. (2002) used a slug test to quantitatively evaluate the hydraulic performance of a 1:11.25 scale physical model of a clearwell system by continuously monitoring the model outlet concentration using a fluorometer. These investigations have shown the slug test is an effective and simple method to investigate the flow behaviour in prototype and model clearwells.

In the continuous feed method, a mass conservative tracer is injected at the inlet at a constant dosage (mass flow rate) until the concentration at the outlet reaches a steady-state. The concentration versus time at the outlet is plotted from the beginning of the injection to the establishment of steady state. Bishop et al. (1993) employed the continuous feed method in full-scale tests of five rectangular clearwells to estimate their hydraulic efficiency. Hurtig (2003) studied the flow characteristics of two clearwells utilizing continuous feed tracer tests in scale physical models of the clearwells. Taras (1956) investigated the difference between the continuous feed method and the slug feed method for determining the retention time distribution curve. He pointed out the continuous feed method eliminated the problem of the large tracer mass needed in the slug test if the tracer test was carried out in a large volume reaction chamber. Also, the continuous feed method was compatible with routine plant operations.

2.3.3 Analysis of Tracer Study Data

In a non-ideal contact chamber each fluid element that enters the reactor will have a different time to pass through the reactor. The distribution of these travel times is called the residence time distribution. This distribution is determined from the results of the above-described types of tracer tests (Levenspiel 1972; Teefy and Singer 1990; Crozes et al. 1999). In fact, two types of residence time distribution curves may be developed: the residence time distribution, *E(t)*; and the cumulative residence time distribution, *F(t)*.

The plot of tracer concentration verses time exiting a clearwell during a slug tracer test gives the residence time distribution of the fluid particles passing through the clearwell. This "flow-through curve", E(t), represents the time distribution of fluid elements in the reservoir (Levenspiel 1972). The cumulative residence time distribution curve is called the F(t) curve. It is derived by numerically integrating the E(t) curve. The cumulative area under the E(t) curve at any time is the value of the F(t) curve, while the slope of F(t) curve is the value of the E(t) curve (Levenspiel 1972; Crozes et al. 1999). The F(t) curve is the age distribution of the tracer exiting the clearwell and directly

illustrates the hydraulic efficiency of the reservoir. In the slug test, two steps are required to derive the F(t) curve, whereas it is directly measured in a continuous feed tracer test.

The T_{10} is determined directly from the F(t) cumulative residence time distribution curve and is the time when F(t) = 0.1 (Thirumurthis 1969; Kothandaraman and Evans 1972; Mitha and Mohsen 1990; Teefy and Singer 1990). Besides the T_{10} value, the T_{50} and T_{90} values are also used as indices to describe the hydraulic efficiency of the clearwell. The 50 and 90 subscripts represent the times for 50 % and 90 % of a tracer mass to pass through the clearwell. The T_{50} is the mean residence time. Comparison of the T_{90} to the T_{10} gives the dispersion in the flow and is called the Morril Index. Ideal plug flow has a Morril Index of 1.0 (Bishop et al. 1993), and a large number for the T_{90}/T_{10} indicates more mixing (Hart 1979). An increase in the baffle factor is typically reflected by a decrease in the Morril Index. A list of other parameters taken from the F(t) curve is given in Table 2.2.

Table 2.2 Performance parameters used in analysis of contact basins (adapted from Marske and Boyle, 1973)

Parameter	Definition
T_d	Theoretical detention time
T_i	Time for the initial observation of the tracer at the outlet
T_p	Time to reach peak concentration
T_g	Time to reach centroid of residence time distribution
T_{10}/T_d	Baffle factor
T_i/T_d	Index of short-circuiting
T_p/T_d	Index of model detention time
T_g/T_d	Index of average detention time
T_{50}/T_d	Index of mean detention time
T_{90}/T_{10}	Morril dispersion index

Further information on the flow behaviour in the clearwell can also be gained from more detailed interpretations of the F(t) based on the function shape (Rebhun and Argaman 1965; Hart and Gupta 1978; Hart 1979; Roy et al. 2002) and statistical methods (Kothandaraman and Evans 1972; Marske and Boyle 1973; Hart and Gupta 1978; Hart and Vogiatzis 1982). These investigations demonstrated how to analyse the entire data

set of a tracer test in order to characterize the residence time distribution rather than using one value such as T_{10}.

Rebhun and Argaman (1965) developed a method to quantitatively assess the percent plug flow, mixed flow, and dead space in a reactor based on the shape of the F(t) curve. They modified earlier work by Wolf and Resnick (1963) and derived the following equation for describing the relationship between the F(t) curve (based on the dimensionless time t/T_d) and the fraction of plug flow and dead space in the reservoir:

$$\ln\left(1 - F\left(\frac{t}{T_d}\right)\right) = -\left(\frac{t/T_d}{(1-p)(1-d)}\right) + \frac{p}{(1-p)} \tag{2.2}$$

where d represents the dead volume fraction and p is the degree of plug flow. Experimental data are used to plot $\ln(1-F(t/T_d))$ vs. t/T_d. Then the intercept of the best-fit linear trend line is used to determine the plug flow proportion (p), and the slope of the line is used to determine the dead space proportion (d). The mixed volume proportion (m) is equal to one minus the sum of the plug flow and the dead space proportions ($m = 1-(p+d)$) (Roy et al. 2002). Many researchers have used Eq. 2.2 to assess the percentage plug flow, mixed flow, and dead space in the reservoir (Kothandaraman and Evans 1972; Hart and Gupta 1978; Hart 1979; McCorquodale and Machina 2002; Roy et al. 2002). It is recommended by the USEPA (1989) as a additional description of the flow behaviour the use of just the T_{10} or T_{90} values, since equation (2.2) takes a larger portion of the entire F(t) curve into account.

Statistical methods are also to describe the flow characteristics by analyzing the residence time distribution or E(t) curve (Bishop et al. 1993). Marske and Boyle (1973) used statistical interpretation of tracer data to evaluate the hydraulic characteristics of a clearwell and to determine the dispersion index (σ^2) generally used in chemical engineering. By this method the dispersion index σ^2 was calculated as the variance of the E(t) curve rather than on the basis of just one or two points on the F(t) curve. The dispersion index σ^2 is expressed as:

$$\sigma^2 = \frac{\delta t^2}{t_g^2} \tag{2.3}$$

$$\delta t^2 = \frac{\sum t^2 C}{\sum C} - \left(\frac{\sum tC}{\sum C} \right)^2 \tag{2.4}$$

$$t_g = \frac{\sum tC}{\sum C} \tag{2.5}$$

where t is time and C is tracer residual concentration. A dispersion index σ^2 equal to zero indicates that no dispersion of the tracer substance has occurred and the clearwell is under ideal plug flow conditions. A symmetrical E(t) represents a model when only dispersion is occurring and this gives $\sigma^2 = 0.01$ (Johnson et al. 1998). Mixing and dead space skew the E(t) curve.

2.4 Physical Modelling of Flow in Clearwells

2.4.1 Background

Physical scale modeling of the flow in clearwells has often been undertaken. This is because, although tracer studies in full-scale clearwells can provide useful information, they cannot be used to assess the effects of proposed modifications to clearwell design. Often the value of a full-scale tracer test is limited due to discontinuities in field data and variable factors such as non steady-state flow conditions. Furthermore, tracer tests can be difficult to conduct in an operating water treatment plant because it is difficult to take the clearwell offline or have it operate at a constant flow and water surface elevation for long periods. Therefore, scheduling of tracer tests can be difficult for potable water service providers who must maintain service to their customers.

As an alternative to tracer studies in the actual clearwells, a scale model test is often employed to determine the residence time distribution (Hart and Gupta 1978; Hart 1979; Falconer and Tebutt 1986; Mitha and Mohsen 1990; Bishop et al. 1993; McCorquodale and Machina 2002; Roy et al. 2002; Hurtig 2003). Louie and Fohrman (1968) stated that physical modelling was not only an efficient method to study flow

within a clearwell, but also a relatively economical way to provide design guidance. Kothandrarman and Evans (1972) investigated the hydraulic characteristics of a rectangular contact tank under various flow conditions using the 1:10 scale model. Roy et al. (2002) investigated the effects of finger baffles, guide vanes, and inlet piping on the hydraulic characteristics of a contact reservoir using a 1:11.25 scale model. The results of the investigation aided in the development of cost-effective modifications to the full-scale reservoir to improve performance. In each of the studies citied above, a scale model was shown to be an effective alternative way to evaluate flow behaviour of an existing contact chamber and a useful tool to assess the effects of retrofits.

2.4.2 Similitude for Clearwells

Physical hydraulic models are usually constructed with much smaller dimensions than the prototype they represent due to space and cost limitations. In order to fairly represent the flow mechanisms in a hydraulic system, and to compare flow characteristics measured in a physical model with the characteristics found in a prototype, it is critical to choose the scale ratios based on the principles of similitude (Falconer and Tebbutt 1986; Bishop et al. 1993; Hurtig 2003). Similitude means that there is geometric, kinematic, and dynamic similarity for the flows in the model and prototype (ASCE 2000). Geometric similarity indicates that all the dimensions in the model are scaled from the prototype value at the same ratio. When kinematic similarity is achieved, there is a constant ratio between velocities and accelerations in the physical model and the prototype at corresponding positions. When dynamic similarity is achieved, there is a constant ratio between the forces in the physical model and the prototype at corresponding positions (ASCE 2000).

It is common practice to design a physical hydraulic model using dynamic similarity by taking the ratio of the dominant force of the system and the inertial force (ASCE 2000). In a physical hydraulic model, there can be many forces in the system that influence the fluid flow including gravitational, viscous, surface tension, and pressure forces. If viscosity (and surface tension) is neglected and gravity dominates, the scale model is considered a Froude model. In a Froude model, the Froude number is the same

in the model and prototype and is used to develop the scale factors for velocity and flow rate. The Froude number, F_r, is expressed as:

$$F_r = \sqrt{\frac{V^2}{gL}} \tag{2.6}$$

where V is average velocity of flow, g is gravity acceleration and L is the length scale for the flow (e.g. depth of flow). For equivalent Froude numbers in the physical model and prototype, the velocity, time, volume and discharge is a function of length scale ratio (see Table 2.3, where L_r is the length ratio between model and prototype).

Table 2.3 Scaling parameters

Parameter in Model	Scale Factor
Length	L_r
Area	L_r^2
Volume	L_r^3
Time	$L_r^{0.5}$
Velocity	$L_r^{0.5}$
Discharge	$L_r^{2.5}$

The water in a clearwell is a free-surface flow which is a gravity-dominated flow. When there is turbulent inflow entering the reservoir, the fluid viscosity has little effect on the flow system and it is assumed negligible compared to gravity forces (ASCE 2000). Froude number similarity has been successfully applied in modelling clearwells by Kothanadaraman and Evans (1972), Hart and Gupta (1978), Falconer and Tebbutt (1986), Roy et al. (2002) and Hurtig (2003).

The validity of Froude number scaling for the flow in a clearwell based on Froude number has been verified by comparing the results of tracer tests performed at full-scale and on the physical model. Bishop et al. (1993) concluded there was good correlation between model and prototype results based on Froude number modelling because the cumulative residence time distribution curve, F(t) vs. dimensionless time t/T_d, simulated

the full-scale system quite well over a range flows. Hurtig (2003) also verified that physical models are an effective method of evaluating clearwell performance by comparing the results of tracer tests on models of two clearwell reservoirs to the results of prototype tests. Falconer and Tebutt (1986) indicated that a hydraulic model based on Froude number similarity was able to closely reproduce general flow parameters in the prototype such as T_i/T_d, T_{10}/T_d, T_{90}/T_d. Hart and Gupta (1978) investigated the effect of various discharges on the parameters T_i/T_d, T_{10}/T_d, T_{90}/T_d, p, m, and T_{90}/T_{10} in the model because they thought that these parameters used to interpret dye tracer data may have different reliability or consistency when compared with the actual prototype values. They found that T_i/T_d, T_{10}/T_d, T_{90}/T_d, p, and m were consistent with prototype results at the high end of the flow operating range; however, T_{90}/T_{10} had good results over the entire range of flow tested. As indicated above, the Froude number similarity criterion is only appropriate when the Reynolds numbers of the flow are large enough (flow Reynolds number in the channel is more than 2000 (Jain 2001)) to ensure the flow is turbulent.

Falconer and Tebutt (1986) conducted tracer tests in distorted physical models which had vertical distortions of two and three times the horizontal scale, i.e. the models had a water depth of two and three times the depth in a non-distorted model. The purpose of the vertically distorted models was to increase the Reynolds number to achieve turbulent flow in the model and to increase the accuracy of flow velocity and depth measurements. They found that there was little difference in test results between the undistorted model and distorted model, even though the undistorted model operated with a Reynolds number stated to be at the lower end of the turbulence scale (although Reynolds number values were not given). They did not provide a quantitative comparison of the results. However they pointed out that there were good agreement between physical model and prototype results for the undistorted model and concluded the undistorted model at the lower end of the turbulence scale had the ability to representatively simulate the prototype flow characteristics.

Hurtig (2003) conducted a tracer test in a physical model with scaled-down pillars to resemble the support columns in the Rossdale Water Treatment Plant Clearwell in Edmonton, Alberta. The objective was to determine if the physical model could reproduce the effects of the columns in the prototype flow behaviour. According to the test results, the columns did not significantly affect the baffle factor compared to the results without columns present. Further, it was noticed that the columns marginally improved the longitudinal mixing based upon visualization tests. Hurtig (2003) suggested that the columns were not a dominant factor in the scale model in representing the flow behaviour of the prototype reservoir. This is contrary to Albers et al. (2005, 2006), who argued that the presence of structural columns in a clearwell greatly improved the mixing between the baffle walls and increased the hydraulic efficiency (also called baffle factor) of a clearwell when compared to the conditions without structural columns. They attributed the increased hydraulic efficiency to internal mixing, which reduced the recirculation and dead zone areas in the clearwell.

2.4.3 Issues with Using Scale Models of Clearwells

One of the issues with using physical scale models to run tracer or mixing studies is that the diffusion in the model is less than the prototype because the turbulence is less at the smaller scale (ASCE 2000). When dye is injected into the water, dispersion of the dye through the flow occurs due to the presence of velocity gradients (Socolofshy and Jirka 2002). In addition to dispersion, diffusion also occurs due to random motion of fluid packets from higher concentration to lower concentration areas (due to turbulence). Diffusion is less in the model than in the prototype. However, longitudinal dispersion is dominant over longitudinal diffusion by several orders of magnitude (Fisher et al. 1979), so the longitudinal dispersion in the direction of flow plays a major role in mixing in a clearwell.

Mitha and Mohsen (1990) conducted tracer studies in four geometrically similar physical models of contact chambers based on the equal detention time criterion to investigate the effect of scale on dispersion characteristics. However, Froude number similarity was not used for the modelling. A lower flow rate was adopted in the model

based on the equal detention time compared with the flow rate based on Froude similarity. It was found that the dispersion appeared to be more dependent on changes in channel size for smaller channels, whereas larger channels were less sensitive to scale. However, the interpretation of the results is uncertain since the scaling was not done on the basis of the Froude number, unlike in other studies. Bishop et al. (1993) also pointed out, besides the effects on dispersion, the model scale ratio needs to provide an adequate depth of flow to avoid surface tension effects, it must provide reasonably sized model (so that measurements can be taken), and model flow rates must be practical.

2.4.4 Flow Visualization in Model Clearwells

In addition to quantitative tracer studies, visual observations of a tracer can also be used to identify short-circuiting, dead zones and longitudinal dispersion by assessing the degree of the dye colour. Louie and Fohrman (1968) investigated the approximate velocity distribution at the locations of interest by flow visualization. They delineated the regions of flow separation and eddy activity in contact chambers for several different model configurations. Falconer and Tebbutt (1986) undertook visual observations of different model configurations and found the trends of dead space identified were compatible with the interpretation of dye concentration analysis. Also, Roy et al. (2002) conducted flow visualization tests with potassium permanganate dye in a 1:11.25 scale model of a chlorination reservoir system in conjunction with a slug test to measure the concentration of tracer. The flow patterns in the scale reservoir model for various configurations were evaluated by flow visualization to identify the short-circuiting and dead zones.

2.5 Numerical Modelling

2.5.1 Why Conduct Numerical Modelling?

Disadvantages of the use of physical models to perform tracer studies are the costs of construction, time to set up model, requirements for the physical space to run such tests, and issues with modelling the diffusion in the flow at a small scale. Also, it is hard to investigate three-dimensional flow characteristics in a physical model unless sophisticated measurements techniques are applied (Hannoun et al. 1998).

An alternative to the use of a physical model is the application of a computational fluid dynamics (CFD) model to assess the flow in a clearwell. CFD models are generally based upon the finite element concept and have been used in fields such as aerodynamics, thermodynamics and chemical reactor engineering. The application of CFD models in the waterworks industry was initiated early in the 1990's and now is widely applied to optimize water storage reservoir and clearwell design (Grayman et al. 1996; Falconer and Ismail 1997; Hannoun et al. 1998; Hannoun et al. 2003; Templeton et al. 2006). CFD models offer several advantages over physical models such as no data limits, flexible parameter selection, and the ability to calibrate the CFD model based on the prototype data (Grayman et al. 1996).

One of the important characteristics of CFD models is the ability to model time-dependent or transient processes resulting in concentrations and flow velocity vectors that vary over time. It is much more difficult to investigate transient processes in field tests in prototypes or in physical models (Hannoun et al. 1998). CFD modelling of clearwells can track the residence time of each fluid packet to obtain a retention time distribution curve from which baffle factors can be determined (Stovin and Saul 1998). Templeton et al. (2006) also note that particle paths and velocity contours can be generated by CFD models. The particle paths can depict the location of dead zones or zones of re-circulation within the clearwell where water is stagnant or moving very slowly relative to the rest of the water (Hannoun and Boulous 1997). Wang and Falconer (1998b) and Wang et al. (2003) reported that CFD models are able to predict the time distribution of tracer injected into the inflow, after a steady-state solution of the velocity field was created.

Hannoun et al. (1998) reported that most CFD software includes a graphical interface that provides users with the ability to modify boundary conditions such as outlet or inlet configurations, clearwell geometry and inflow and outflow conditions. After a basic CFD model of a clearwell is established, it can then be extended to more complicated situations to simulate modifications such as alternative inlet-outlet

conditions and the effects of thermal and buoyancy induced flow, which are difficult to do in physical model tests and not possible in prototype studies.

Hannoun et al. (2003) applied CFD modelling to circular and rectangular clearwells to demonstrate that simple modifications to the original design can achieve required CT results easily and cost-effectively, and increase the disinfection effectiveness**.** Reddy et al. (1999) applied CFD modelling to improve clearwell design and to alleviate short-circuiting problems in existing reservoirs. They reported that CFD modelling is an especially economical method of evaluating different reservoir layouts, configurations and operating conditions compared to field tracer or scaled-down physical model studies.

A limitation of CFD modelling is that the computational model should be validated using field data before it is applied to a wide range of operating conditions (Grayman et al. 1996). Only after comparing the CFD simulation results with measured field data can the predictive capability of the CFD models be verified (Reddy et al. 1999).

2.5.2 Numerical Models Used for Flow Assessment in Clearwells

Hannoun and Boulos (1997) and Hannoun et al. (1998) solved the three-dimensional time-averaged Navier-Stokes fluid flow equations with a k-ε turbulence model applied to a water treatment plant clearwell and compared the numerical results with the prototype tracer test data. The effects of baffling on disinfection efficiency also were investigated. The CFD model included a geometrical description of the reservoir, a reaction rate expression for the tracer, and initial flow and boundary conditions as the input. Using the computer language Fortran 77, a computational mesh was established by subdividing the domain into discrete computational volumetric cells. The residence time distribution of particles was determined from the simulation. The CFD model was used to assess the flow through the clearwell in the Tulsa, Oklahoma, water treatement plant. However, no prototype tracer study results were available for comparison.

Hannoun et al. (2003) further discussed the application of CFD modelling using the program FLOWMOD. This program is based on the theory presented in Hannoun

and Boulous (1997). The FLOWMOD model was applied in several studies of the flow behaviour within different structures and water treatment facilities (clearwells, tanks, and distribution storage reservoirs). The study results showed the FLOWMOD model was capable of producing highly accurate results in comparison to field test measurements. Hannoun et al. (2003) simulated the flow behaviour in a clearwell (Palmdale, California) using three different configurations of intra-baffle walls to explain how to apply CFD models to optimize water quality in a clearwell.

Ta and Brignal (1998) used a CFD model (Fluent) to simulate the flow dynamics in a water storage reservoir. The three-dimensional, finite-volume model was used to investigate the interior flow pattern, short-circuiting, stagnant zones and residence time distribution curves for different inlet and outlet configurations. Even though they did not undertake a comparison between the simulated and measured results (i.e. they did not validate their model), they concluded that a manifold inlet option can produce good plug flow conditions and a smaller stagnation zone when the residence distribution and cumulative residence distribution were compared between the four types of inlet arrangement.

Crozes et al. (1999) applied the computational model FIDAP to model the flow through a clearwell of a water treatment plant (Oak Creek, Wisconsin). FIDAP can simulate steady or transient two- or three-dimensional flows based on Navier-Stokes, continuity, and convective-diffusion equations. In this study, they employed a two-dimensional simulation because the computational time required for solving the equations of mass and momentum transport in three dimensions is significantly more than for two dimensions. The results included the residence time distribution curve and fluid dynamic simulation to illustrate the effect of baffling on the flow patterns within a contactor. After comparing with full-scale tracer tests, FIDAP was able to predict the flow behavior in the disinfection contactors like the prediction of T_{10}/T within 10-15% of the measured value.

Reddy et al. (1999) used a CFD model to simulate the clearwell in Phoenix, Arizona to investigate short-circuiting problems. The results included the cumulative residence time distribution curve and the flow patterns within the clearwell for various baffle configurations. The simulation results were able to predict the flow behavior in the clearwell when CFD data matched the field tracer test data with 10 %. However, they did not specify what model was used.

Falconer and Liu (1988) used a two-dimensional depth-integrated numerical model (QUICK scheme which is a method of quadratic upstream interpolation for term of convective kinematics in the governing differential equation) to predict the depth mean velocity field and the spatial concentration distribution in a chlorine contact tank. Falconer and Ismail (1997) further applied the QUICK scheme to model the transport of a tracer in a scale physical model of a chlorine contact disinfection tank with a serpentine baffle system. The numerical model results for different tank configurations were compared with corresponding physical model results. The predicted mass flow curves assuming two-dimensional (depth-averaged) flow for a conservative tracer were compatible with the corresponding laboratory model results.

Wang and Falconer (1998a, 1998b) and Wang et al. (2003) also investigated application of flow and transport simulation models to the prediction of flow-through curves of a chlorine contact tank. Two-dimensional numerical models using various combinations of turbulence stress models and numerical schemes were developed to solve the two-dimensional flow and transport equations. Predicted flow patterns using various turbulence models (depth mean mixing length model, depth mean k- ε model and Smagorinsky model) and numerical schemes (first-order upwind scheme, QUICK scheme, and third-order upwind difference scheme) were compared with measurements from a physical model. It was concluded that the depth-mean k-ε model gave the most accurate prediction of turbulent flow and mixing over a cross-section. Meanwhile, Wang and Falconer (1998a) pointed out that one of testing criteria of a mathematical model was whether a mathematical model can predict the sizes and locations of recirculation zones in a contact tank or not.

Baawain et al. (2006) investigated the chlorine contact chamber performance of the E.L. Smith Water Treatment Plant in Edmonton, Alberta by creating a three-dimensional (3-D) computational fluid dynamics model (CFX^{TM}5.6). The results of the computational fluid dynamic model were compared to experimental residence time distribution (RTD) curves from a scale model test of the clearwell given in Hurtig (2003). The three-dimensional computational fluid dynamic model was able to predict the measured RTD curves. However, they noted the inlet geometry had a great impact on the flow pattern in the clearwell and noted that 3-D computational modeling was required for this inlet region. Wang and Falconer (1998a) also indicated that it is typical that 3-D water flow with strong horizontal and vertical recirculation regions commonly exists at the inlet and outlet of a contact tank. However, the flow tends to be uniform over the water depth at locations away from the inlet region and 2-D modelling is acceptable in these regions.

Templeton et al. (2006) applied two–dimensional CFD modeling to simulate tracer tests results in a full-scale clearwell. A two-dimensional model was used instead of a three-dimensional model to simplify the modelling procedure and reduce computation time. It was thought possible to use the 2-D model due to the large surface area to depth ratio (> 180) of the modeled clearwell. The model was created using Fluent 6.0 software and was used to predict the residence time distribution curve for various clearwell configuration and flow rate conditions and to determine the baffle factors. The standard k-ε turbulence model was applied in the model. A particle tracking function was used to simulate the tracer movement at specified locations. The study demonstrated that the two-dimensional model could successfully predict clearwell residence times for a range of baffle configurations and flow rates. CFD predictions were verified using tracer study results in the prototype.

Albers and Maksymetz (2004) and Albers et al. (2005a and 2005b) applied River2DMix to investigate the effect of structural columns within the Calgary Glenmore WTP on the baffle factor. The 2D computational model was used to simulate field tracer tests, generate cumulative retention time distribution curves and baffle factors. In the

simulation process, the same clearwell geometry and flow conditions were modelled without columns and with columns. This research showed that River2DMix was sufficiently accurate to describe the flow behaviour in the clearwell compared to field tests conducted by Maksymetz (1998). By comparing the simulation results for the without columns condition and the with columns condition, a significant difference was identified. Albers et al. (2005a and 2005b) suggested that the structural columns in the clearwell enhanced internal mixing and minimized the presence of dead zone and short-circuiting in the clearwell. Further, the assumption of uniform concentration in the water used by the depth-averaged finite element approach agreed well with the +/- 4% difference in measured tracer concentration between the water surface and the bed at the 6 m deep clearwell outlet.

2.6 River2DMix

River2DMix, the program used to simulate the flow in the Glenmore clearwell herein, is a modified version of the River2D software developed at the University of Alberta to simulate hydrodynamic flow and mass transport in a river. The software utilizes a depth-averaged finite element approach to simulating the St. Venant equations (Albers et al. 2005a and 2005b). The hydrodynamic simulation within River2DMix initially runs to converge upon a solution. Then the mixing model runs to simulate mass transport and to determine concentration profiles in the two horizontal directions. Velocity vectors from the hydrodynamic simulation can be used to trace the path of particles that travel through a modelled system (Stovin and Saul 1998). A time series of concentrations from the mass transport and mixing model can be used to depict residence time distribution curves at selected locations.

In River2DMix, a Boussinesq type eddy viscosity formulation is used for the transverse turbulent shear stress τ_{xy} and τ_{yx} in the hydrodynamic model and mixing model. The terms τ_{xy} and τ_{yx} are estimated using the turbulent kinematic viscosity ν_t. The ν_t term includes the eddy viscosity coefficient, which is assumed to be composed of three components: a constant ε_1 (default value 0), a bed shear generated term ε_2, and transverse shear generated term ε_3 (Steffler and Blackburn 2002). All three components are

adjustable parameters within the hydrodynamic and mass transport simulation in River2DMix.

The general modeling procedure is to develop a bed topography file from available engineering drawings. The resulting .bed file is loaded into R2D_Mesh to generate the computational mesh files for the River2DMix model. Next, the River2DMix program executes the hydrodynamic simulation until the inflow discharge is equal to the outflow discharge. Finally, the mass transport simulation runs utilizing the fluid flow field determined in the hydrodynamic simulation (Steffler and Blackburn 2002).

In River2DMix, hydrodynamic boundary conditions usually take the form of a specified total discharge at inflow sections; fixed water surface elevations or rating curves at outflow sections and no-flow vertical walls. There is also a function in River2DMix called "simple tracer mass initial condition specification" that is used in mass transport mixing simulation. Some key assumptions in the model are a hydrostatic pressure distribution in the vertical, a constant horizontal velocity distribution over the depth, and negligible Coriolis and wind forces (Steffler and Blackburn 2002).

2.7 Flow Dynamics Around Columns

In order to better understand the flow behaviour around structural columns, the following paragraphs review some previous and current research regarding flow around columns with circular and square cross sections. In particular, the variation of the flow behaviour with Reynolds number is described to better understand the changes in flow behaviour around columns present in the model studied herein.

Firstly, in considering the flow around a single cylinder that is circular in cross-section, it is known that the flow behavior depends strongly on the Reynolds number. Here Reynolds number is based on the cylinder diameter and is defined as follows:

$$Re_D=\rho U D_c/\mu \tag{2.7}$$

where ρ is the free-stream density; μ is the free-stream dynamic viscosity; U is the velocity of the approach flow; and D_c is the cylinder diameter. When Re_D is less than 5, the flow is mirrored on the front side and back side of the cylinder (Williamson 1996). When $Re_D > 5$, the flow begins to separate at the rear stagnation point and the flow pattern changes to the steady twin vortex regime where two steady symmetric vortices are formed behind the cylinder (Li 2008). Williamson (1996) defined flow with Re_D less than 49 as the laminar steady regime including the creeping flow regime and steady twin vortex regime (Figure 2.1(a)). The wake starts to become unstable at the end of the recirculation region behind the cylinder when Re_D is greater than 49 (Williamson 1996). The recirculation region

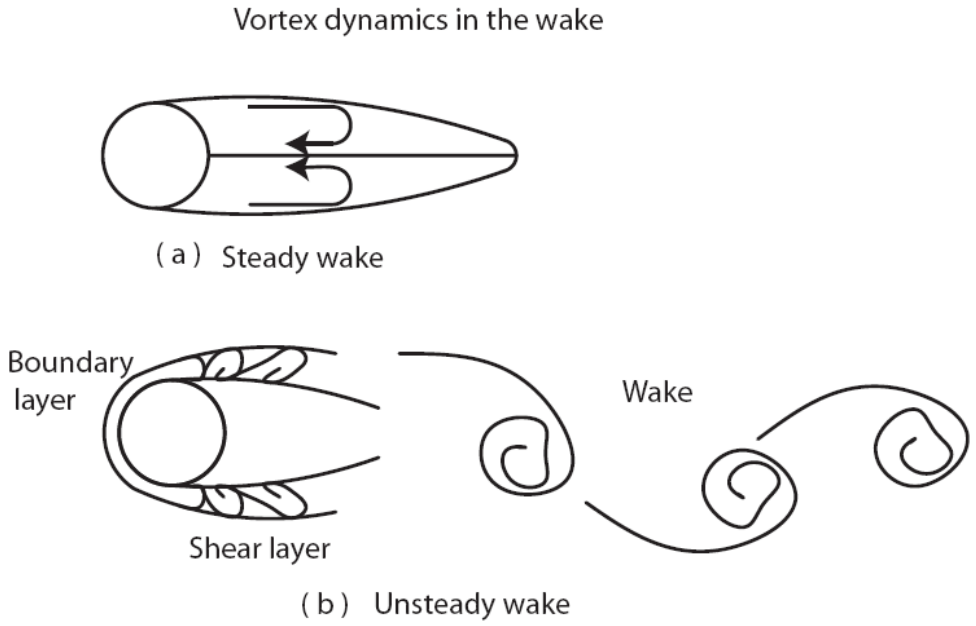

Figure 2.1 The vortical wakes from a bluff body (a) at low Reynolds numbers and (b) at higher Reynolds numbers (adapted from Williamson 1996).

becomes larger with increasing Re_D. As the Re_D increases further, vortices begin to be shed alternately from each side the cylinder (i.e. vortex shedding). When Re_D is 190 to 260, instabilities are amplified to develop turbulence in the wake (Williamson 1996). The flow develops into an irregular vortex shedding regime where the separated shear layers transition to turbulence before roll-up into a Karman vortex street. This causes turbulent fluctuations of the wake. When Re_D is 260 to 1000, the length of recirculation region

increases with disordered three-dimensional vortices (Williamson 1996). When Re_D is 1000 to $2x10^5$, the transition point of the shear layer from laminar to turbulent flow moves upstream and the vortex shedding from the cylinder has a three-dimensional structure. Additional changes happen at even higher Reynolds numbers.

In contrast to flow around circular columns, the flow around a square column has a different flow pattern because the geometry differences provide a different relationship between the vortex structure and flow characteristics (Lyn et al. 1995). Also, features which are less obvious in the circular geometry may be accentuated in the square geometry (Okajima 1982). Kumar et al. (2008) reported that square columns tend to fix the separation point, which increases the shedding frequency and hydrodynamic force. The separation mechanism also was greatly different from the flow around the circular columns. Generally speaking, the flow behaviour around square and rectangular columns is more complicated than flow around a circular column. However, the flow around a sharp-edged column has received far less attention than the flow around circular columns (Lyn et al. 1995, Kumar et al. 2008).

Okajima (1982) reported that variation of the width-to-depth (width is the normal to the flow direction, and depth is parallel to the flow direction) ratio of a square column is closely correlated with changes in the flow pattern. The flow pattern around a square or rectangular column is dependent on the Reynolds number for a sharp-edged object where the separation points are fixed at the leading edges or trailing edges (Figure 2.2 and Figure 2.3). The Okajima (1982) experiments measured the vortex-shedding frequencies of various rectangular columns to investigate how Strouhal number varies with width-to-depth ratio in a range of Reynolds number ($R_e=UH/\nu$ where U is velocity, H is depth of column and ν is kinematic viscosity) between 70 and 2×10^4. Strouhal number is defined as:

$$S_t = \frac{fD}{U} \tag{2.8}$$

where : f is the frequency of vortex shedding, D is diameter of the cylinder and U is the average flow velocity. The experiments showed that the wake velocity fluctuates in a

fairly sinusoidal pattern and Strouhal numbers of a square column have slight and continuous change around a constant value in the wide range of R_e = 100 to 2 x10^4. These findings have been verified by Turki et al. (2003). When R_e = 80, the flow has been calculated to separate just at the trailing edge (Daiguji and Kobayashi 1981). When R_e = 150, the flow is separated at the leading edge and is seen to detach itself on either the upper or the lower surface (Okajima 1982). When there are incidence angle θ between the square column and flow direction, there are still some wake and vortex shedding behind the columns with the different drag coefficient comparing to the no incidence angle situation. For incidence angle θ = 0, the coefficient is 1.05 when Reynolds number is more than 10^4; and for incidence angle θ = 45, the coefficient is 0.8 with the same Reynolds number (Bruce et al. 2002).

The study of uniform flow around a cylindrical obstacle has a lot of detailed information pertaining to it in the literature. The above paragraphs described some previous and current studies on the behaviour of flow around individual columns and groups of columns including variation in flow behaviour with different Reynolds numbers. It is seen that the flow behavior around the cylinder (square column) is complex. At lower Reynolds numbers, there is no discernible vortex shedding from the trailing edge of the column; at higher Reynolds numbers, there is vortex shedding rolling up behind the square column while the flow separation starts at the leading edge of the column.

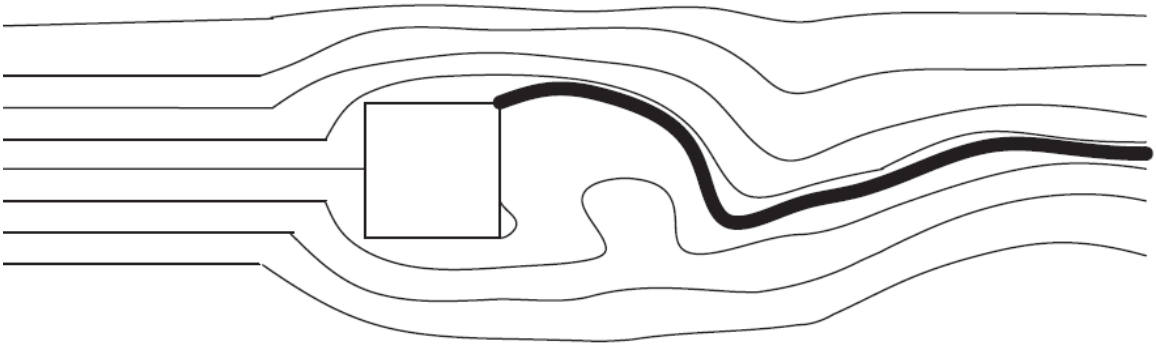

Figure 2.2 Flow pattern for a square cylinder at Reynolds number 80 (adapted from Daiguji and Kobayashi 1981).

Figure 2.3 Flow pattern for a square cylinder at Reynolds number 150 (adapted from Okajima 1982).

CHAPTER 3: DEVELOPMENT OF THE PHYSICAL MODEL, EXPERIMENTAL SETUP, AND TESTING PROGRAM

3.1 Background

The Glenmore Water Treatment Plant (GWTP) clearwell consists of two parts: the southwest (SW) cell and the northeast (NE) cell. Preceding the northeast cell of the clearwell, the flow moves from the treatment plant through a box culvert about 1.83 m high and 1.22 m wide, which is about 300 m upstream of the inlet gate structure to the clearwell. Fluoride is injected into the flow just upstream of the culvert. The flow then moves over a weir and enters into a large chamber. Next, it moves through a perforated baffle wall with circular openings of 400 mm diameter and then through a system of serpentine baffles through the main portion of the clearwell. Finally, the flow then moves into the southeast cell of the reservoir by flowing over another weir. The research presented herein focuses on the northeast cell of the clearwell, for which tracer studies have been carried out for three flow rates by Maksymetz (1998).

In the Maksymetz (1998) tracer tests, the northeast cell of the clearwell was studied over the full range of operating conditions. The minimum and maximum operating flow rates were 115 ML/d and 390 ML/d, respectively. One intermediate flow of 280 ML/d was also tested. These flows correspond to flow depths near the outlet of the northeast portion of clearwell of 5.91, 6.00 and 5.96 m, respectively. For these prototype tracer studies, when the flow rate through the reservoir reached steady-state, the supply of fluoride to the clearwell was shut off at the injectors. This marked the start of the tracer test. The decrease in concentration of fluoride with time was monitored at the end of the NE cell. Five sample lines near the weir at the outlet of the cell were placed vertically at a 1 m spacing to collect samples at a typical frequency of every 10 minutes. The three tests ran 313, 122, and 92 minutes duration for the flow rates of 115 ML/d, 280 ML/d and 390 ML/d, respectively. From the tracer test data, the cumulative residence time curves were developed from which the baffle factors were assessed. The estimate error of prototype data was ± 2.5 % over the three flow rate.

For the experiments described herein, a scale physical model of the NE cell of the Glenmore clearwell was set up and tested using tracer studies and flow visualization. Tests were conducted under flow conditions to model the prototype tests described above, plus one other intermediate flow. Test flows were selected according to the guidelines for testing reservoirs specified by USEPA (1989). For the experiments, the physical model of the reservoir was run with and without the many structural columns in the clearwell. These physical model studies were followed by a study using the software River2DMix to model the flow and retention times in the model clearwell under the same conditions.

This chapter gives the details of the development, construction, and operation of the hydraulic model. Next, the tracer tests run in the model are described, including the method of preparation of tracer used in the experiments, the calibration of the instrument used to measure the concentration of the tracer, and how these measurements were taken. It also gives details of the test program. Finally, some details are given about how the computational model River2DMix was set up to simulate the flow behaviour in the model clearwell.

3.2 Hydraulic Model

3.2.1 Development of Physical Model

Hydraulic models have a scaled-down geometry of the actual structure (prototype). In order to fairly represent the physical processes in a hydraulic system, the dimensions of a physical model compared to the prototype must be chosen based on the principles of similitude (ASCE 2000).

As discussed in Chapter 2, the hydraulic model of the clearwell can be considered a Froude model. For the model clearwell, the Reynolds number also needs to be high enough to create a turbulent jet through the perforated baffle wall at the entrance of the reservoir and to ensure turbulent flow within the reservoir. For the flow through the perforated baffle wall at the inlet, it is known that a jet Reynolds number R_i = 500 is about the lowest R_i that will create a turbulent jet (Rajaratnam and Flint-Peterson 1989). The Reynolds number is $R_i = U_i D/\nu$, where U_i is the average velocity of flow through the

holes of the perforated baffle wall, D is the diameter of one of the holes in this wall (the hole size is constant in the wall), and v is the kinematic viscosity of the fluid. Rajaratnam and Flint-Peterson (1989) note that although the minimum Reynolds number for turbulence for a single circular free jet is about 500, the growth of the jet does not depend on Reynolds number for about R_i >10,000. Meanwhile, the flow within the reservoir must also be in the turbulent range. The Reynolds number of the flow in the reservoir is expressed as $R_r = 4VR_h/v$, where V is the average velocity of flow in the reservoir through the section of interest and R_h is the hydraulic radius, where $R_h = A/P$ and A and P are the cross-sectional area and wetted perimeter of the flow, respectively. R_r has to be larger than 2000 to ensure turbulent flow (Jain 2001). The Reynolds number of column is $Re_D = VD_c/v$, where D_c is the square column diameter (width). In model design, the Reynolds number for columns was neglected.

Based on a desired minimum reservoir Reynolds number R_r of 2000 and space and flow handling limitations in the Hydraulics Laboratory at the University of Saskatchewan, an undistorted scale model of 1:19 was chosen. In the model tests, R_r then varied from 2011 to 6776 and the R_i for the perforated baffle wall varied from 1240 to 4200. Although the Reynolds numbers for the jet is not in the range of R_i >10,000, where the growth of a turbulent jet does not depend on R_i, the several jets that move through the perforated baffle wall will quickly merge together. Thus, the growth rate of an individual jet is less important. Table 3.1 gives a comparison of the Glenmore clearwell and physical model parameters for the minimum and maximum flow rate. At the 1:19 scale, the flow rates of 115 ML/d, 280 ML/d and 390 ML/d give model flow rates of 0.85, 2.06, and 2.87 L/s, respectively. The depths of 5.91, 5.96, and 6.00 m in the actual clearwell gave respective depths of 0.311, 0.314, and 0.316 m in the scale model. This corresponds to Froude numbers in the clearwell through the widest channel from 0.002 to 0.008.

3.2.2 Construction of Physical Model

A 1:19 scale model of the Glenmore Reservoir NE cell was constructed in the Hydraulics Laboratory of the University of Saskatchewan. It was constructed of plywood, which was waterproofed using oil based primer and glossy oil paint. Figure 3.1 shows

the schematic layout of the physical model with columns. Information on the layout of the reservoir was available from drawings provided by the City of Calgary. Figure 3.2 shows a photograph of the model without the columns. The model included a

Table 3.1 Glenmore Water Treatment Plant clearwell and hydraulic model parameters

Parameters	Prototype	Physical model
Width of Widest Channel, W (mm)	16200	853
Highest Flow Rate (ML/D)	390	0.248
Highest Flow Rate (L/s)	4514	2.868
High Flow Depth (m)	6	0.316
Average Velocity at Highest Flow Rate in Widest Channel (m/s)	0.0464	0.0107
Minimum Flow Rate (ML/D)	115	0.073
Minimum Flow Rate (L/s)	1331	0.846
Minimum Flow Depth (m)	5.91	0.311
Average Velocity at Minimum Flow Rate in Widest Channel (m/s)	0.0139	0.0031
Reynolds No. R_r (Minimum - Maximum)	1.5E+05 - 5.6E+05	2011 - 6776
Reynolds No. R_i (Minimum - Maximum)	1.03E+05 - 3.5E+05	1240 - 4200
Reynolds No. Re_D (Minimum - Maximum)	4.8E+03 - 1.6E+04	59 - 197

perforated baffle wall at the inlet (Figure 3.3(a)) and three serpentine intra-baffle walls as shown in Figure 3.1. There was a bit of difference between the prototype baffle wall (Figure 3.3 (b)) and one used in the physical model. The height of the baffle wall used in the physical model was higher than the height of the prototype baffle wall scaled down in terms to 1:19 with 184 mm difference. Due to these change, the flow was jet flow after it passed through the perforate baffle wall in the physical model. However, in the prototype clearwell, the top parts flow over the perforated baffle wall is overflow and rest of flow below that is the jet flow through the perforated baffle wall. The change have no effect on the test results, because the purpose of two type perforated wall is to make fully mixing in width and depth direction of channel at the beginning of the channel. There is a sharp-crested rectangular weir at the clearwell outlet that was used to adjust the flow depth in the reservoir. In order to allow visualization of the tracer movement using photographs or video of the tests, a 100 mm x 100 mm grid of black twine was attached

on top of the model. A camera or video recorder was suspended above the model for taking pictures or video used for flow visualization.

Based on the research objectives, there were two separate test conditions for the model: without the structural columns and with the columns. For the second phase of the experiments, when the columns were added, there were 122 columns fixed to the floor of the model at locations simulating the Calgary Glenmore Water Treatment Plant northeast cell as shown in Figure 3.1. The square columns were 19 mm a side in the model corresponding to the actual columns that were 400 mm a side. The model columns were also painted with oil-based primer and glossy oil paint. As well, the columns were covered with a plastic screen to increase the roughness of the columns in hopes of increasing some of additional turbulence that might be seen at full-scale (Krogstad et al. 1992; Zdravkovich 1997).

In the physical model, the water enters the clearwell after passing through an inlet flow chamber (Figure 3.4). A diffuser (Figure 3.5(a) and (b)) was designed and used to evenly distribute the flow rate into the model clearwell across the channel and was set 250 mm upstream of the perforated baffle wall. The diffuser was set at two-thirds the depth of water in the inlet chamber and the centres of the holes in the diffuser were set about 105 mm from the floor of the inlet chamber. The perforated baffle wall separated this chamber from the rest of the clearwell. Flow passed through the baffle wall and into the serpentine baffle system of the clearwell. To exit the model clearwell, the flow passed over the weir at the outlet of the clearwell and dropped into another chamber. Two gate valves of 76.2 mm diameter were attached to the wall of this chamber. These valves were used to control whether the flow moved to the sewer or entered a tank used for volumetric measurements of flow.

3.2.3 Operation of the Model and Tracer Tests

As noted in the previous section, in operating the model, water was pumped into a diffuser set in the inlet chamber before the baffle wall. A valve was used to control the inflow rate and a rotameter made by Muis Control Ltd (Model 7205-0211-33W,

maximum capacity 190 Lpm, 6 % accuracy at full scale) was used to set the flow rate for a test (Figure 3.6 (a)). This flow measurement was checked by collecting the overflowing water using a known volume and measuring the time to fill a 125 L

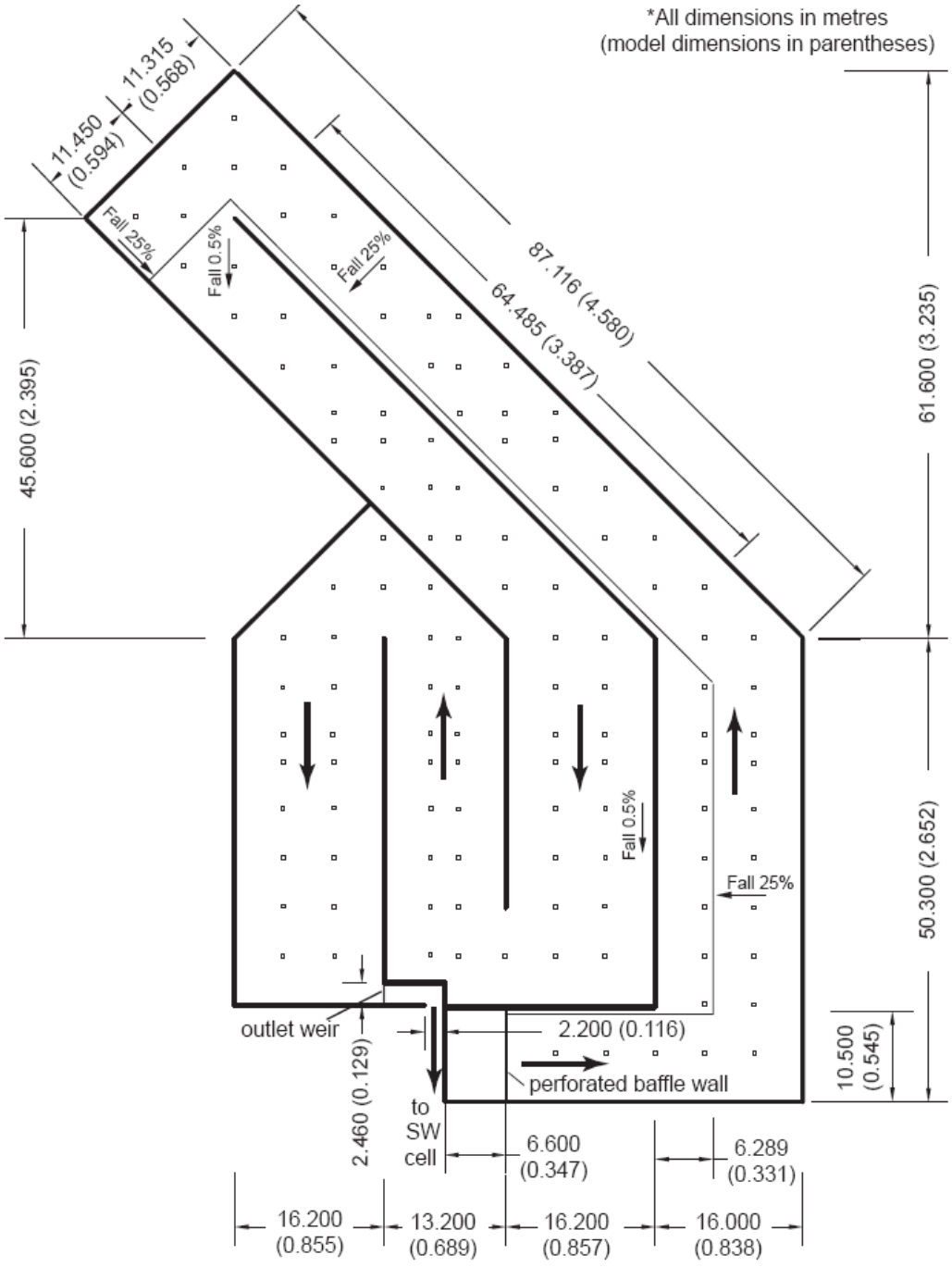

Figure 3.1 Plan view NE Cell of the Calgary Glenmore Water Treatment Plant Clearwell (prototype and model dimensions in metres).

(a)

(b)

Figure 3.2 Physical model of NE cell without the columns (a) looking from the inlet/outlet end of the reservoir and (b) looking at the serpentine baffling from the opposite end of the reservoir.

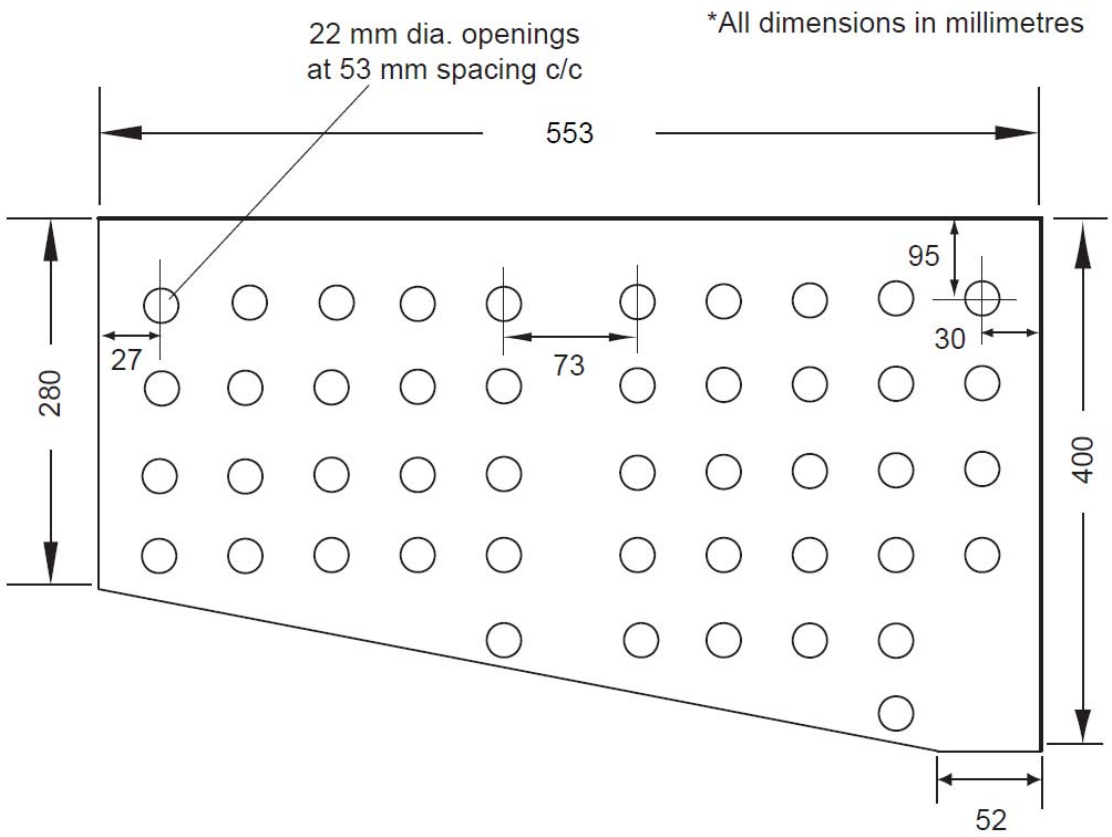

(a)

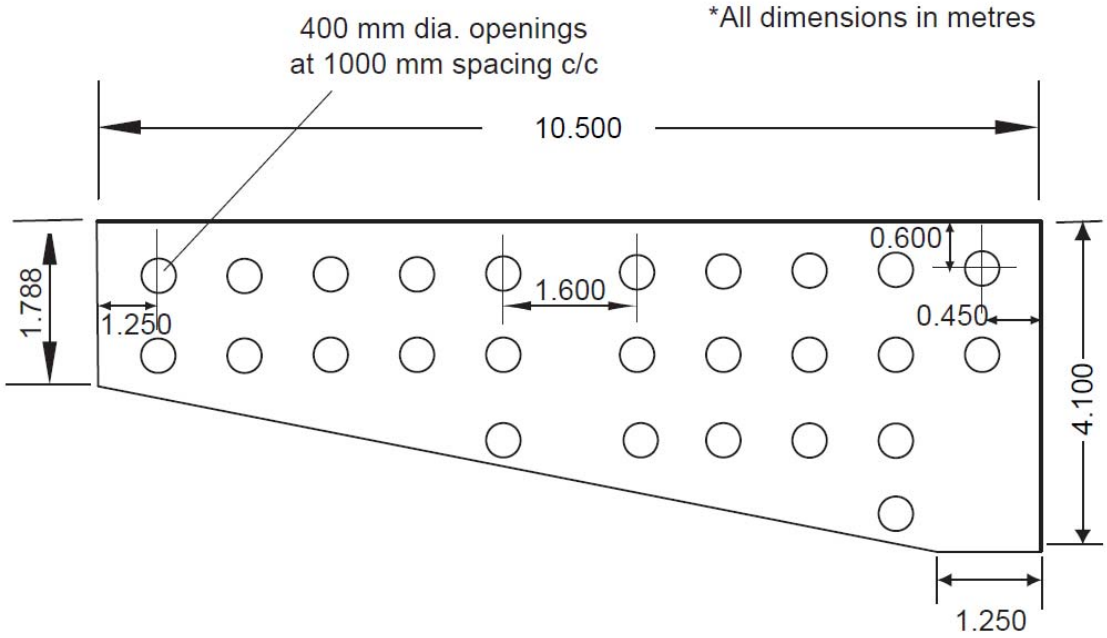

(b)

Figure 3.3 Perforated baffle wall (a) in the scale model looking from downstream of the inlet (b) in the prototype.

Figure 3.4 Diffuser and inlet chamber of the physical model.

container (Figure 3.6 (b)). To avoid build-up of the background concentration of tracer, water was not recirculated in the model. For the experiments without columns, the water was pumped into the model from the sump of the Hydraulics Lab. The tests were run when the temperature of the water in the model was approximately 15-26°C. For the second set of tests when the model was run with columns, the water was supplied by pumping from a steel tank that was fed continuously with tap water. There was no technical reason to change the way that water was supplied to the reservoir. However, the second method of supplying water allowed the model to operate independently of the activities of the other students in the laboratory. And the tests in the second method were implemented after the experiments without columns were completed.

One issue that arose during testing was the length of time required for the model to operate before the tracer tests were initiated. Initially, the tracer tests were conducted after about 1 h of operation of the model. Initial tracer study results at the lowest flow

rate showed a markedly lower baffle factor in the model than the prototype (detailed results are given in Chapter 4). In investigating potential explanations for this difference, it was found the time allowed for flow development before the tracer test was initiated could strongly affect results. Flow development time thus became another variable for the tests.

For the tracer tests, two methods were chosen to input the tracer: as a slug, and as a continuous feed. For the slug input of tracer, three 140 cc syringes filled with the required amounts of Rhodamine WT (175 ppm) were set at a height of half the water depth. The syringes were quickly pushed simultaneously to almost instantaneously inject tracer into the tank just upstream of the perforated baffle wall. For the continuous feed tests a peristaltic pump with flow rate of 1.25 mL/s was used to continuously pump a specified concentration (100 ppm) of Rhodamine WT from a vessel of known volume into the flow through a small tube connected to the pipe just upstream of the diffuser (see Figure 3.5(b)).

Samples for assessing the concentration of tracer at the clearwell outlet were taken by continuously drawing fluid from just above the weir through a fluorometer (Turner Designs Model 10) using a peristaltic pump (Figure 3.7). The fluorometer was connected to a data acquisition system that used LabView software to record the concentration every 5 seconds. Other measurements during a tracer test included the pump delay time for the sampling flow to move between the sampling point at the reservoir outlet and the fluorometer detection cell, and the test temperature. Hudson (1975) recommended that at least two theoretical detention time periods be used to monitor a tracer test and suggested that three or four theoretical detention times may be required to ensure complete recovery of the tracer. Therefore the duration used for each tracer test was three theoretical detention times.

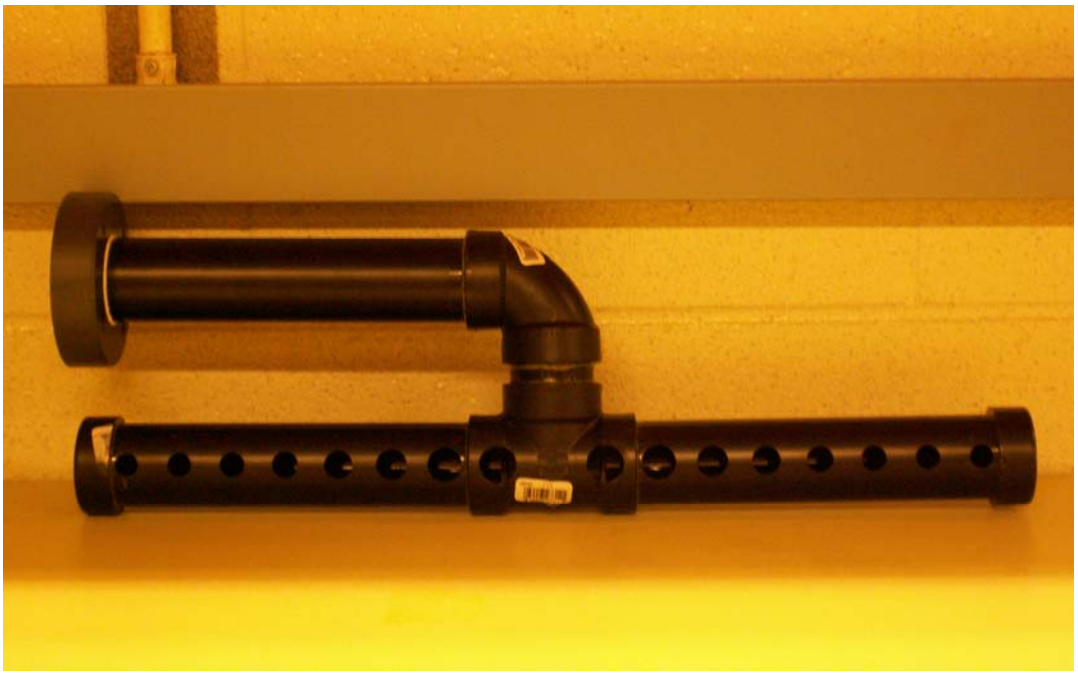

(a)

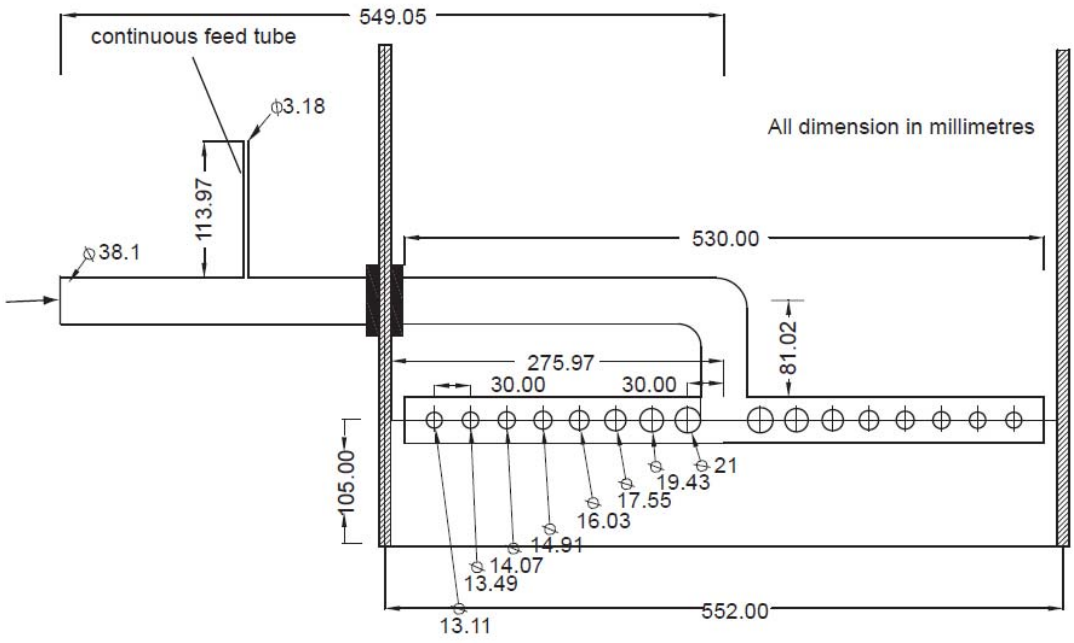

(b)

Figure 3.5 Diffuser (a) side view (b) dimensions.

(a)

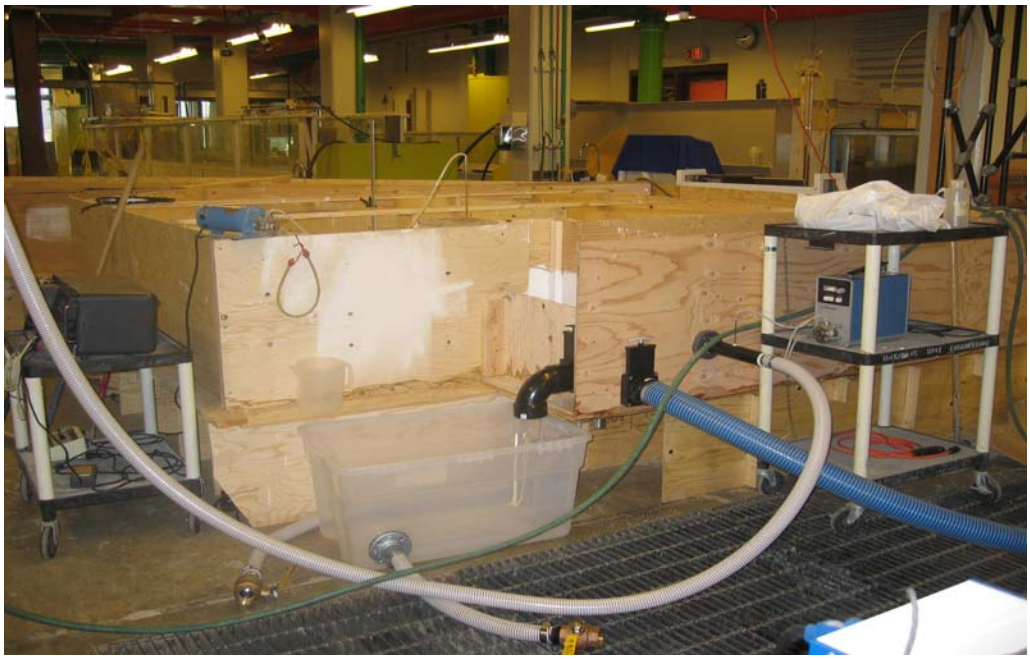

(b)

Figure 3.6 (a) Rotameter used for flow measurements and (b) tank used for volumetric flow measurements.

Figure 3.7 Fluorometer (Turner Designs Model 10) used in tracer tests.

3.3 Test Program

For the experiments, the test variables included the flow rate, the flow development time, and whether or not the structural columns were present in the model. Table 3.2 summaries the details of the testing program. In Experiments 1-6, three trials under the same hydraulic conditions (same flow rate Q = 2.06 L/s and depth of 0.314 m, without columns) were conducted each for the slug and the continuous feed tracer additions to test for repeatability and to decide which tracer feed gave the most consistent results. These tests were conducted allowing for a flow development time of only one hour. Since the slug feed produced the most consistent results and was easier to implement, this method of tracer addition was used for the rest of the tests. Finally, the mass recovery was computed for each tracer test experiment to investigate the quality of the tracer test according to Liem et al. (1999).

3.4 Flow Visualization

Flow visualization tests were conducted to assess the flow pattern in the model clearwell. These tests provided information to be able to delineate the main flow channel and dead zones in the model. For the visualization tests, a slug of dissolved potassium

permanganate was added to the flow and a video camera that was suspended above the model was used to take pictures of the coloured flow. To visualize the flow contours at the inlet area of the model, a slug of dye was dumped into the flow upstream of the perforated baffle wall. However, this dye plume dispersed too quickly to make observation further downstream in the model. Therefore, dye was also injected across the width of channel just upstream of five other locations of interest along the flow in the clearwell. All flow visualization tests were run as separate tests from the tracer tests. Table 3.2 shows the experimental conditions for which flow visualization tests were carried out.

To better identify the dead zone in the clearwell of physical model, the sketch of the line of dead zone and circulation area was drawn at the same time as the dye injected into the flow (see example Figure 3.8). The layout of clearwell of physical model with the 100 mm x 100 mm reference line was used to delineate the circulation zone while dye moving downstream with the flow. There were tab fixed on the twine on the top of the physical model with 500 mm space as the marker to identify the location of dye when it moving, then found the same location on the layout of clearwell of the physical model. These sketches were combined with the images from the video mentioned above, and finally provided the dead zones in the clearwell of the physical model.

Table 3.2 Master table of the Glenmore WTP NE Clearwell model study test program

Test No.	Flow Development Time (Hours)	Tracer Input	Model Condition*	Prototype Flow Rate (m^3/s)	Depth of Prototype Flow (m)	Model Flow Rate (L/s)	Depth of Model Flow (m)	Average Reservoir Velocity (m/s)	Reservoir Reynolds Number (R_r)	Reservoir Froude Number (F_r)	River2DMix Simulated (#)
1	1	s	N	3.24	5.97	2.06	0.314	0.0076	4875	0.006	
2	1	s	N	3.24	5.97	2.06	0.314	0.0076	4875	0.006	
3	1	s	N*	3.24	5.97	2.06	0.314	0.0076	4875	0.006	
4	1	c	N	3.24	5.97	2.06	0.314	0.0076	4875	0.006	
5	1	c	N	3.24	5.97	2.06	0.314	0.0076	4875	0.006	
6	1	c	N	3.24	5.97	2.06	0.314	0.0076	4875	0.006	
7	1	s	N*	4.51	6.00	2.87	0.316	0.0107	6776	0.008	
8	1	s	N*	1.97	5.95	1.25	0.313	0.0047	2964	0.004	
9	1	s	N	1.33	5.91	0.85	0.311	0.0032	2011	0.002	
10	1	s	N*	1.33	5.91	0.85	0.311	0.0032	2011	0.002	
11	1	s	N	1.33	5.91	0.85	0.311	0.0032	2011	0.002	
12	3.5	s	N*	1.33	5.91	0.85	0.311	0.0032	2011	0.002	
13	7	s	N*	1.33	5.91	0.85	0.311	0.0032	2011	0.002	
14	10.5	s	N*	1.33	5.91	0.85	0.311	0.0032	2011	0.002	#
15	14	s	N	1.33	5.91	0.85	0.311	0.0032	2011	0.002	
16	14	s	N*	1.33	5.91	0.85	0.311	0.0032	2011	0.002	
17	30	s	N	1.33	5.91	0.85	0.311	0.0032	2011	0.002	

Table 3.2 cont'd

Test No.	Flow Development Time (Hours)	Tracer Input	Model Condition*	Prototype Flow Rate (m^3/s)	Depth of Prototype Flow (m)	Model Flow Rate (L/s)	Depth of Model Flow (m)	Average Reservoir Velocity (m/s)	Reservoir Reynolds Number (R_r)	Reservoir Froude Number (F_r)	River2DMix Simulated (#)
18	4	s	N*	4.51	6.00	2.87	0.316	0.0107	6776	0.008	#
19	5	s	N*	3.24	5.97	2.06	0.314	0.0076	4875	0.006	#
20	9	s	N*	1.97	5.95	1.25	0.313	0.0047	2964	0.004	
21	1	s	FW.*	1.33	5.91	0.85	0.311	0.0032	2011	0.002	
22	3.5	s	FW.*	1.33	5.91	0.85	0.311	0.0032	2011	0.002	
23	7	s	FW.*	1.33	5.91	0.85	0.311	0.0032	2011	0.002	
24	10.5	s	FW.*	1.33	5.91	0.85	0.311	0.0032	2011	0.002	#
25	14	s	FW.*	1.33	5.91	0.85	0.311	0.0032	2011	0.002	
26	1	s	FW.*	4.51	6.00	2.87	0.316	0.0107	6776	0.008	
27	1	s	FW.*	3.24	5.97	2.06	0.314	0.0076	4875	0.006	
28	1	s	FW.*	1.97	5.95	1.25	0.313	0.0047	2964	0.004	
29	4	s	FW.*	4.51	6.00	2.87	0.316	0.0107	6776	0.008	#
30	5	s	FW.*	3.24	5.97	2.06	0.314	0.0076	4875	0.006	#
31	9	s	FW.*	1.97	5.95	1.25	0.313	0.0047	2964	0.004	

FW= With full columns; N= Without columns; s= Slug test; c= Continuous test; *= Flow visualization test conducted; #= simulated by River2DMix

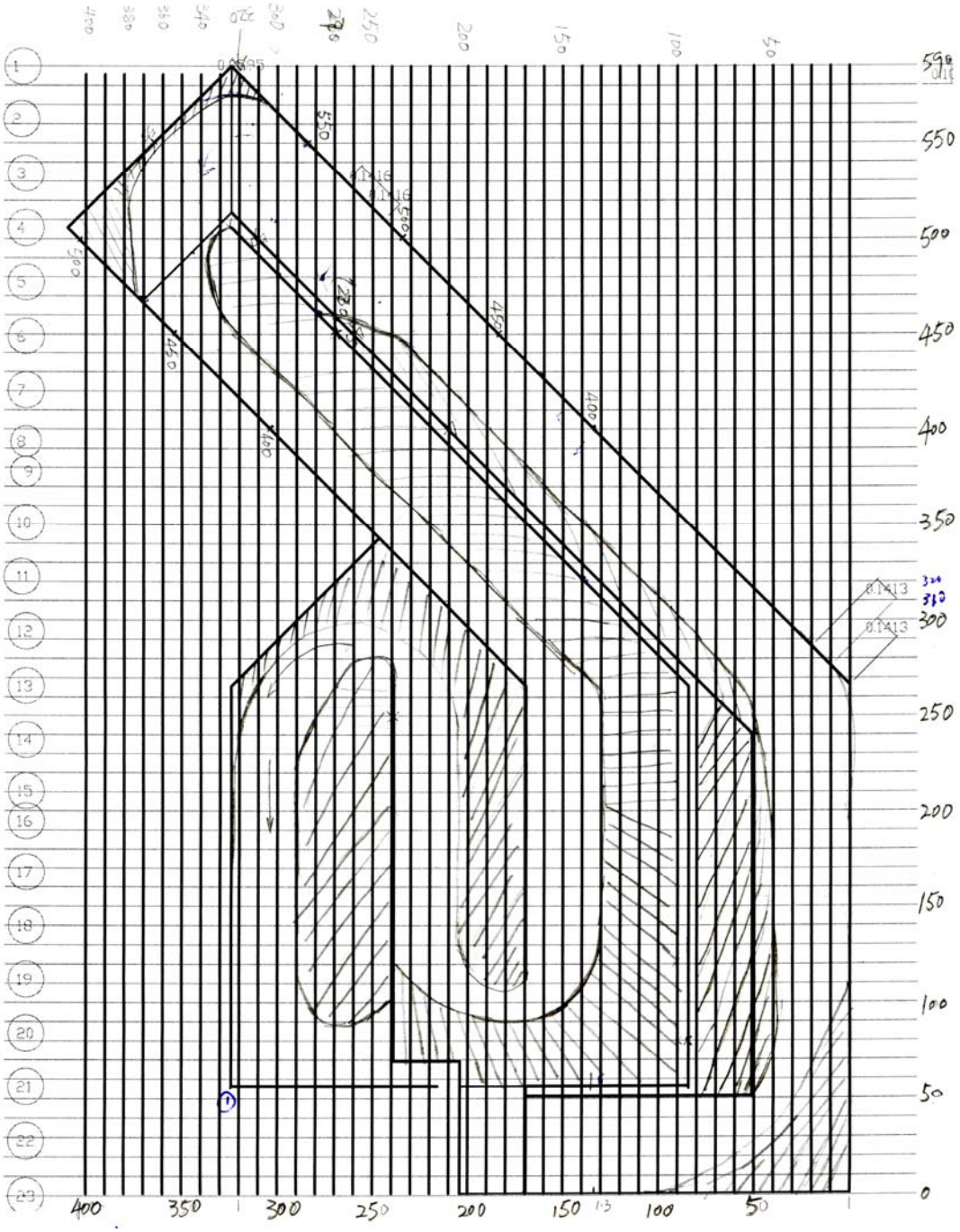

Figure 3.8 Sketch of dead zone of clearwell of physical model used in the flow visualization test.

3.5 Selection and Preparation of Tracer for Tracer Study Tests

For the experiments, Rhodamine WT (concentration of 20% by weight with a specific gravity of 1.19) was used as the tracer since it is a commonly used chemical and meets the requirements that it is non-toxic, economical, and detectable in low

concentrations (Wilson et al. 1986). The tracer was prepared by diluting concentrated liquid Rhodamine WT with distilled water. The standard for fluorometer calibration (100 ppb) and the injection solution for test tracers (175000 ppb) were prepared step-by-step by making serial dilutions of the stock Rhodamine WT liquid (20% by weight, SG 1.19). The dilution concentration was computed following the equation

$$C_n = C_i\left[\frac{V_d}{V_w + V_d}\right] \tag{3.1}$$

where V_w = volume of the added diluent; V_d = pipette volume of the dye solution; C_i = initial concentration; and C_n = new concentration after each dilution step. Table 3.3 gives details of the three-step of serial dilution preparations.

Table 3.3 Serial dilutions for preparation of working tracer solutions

Dye used in test	Serial dilutions (mL)						Working solution (ppb, ug/L)
	First step (Dilution 1)		Second step (Dilution 2)		Third step (Dilution 3)		Final dilution (Dilution 3)
Rhodamine WT (20%, SG 1.19)	V_d	V_d+V_w	V_d	V_d+V_w	V_d	V_d+V_w	
	5	1000	10	1000	10	1000	100
	10	500	43.75	1000			175000

To get the 100 ppb working solution, the serial dilution procedure was carried out as follows: (1) add distilled water into 5 mL Rhodamine WT to get 1000 mL total volume (Dilution 1); (2) took out 10 mL of Dilution 1, added distilled water to get 1000 mL total volume (Dilution 2); (3) took 10 mL of Dilution 2, added distilled water again to get 1000 mL total volume (Dilution 3). The working solution at 175000 ppb was prepared using the same procedures but with different values of V_d and V_w as shown in Table 3.3. To avoid concentration stratification, all final solutions were agitated until each was thoroughly mixed. All working solutions were retained in an airtight bottle and were stored in a dark place to avoid degradation by UV light.

3.6 Fluorometer Calibration

In this study, a Turner Designs Model 10-AU Fluorometer was used for the tests to measure tracer concentration. The detection limits of the Turner Model 10-AU can be as low as 0.01 ppb and as high as 100 ppb (Turner Designs 1993). The calibration procedure for this fluorometer consist of two steps: (1) running the "blank", which is the matrix of the background solution that is used to set the instrument to read zero; and (2) adjusting the fluorometer to read out a known concentration of sample called the standard. For the present experiments, the blank was taken as the tap water which was used to fill the physical model. Once the fluorometer warmed for at least 30 minutes, the fluorometer calibration process was started. First, the background concentration influence on the final concentration readout was eliminated by running the blank solution and choosing "subtract blank" on the instrument. Secondly, the standard solution was used to adjust the span and instrument sensitivity until the reading on the full scale value was 100 ppb. After calibration of the fluorometer, the readout on the screen of the fluorometer is the concentration of Rhodamine in the sample without influence of any background concentration in the water. Note it was recommended to keep the calibration within fluorometer specifications during the tests (Turner Designs 1993).

3.7 Modeling with River2DMix

3.7.1 Background

The second aspect of this research project was to develop a computational model of the NE part of the Glenmore Water Treatment Plant clearwell at the same scale as the physical model using River2DMix software developed at the University of Alberta. River2DMix was used to simulate the flow field in the clearwell and to predict the cumulative residence time distribution curve of a tracer in the clearwell. The model was run for conditions with and without columns in the clearwell. The River2DMix software is a modification of the River2D software developed to simulate the hydrodynamics of flow in a river. In River2D, the simulation results is related with the hydrodynamic part, like flow velocity, shear stress and flow pattern. In River2DMix, besides the hydrodynamic results same as River2D, it also has the mixing results of a tracer like residence time distribution.

The two-dimensional depth-averaged River2D software simulates the governing equations of flow based on a finite element approach. Some key assumptions in the model are hydrostatic pressure distribution in the vertical, constant horizontal velocities over the depth and negligible Coriolis and wind forces. Steffler and Blackburn (2002) describe the two-dimensional depth-averaged St. Venant equations of the hydrodynamic model applied in River2D. The St. Venant equations are the transformation of the depth-averaged Reynolds equations and they are solved by a finite element method (Streamline Upwind Petrov-Galerkin Weighted Residual formulation) in River2D. The Streamline Upwind Petrov-Galerkin Weighted Residual formulation is a way to ensure solution stability under the different flow conditions by more weighting of an element upstream of a node comparing to the an element downstream of a node (Steffler and Blackburn 2002).

In River2D (Steffler and Blackburn 2002), the St. Venant equations include the two-dimensional; depth averaged conservation of mass, and the depth averaged, two-dimensional Reynolds equations (x and y direction). In equations, the depth and discharge intensities are basic variables.

Conservation of mass:

$$\frac{\partial H}{\partial t}+\frac{\partial q_x}{\partial x}+\frac{\partial q_y}{\partial y}=0 \tag{3.2}$$

Conservation of x-direction momentum:

$$\begin{aligned}&\frac{\partial q_x}{\partial t}+\frac{\partial}{\partial x}(Uq_x)+\frac{\partial}{\partial y}(Vq_x)+\frac{g}{2}\frac{\partial}{\partial x}H^2\\&=gH(S_{0x}-S_{fx})+\frac{1}{\rho}\left(\frac{\partial}{\partial x}\left(H\tau_{xx}\right)\right)+\frac{1}{\rho}\left(\frac{\partial}{\partial y}\left(H\tau_{xy}\right)\right)\end{aligned} \tag{3.3}$$

Conservation of y-direction momentum:

$$\begin{aligned}&\frac{\partial q_y}{\partial t}+\frac{\partial}{\partial x}(Uq_y)+\frac{\partial}{\partial y}(Vq_y)+\frac{g}{2}\frac{\partial}{\partial y}H^2\\&=gH(S_{0y}-S_{fy})+\frac{1}{\rho}\left(\frac{\partial}{\partial x}\left(H\tau_{yx}\right)\right)+\frac{1}{\rho}\left(\frac{\partial}{\partial y}\left(H\tau_{yy}\right)\right)\end{aligned} \tag{3.4}$$

Where H is the depth of flow, U and V are the depth averaged velocities in the x and y directions respectively, q_x and q_y are the respective discharge intensities, g is acceleration due to gravity and ρ is the density of water, S_{0x} and S_{0y} are the bed slopes in the x and y directions, S_{fx} and S_{fy} are corresponding friction slopes. The River2D (Steffler and Blackburn 2002) software uses a Bossinesq type eddy viscosity formulation for transverse turbulent shear stress (τ_{xy}). It is expressed as

$$\tau_{xy} = \nu_t \left(\frac{\partial U}{\partial y} + \frac{\partial V}{\partial x} \right) \tag{3.5}$$

ν_t is eddy viscosity given by

$$\nu_t = \varepsilon_1 + \varepsilon_2 \frac{H\sqrt{U^2 + V^2}}{C_*} + \varepsilon_3{}^2 h^2 \sqrt{2\left(\frac{\partial U}{\partial x}\right)^2 + \left(\frac{\partial U}{\partial y} + \frac{\partial V}{\partial x}\right)^2 + 2\left(\frac{\partial V}{\partial y}\right)^2} \tag{3.6}$$

Where $\varepsilon_1, \varepsilon_2, \varepsilon_3,$ represent the only user definable calibration coefficients, usually, $\varepsilon_1 = 0$. C_* is the dimensionless Chezy coefficient given by

$$C_* = \frac{1}{\kappa} \ln\left(12 \frac{h}{k_s}\right) \tag{3.7}$$

Where K is Von Karmen's constant and k_s is the equivalent sand grain roughness of the bed.

3.7.2 Building the Model

In order to run River2DMix, the bed topography files (a text file with a .bed file name extension) are first developed based on the position and elevation of the geometrical characteristics and bed roughness of the physical model of the NE clearwell. The file also includes the boundary conditions. The inflow boundary condition took the form of a specified total discharge (flow rate of 2.87 L/s, 2.06 L/s or 0.85 L/s) at the inflow section. The outflow boundary condition was specified as a fixed water depth (0.316 m, 0.314 m or 0.311 m) at the outlet of the clearwell. Another boundary condition that had to be specified was that there were no-flow vertical walls (no lateral discharge through the walls) and no-slip wall and columns. Each square was modeled as a conical frustum, in which the same presentation area to the flow for the frustum shapes as for the square column shape of the physical model. By this way, the same drag would be

experienced by both the physical model column and the simulated column. The frustum columns were 31.6 mm in width at the bed and 10.5 mm in width at the top. The resulting bed file was then input into "R2D_Mesh" to develop a computational discretization finite element mesh file. Figure 3.9 showed the mesh of computational model of scale clearwell under "without column" condition and Figure 3.10 showed the mesh of computational model of scale clearwell under "with column" condition. There are 4906 elements used under "without column" and 10,488 elements used under "with column" condition, respectively. The output of "R2D_Mesh" was used to generate the input files for the "River2DMix" model. Finally, the River2DMix program executed the hydrodynamic simulation until the inflow discharge was equal to the outflow discharge. Then, the tracer transport simulation was run once the fluid flow field was determined.

For the tracer transport simulations, there is a check box in "River2DMix" that is called the simple tracer mass initial condition specification. It is used to set the initial normalized tracer mass concentration equal to 1. The output of "River2DMix" is then the normalized concentration of tracer remaining in the clearwell. With water entering the River2DMix, inflow boundary have a concentration of zero. The normalized concentration of tracer exiting the clearwell is then equal to unit 1 minus the normalized concentration of tracer remaining in the clearwell**.**

3.7.3 Calibration of the River2DMix Model

In operating the "River2DMix" model, the hydrodynamic simulation portion of the program runs to reach convergence and a steady-state solution for the velocity field is obtained through iteration. Then, the tracer transport mixing model is run to provide the tracer cumulative residence time in the model. For the "River2DMix" model, a Bossinesq type eddy viscosity formulation is used for the transverse turbulent shear stress τ_{xy} and τ_{yx} in the hydrodynamic model and mixing model. τ_{xy} and τ_{yx} are estimated using the turbulent kinematic viscosity v_t. The v_t term includes the eddy viscosity coefficient, which is assumed to be composed of three components: a constant ε_1 (default value 0), a bed shear generated term ε_2, and transverse shear generated term ε_3 (Steffler and Blackburn 2002). All three components are adjustable parameters within the

hydrodynamic and mass transport simulation in River2DMix.

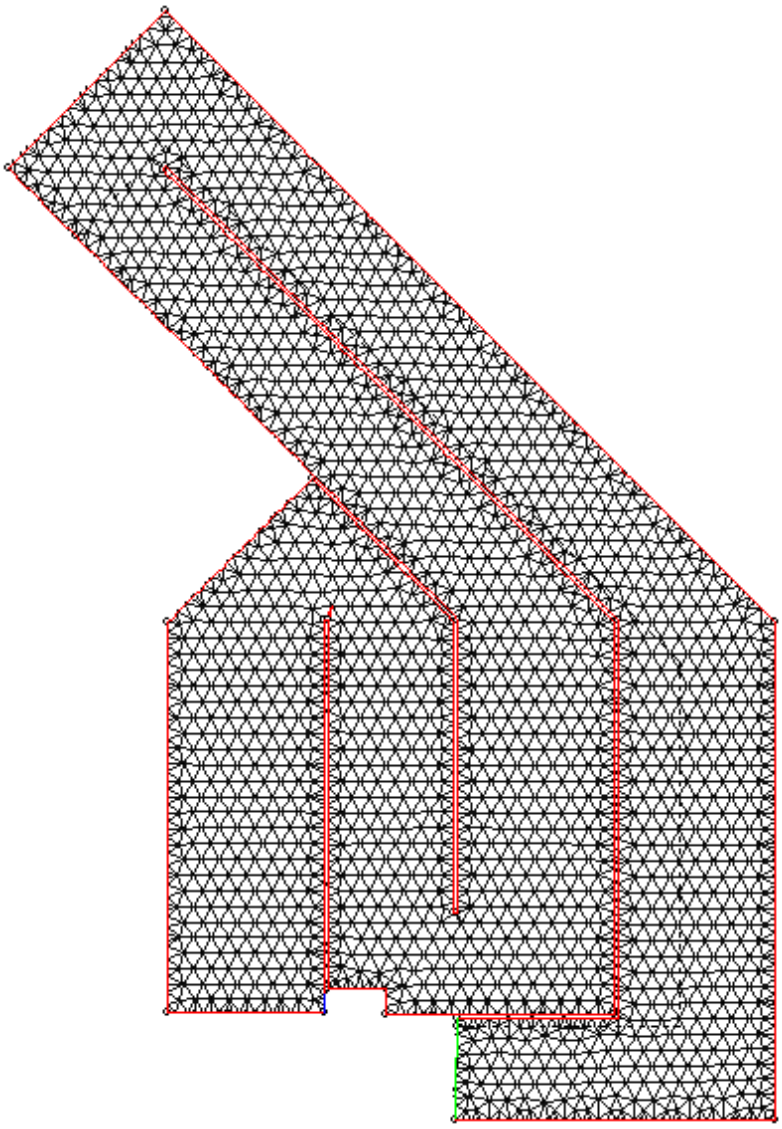

Figure 3.9 Full computational mesh used in computational model of scale clearwell under without columns condition.

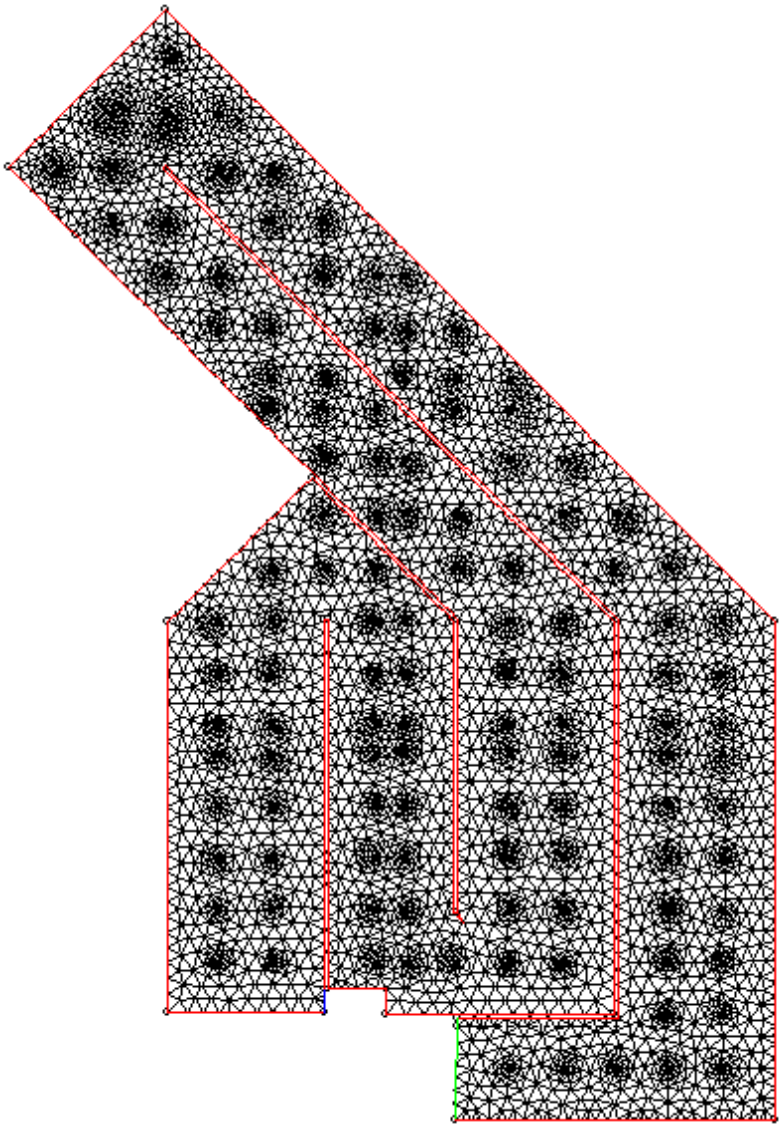

Figure 3.10 Full computational mesh used in computational model of scale clearwell under with columns condition.

River2DMix was first calibrated for the “without columns” condition and then for the “with columns” condition. For each case, the model was calibrated at both the minimum and maximum flows. A hydrodynamic and a mixing calibration were conducted for each condition. In the hydrodynamic calibration, the difference between the flow rate at the inlet and the flow at the outlet are minimized. In the hydrodynamic

calibration, first, initial values for ε_2 =0.2 and ε_3 =0.1 were set (based on the River2D manual). Then the velocity field was created by the hydrodynamic model and the minimum flow continuity tolerance in the hydrodynamic model is reached by adjusting ε_2. Then, for the mixing calibration, the cumulative RTD curve was compared to physical model results and the results of the simulation were improved by adjusting ε_3 but not ε_2. The goal was to minimize the root mean square error between the measured F(t) in the model and the simulated F(t) between the times corresponding to the start of the test to t_{99} on the F(t) curve. The time T_{99} is the time for 99 % of the tracer mass to exit the clearwell. Because there was no velocity distribution data to calibrate the model, the hydrodynamic and mixing calibration can only be validated using the tracer test data.

For the condition where the model had columns, the bed shear generated term ε_2 and transverse shear generated term ε_3 were adjusted to fit the physical model data as for the calibration process in the without columns condition. First, ε_3 was set to equal to the final value of ε_3 found for the without column simulation, then ε_2 was adjusted so that the outflow equalled the inflow. Albers et al. (2005) suggested that the bed shear generated term ε_2 is not sensitive to adjustments because turbulent bed shear resistance should be small compared to form drag generated as water flows past the structural columns. When calibrating the computational model under “with column condition”, the same procedure was taken as the one for “without columns condition”. The results of the calibration procedure and analysis are given in Chapter 4. The test conditions simulated using River2DMix are listed in Table 3.2.

CHAPTER 4: EXPERIMENTAL RESULS, ANALYSIS AND DISCUSSION

4.1. Introduction

In this chapter, the results of the experiments and the analysis of data are given. First, the methods of analysis for the tracer tests and flow visualization experiments are presented. Next, the repeatability of the experiments is discussed. Following this, the effect of flow development time and columns are given. Finally, the results of River2DMix are compared to the hydraulic model results.

4.2. Analysis of Data

4.2.1. Tracer Study Results

In order to present the results of the tracer tests, firstly there must be a discussion of how the tracer study data were analyzed. To determine the residence time distribution and associated baffle factor, the method for analyzing the concentration of tracer at the outlet with time discussed in Fogler (1992) was followed. In this method, for a slug input of tracer, the mass of tracer ΔN leaving the reservoir in a time period Δt is

$$\Delta N = \frac{1}{2}(C_t + C_{t+\Delta t})Q\Delta t \tag{4.1}$$

where C = concentration of tracer measured by the fluorometer; Q = flow rate; and t = time. If ΔN is summed over the test duration, the result should equal the total mass of tracer inputted into the reservoir, N_o. The ratio of this sum to N_o is called the mass recovery, which USEPA (1989) recommends should be greater than 90 % for a tracer test. The residence time distribution function $E(t)$ is given by

$$E(t) = \frac{\Delta N}{N_o \Delta t} \tag{4.2}$$

$E(t)$ is typically plotted against the dimensionless time t/T_d to show the residence time distribution for the reservoir. The fraction of the flow that has resided in the reservoir for a time shorter than time t is given by the cumulative residence time distribution $F(t)$, where

$$F(t) = \int_0^t E(t)\,dt \tag{4.3}$$

$F(t)$ is also plotted against t/T_d. As noted previously, the baffle factor is determined from the cumulative residence time distribution plot and is the time t/T_d for which $F(t) = 0.1$ (USEPA 1989). The Morril dispersion index is also determined from $F(t)$; it is the ratio T_{90}/T_{10}, where T_{90} is the time for $F(t) = 0.9$ and T_{10} is the time for $F(t) = 0.1$ (USEPA 1989).

4.2.2. Analysis of Data for Flow Visualization

For the flow visualization tests, the video recordings made during each visualization test were used to prepare still images of various sections of the model. The images were arranged together to form a composite image of the entire reservoir. In the visualization tests, firstly, a slug of dye was dumped into the flow upstream of the perforated baffle wall (same location as the tracer test). As the slug of dye advanced in the physical model, a video camera fixed on a movable support was used to track and record the movements of the dye plume front. The degree of color was used to identify the preferential flow paths. Dye in the channel indicated a preferential flow path since dead zone space had no visible colorimetric dye present. Because the dye plume dispersed as it moved downstream, it became increasingly more difficult to define the dead zones in the flow at the downstream end of the clearwell. Therefore, dye was also injected at five other sections, which were just upstream of each corner of the channel. These plumes were also videotaped to better identify the flow patterns and dead zones in that region of the model. For these tests the video camera was fixed in place above the corner of interest in the model to record the dead zone locations. Depending on the dye injection location and the time delay between dye injection and when the photograph was taken, preferential flow paths could be highlighted by dark or clear water.

4.3. Results

4.3.1. Assessment of Repeatability of Experiments

At the beginning of the study, tests were conducted to assess the repeatability of the experiments. In this study, three replicate tests were each carried out for the 0.85 and

2.06 L/s flows in the model (115 and 280 ML/d in the prototype). Figure 4.1 shows the residence time distributions (RTDs) for the replicate tests for the 0.85 L/s flow rate. Figure 4.2 shows the results for Q=2.06 L/s. For convenient reference, all the experimental analysis data and mass recovery have been included in Table 4.1.

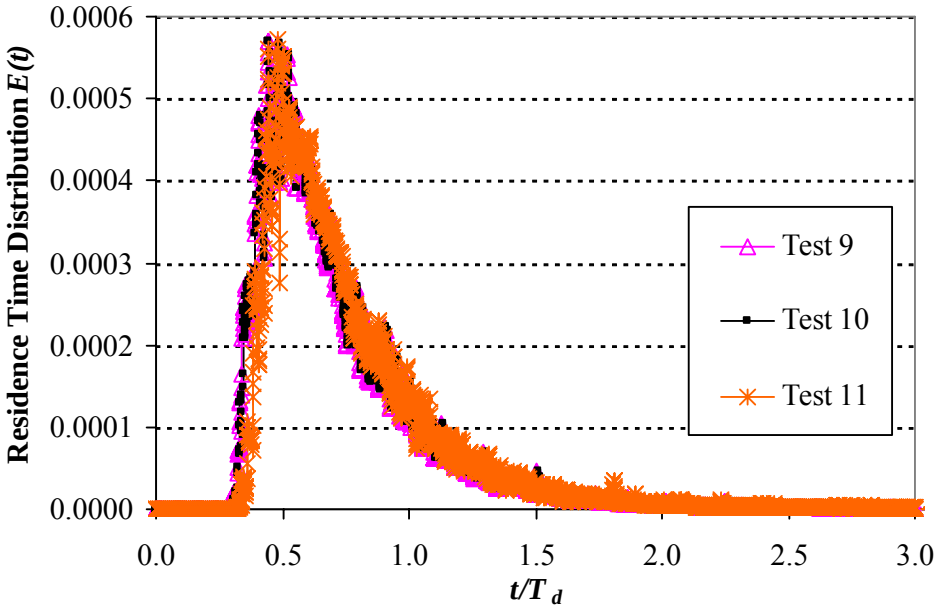

Figure 4.1 Residence Time Distribution for replicate experiments at 0.85 L/s in model (115 ML/d in prototype).

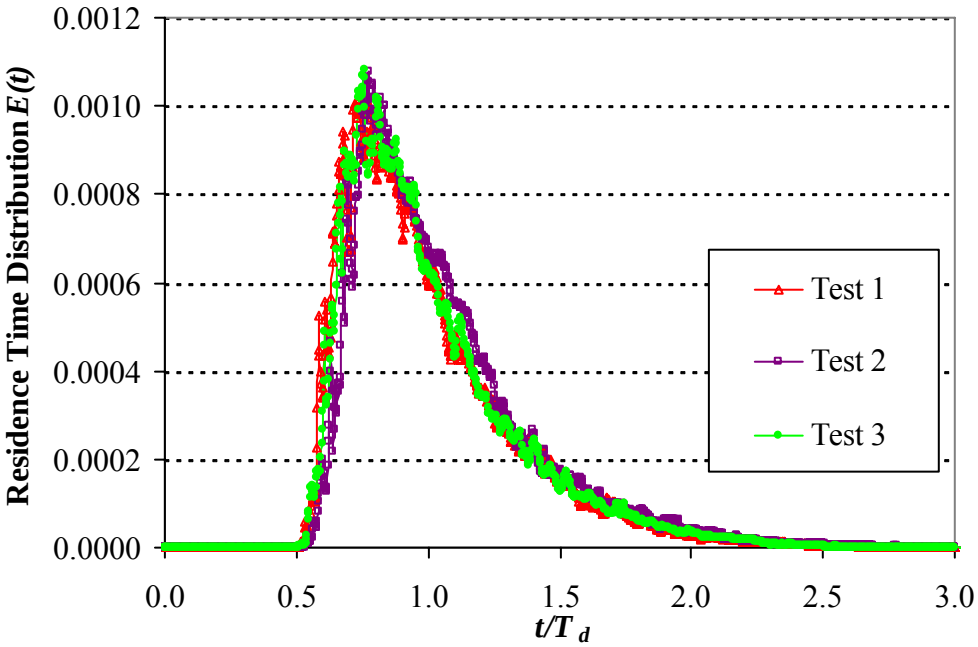

Figure 4.2 Residence Time Distribution for replicate experiments at 2.06 L/s in model (280 ML/d in prototype).

Table 4.1 Master table of physical model tracer test

Test NO.	Flow Development Time (Hours)	Tracer Input	Model Condition *	Prototype Flowrate (m^3/s)	Model Flowrate (L/s)	Test Date	T_{10}/T_d	T_{50}/T_d	T_{90}/T_d	T_{90}/T_{10}	Plug Flow Fraction (p)	Mixed Flow Fraction (m)	Dead Space Fraction (d)	Mass Recovery
1	1	s	N	3.24	2.06	5/3	0.67	0.92	1.46	2.19	39.76	21.28	38.96	119.5%
2	1	s	N	3.24	2.06	5/4	0.72	0.96	1.51	2.10	41.86	16.93	41.21	118.6%
3	1	s	N*	3.24	2.06	5/7	0.68	0.92	1.46	2.14	40.30	19.12	40.58	112.2%
4	1	c	N	3.24	2.06	5/11	0.72	0.98	1.53	2.12	~	~	~	~
5	1	c	N	3.24	2.06	5/15	0.71	0.99	1.55	2.18	~	~	~	~
6	1	c	N	3.24	2.06	5/23	0.74	1.02	1.65	2.22	~	~	~	~
7	1	s	N*	4.51	2.87	5/8	0.73	0.99	1.44	1.97	42.20	19.19	38.61	116.8%
8	1	s	N*	1.97	1.25	5/14	0.71	0.97	1.47	2.09	41.52	18.13	40.34	114.2%
9	1	s	N	1.33	0.85	5/1	0.41	0.63	1.14	2.77	29.08	15.46	55.46	117.4%
10	1	s	N*	1.33	0.85	5/2	0.42	0.63	1.15	2.77	29.58	15.31	55.11	118.4%
11	1	s	N	1.33	0.85	5/9	0.45	0.66	1.19	2.66	31.03	14.74	54.23	110.4%
12	3.5	s	N*	1.33	0.85	6/7	0.64	0.86	1.31	2.04	38.27	14.18	47.55	120.6%
13	7	s	N*	1.33	0.85	6/8	0.70	0.94	1.39	1.98	41.52	13.99	44.49	117.5%
14	10.5	s	N*	1.33	0.85	6/12	0.74	0.98	1.38	1.86	42.85	11.26	45.88	115.2%
15	14	s	N	1.33	0.85	6/5	0.74	0.96	1.40	1.90	42.53	13.91	43.56	114.7%
16	14	s	N*	1.33	0.85	6/6	0.75	0.97	1.40	1.88	42.85	12.87	44.27	115.9%
17	30	s	N	1.33	0.85	8/1	0.74	0.97	1.40	1.89	42.69	13.49	43.82	114.9%

Table 4.1 cont'd

Test NO.	Flow Development Time (Hours)	Tracer Input	Model Condition *	Prototype Flowrate (m^3/s)	Model Flowrate (L/s)	Test Date	T_{10}/T_d	T_{50}/T_d	T_{90}/T_d	T_{90}/T_{10}	Plug Flow Fraction (p)	Mixed Flow Fraction (m)	Dead Space Fraction (d)	Mass Recovery
18	4	s	N*	4.51	2.87	6/11	0.73	0.98	1.37	1.87	42.20	18.58	39.22	109.6%
19	5	s	N*	3.24	2.06	6/14	0.75	1.00	1.43	1.91	43.82	13.61	42.57	109.7%
20	9	s	N*	1.97	1.25	6/15	0.76	1.00	1.40	1.86	43.18	13.05	43.76	114.0%
21	1	s	FW.*	1.33	0.85	10/12	0.67	0.91	1.52	2.25	39.76	19.62	40.62	110.3%
22	3.5	s	FW.*	1.33	0.85	10/13	0.70	0.95	1.52	2.18	41.25	18.81	39.94	97.4%
23	7	s	FW.*	1.33	0.85	10/24	0.72	0.99	1.55	2.09	41.52	16.81	41.67	98.0%
24	10.5	s	FW.*	1.33	0.85	10/15	0.74	0.99	1.54	2.09	43.18	16.24	40.58	97.9%
25	14	s	FW.*	1.33	0.85	10/13	0.74	1.00	1.55	2.10	43.18	17.20	39.62	101.0%
26	1	s	FW.*	4.51	2.87	10/12	0.73	1.00	1.57	2.14	42.20	21.48	36.33	106.8%
27	1	s	FW.*	3.24	2.06	10/13	0.72	0.99	1.53	2.12	41.86	18.51	39.63	115.2%
28	1	s	FW.*	1.97	1.25	10/16	0.72	0.96	1.49	2.07	41.86	17.76	40.38	100.0%
29	4	s	FW.*	4.51	2.87	10/12	0.73	1.01	1.55	2.13	42.20	20.02	37.78	111.0%
30	5	s	FW.*	3.24	2.06	10/10	0.72	0.99	1.51	2.11	41.86	17.31	40.83	110.0%
31	9	s	FW.*	1.97	1.25	10/16	0.71	0.97	1.44	2.03	41.52	15.28	43.20	102.7%

FW= With full columns; N= Without columns; s= Slug test; c= Continuous test; *= Flow visualization test conducted.

The results show the RTD produced in the replicates are similar. For Q=0.85 L/s, the baffle factors(T_{10}/T_d) found from the tests were 0.41, 0.42, and 0.45 and the Morril dispersion indices(T_{90}/T_{10}) were 2.77, 2.77, and 2.66. For Q=2.06 L/s, the baffle factors were 0.67, 0.72, and 0.68 and Morril dispersion indices were 2.19, 2.10, and 2.14. The percent difference between the smallest and largest values for the baffle factor for replicate tests were 8.7 % for the 0.85 L/s flow (115 ML/day in prototype) and 7.1 % for the 2.06 L/s flow (280 ML/d in prototype). The percent difference between the smallest and largest values for the Morril index for replicate tests were 4.0 % for the 0.85 L/s flow (115 ML/day in prototype) and 4.0 % for the 2.06 L/s flow (280 ML/d in prototype). It is noted these experiments had been run for a flow development time of 1 h.

In these experiments, the baffle factors observed in the physical model were lower compared to the prototype tracer study results. The average baffle factor found in the model was 0.43 for 0.85 L/s flow, whereas the prototype baffle factor was 0.74 from Maksymetz (1998), which is a 42.7 % difference. The dispersion index, T_{90}/T_{10}, in the model at this flow was 2.73, whereas in the prototype it was found to be 1.82. Figure 4.3 shows this departure from the prototype results using the cumulative residence time distribution. For 2.06 L/s flow, the average baffle factor found in the model was 0.69, whereas the prototype factor was 0.69 from Maksymetz (1998) and thus the averaged baffle factor in the scale model was same as the prototype. The dispersion index, T_{90}/T_{10}, in the model at this flow was 2.14, whereas in the prototype it was found to be 1.84. This difference between the model and the prototype results for the 2.06 L/s flow are shown in Figure 4.4. The significant difference of baffle factor between the scale model and prototype results may be induced by the lower flow Reynolds number (2100) in the channel for the scale model at the minimal flow rate.

4.3.2. Flow Development Time

As mentioned above, the baffle factors observed in the physical model were lower compared to the prototype tracer study results at the minimum flow rate (0.85 L/s). In assessing potential causes for this discrepancy, it was decided to check whether the time for flow development before initiation of the tracer tests would affect test results.

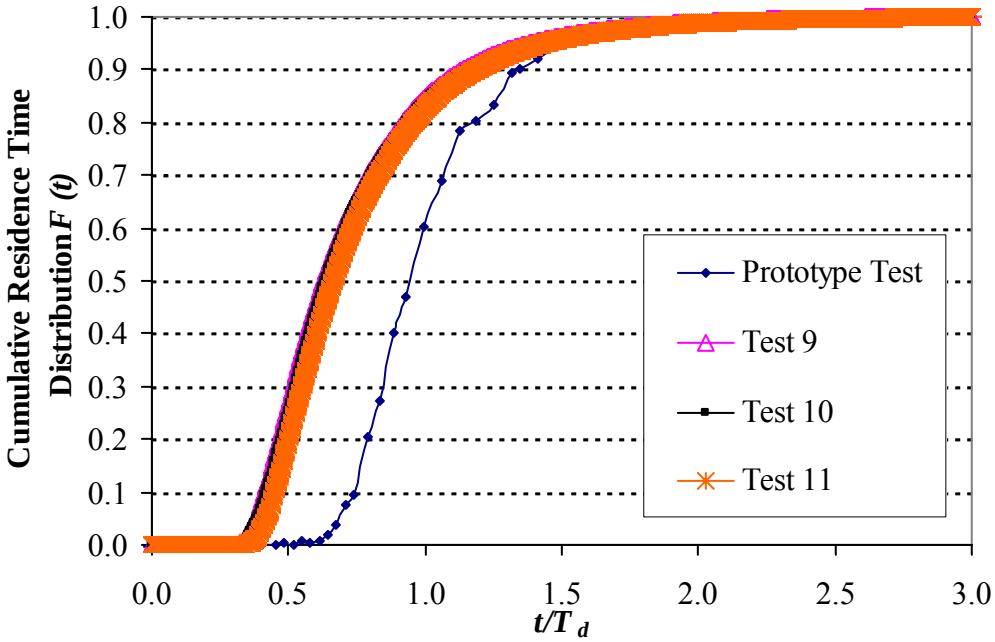

Figure 4.3 Cumulative Residence Time Distribution for 0.85 L/s flow (115 ML/d in Prototype).

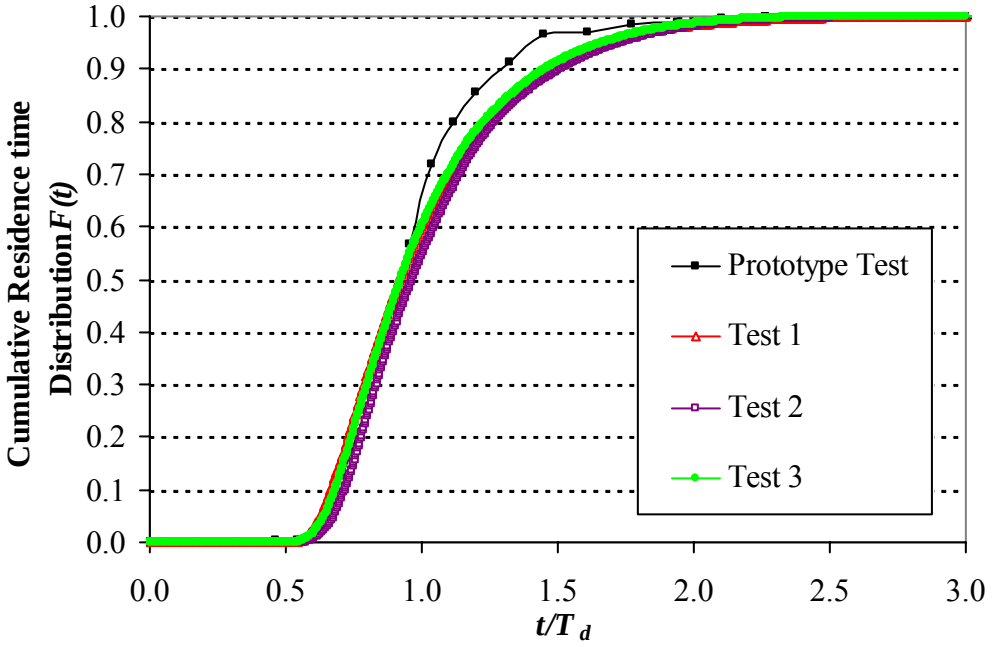

Figure 4.4 Cumulative Residence Time Distribution for 2.06 L/s flow (280 ML/d in Prototype).

Therefore, two tests were conducted when the flow was allowed to develop for 14 h (equivalent to $12T_d$) before the tracer test was carried out at Q = 0.85 L/s. Analysis of the RTD from the tests, shown in Figure 4.5, showed that in these experiments the baffle

factor T_{10}/T_d differed on average only 0.1 % and the dispersion index differed only 3.8 % between the model and prototype. It is seen in Figure 4.5 that there is an obvious displacement of the RTD in time between a flow development time τ =1 ($0.9T_d$) and 14 14 h ($12T_d$).

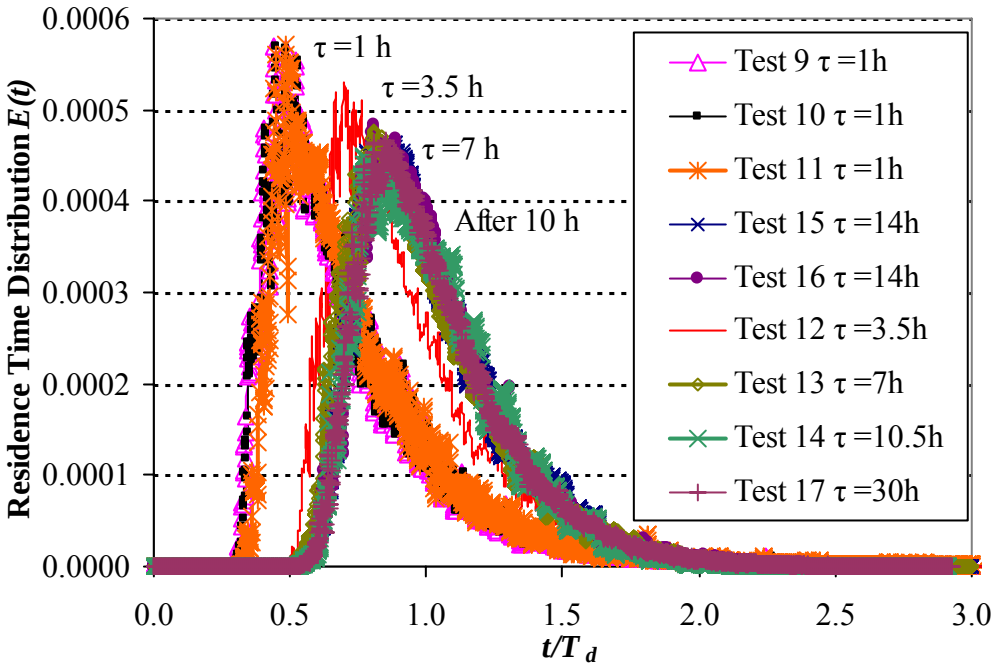

Figure 4.5 Residence Time Distribution for minimum flow rate (0.85 L/s) tests for various flow development times.

Additional tests were then carried out to assess how the time allowed for flow development affected the tracer test results after 3.5, 7 and 10.5 h of flow development (equivalent to $3T_d$, $6T_d$, and $9T_d$). Figure 4.6 shows the cumulative residence time distributions for flow development (τ). Figure 4.7 shows the variation of the baffle factor and dispersion index with flow development time. It is seen that the physical model baffle factor and dispersion index asymptotically approach the prototype values and seem to reach a stable value after about 10.5 h of flow development at the minimum flow rate. For τ = 10.5 h, the difference in baffle factor between the model and prototype is only 0.2 % and dispersion index is only 2.1 %. It is also seen that the increased baffle factor is related to a decreased dispersion index. Finally, a tracer test was conducted with τ = 30 h (equivalent to $25.6T_d$) to fully make sure that the flow parameters had reached their

asymptotic values. It is seen (Figure 4.7) there is little change in results between τ = 30 and 10.5 h.

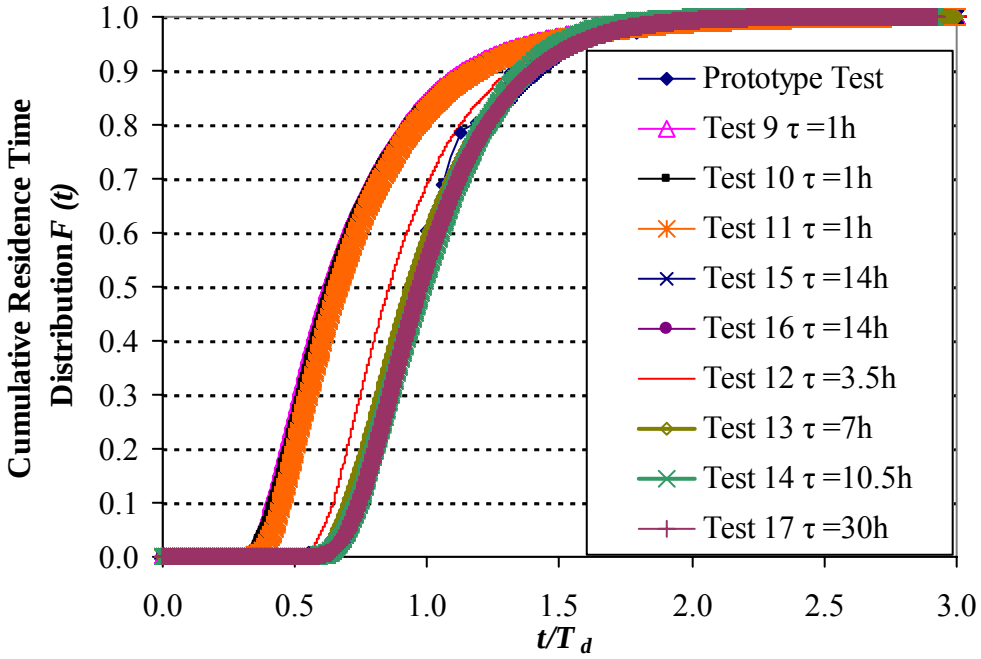

Figure 4.6 Cumulative Residence Time Distribution for minimum flow rate (0.85 L/s, 115 ML/d in prototype) tests without column condition.

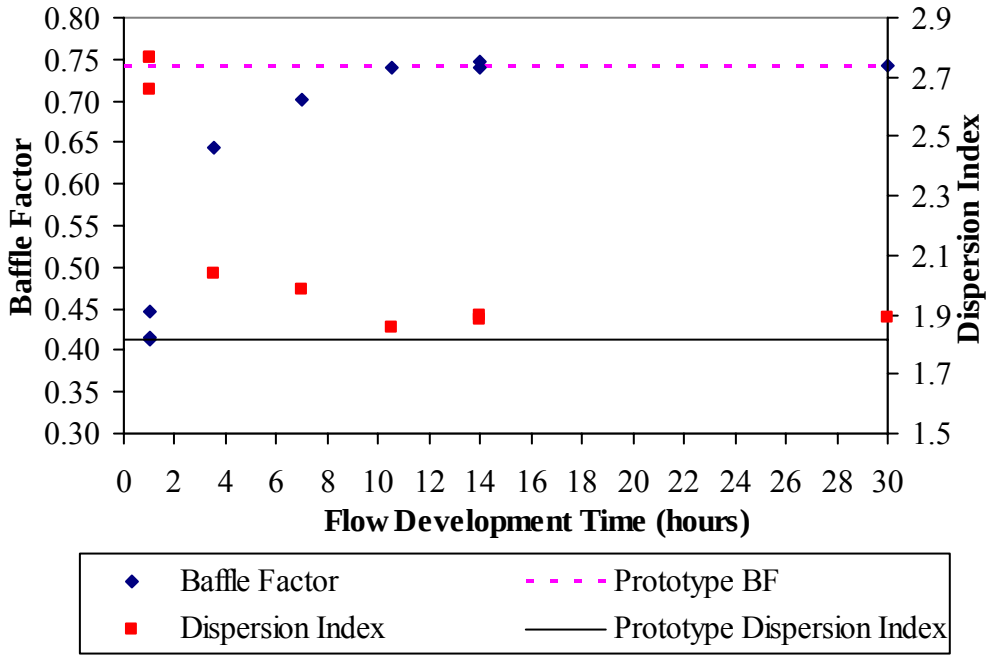

Figure 4.7 Baffle factor and dispersion index for minimum flow rate (0.85 L/s in model, 115 ML/d in prototype) tests without column condition.

The difference in the baffle factor is 0.2 % and dispersion index is 1.7 % between the 10.5 and 30 h tests. Note that these tests are all for the "without columns" condition in the clearwell.

Figure 4.8 shows the RTD from three replicate tests with a flow development time τ =1 h (equivalent to 2.0T_d) and another with a flow development time τ = 5 h (equivalent to 9.8T_d) for the flow rate of 2.06 L/s (without columns in the model). Figure 4.9 shows the equivalent cumulative residence time distributions for these tests. The difference of baffle factor is 8.8 % and dispersion index is 10.8 % between the results for τ = 1 and τ = 5 h. The increased flow development time affected the dispersion index as compared to the τ = 1 h, but not the baffle factor. With τ = 5 h, the model and prototype showed a difference in baffle factor of 8.6 % and in dispersion index of 1.5 %. Thus, there is only improvement in the dispersion index with increased flow development time at this flow rate.

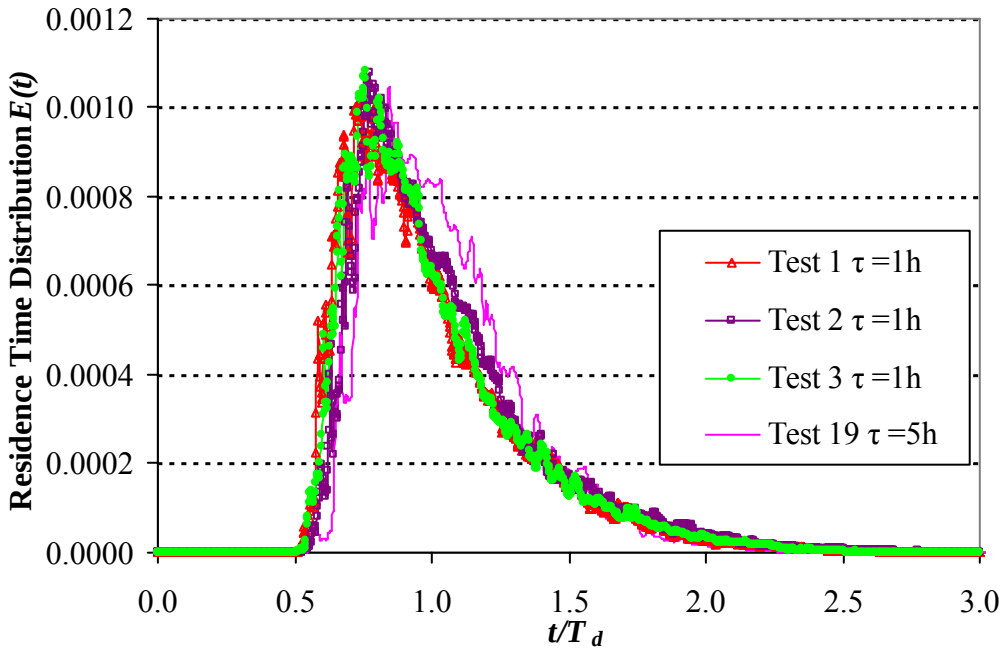

Figure 4.8 Residence Time Distribution for 2.06 L/s flow rate (280 ML/d in prototype) for various flow development time.

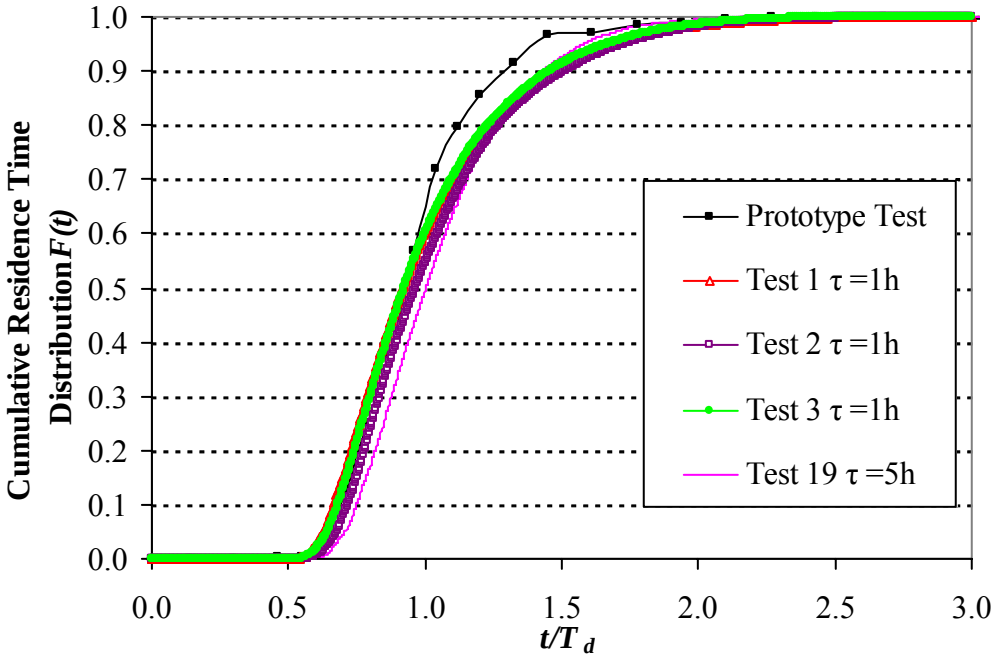

Figure 4.9 Cumulative Residence Time Distribution for 2.06 L/s flow rate (280 ML/d in prototype) for various flow development time.

For the highest flow rate tested of 2.87 L/s (390 ML/d in the prototype), a comparison of the RTD and cumulative RTD curve between the model and the prototype for various τ is shown in Figures 4.10 and 4.11. These tests were conducted after 1 h (equivalent $2.6T_d$) and 4 h (equivalent $10.6T_d$) after initiation of flow through the model. For the test with τ =1 h, the baffle factor determined from the scale model was 0.73 as compared to the prototype value of 0.71 , which gives a marginal 2.8 % difference. The dispersion index was 1.97 in physical model and 1.82 in prototype test with a 7.9 % difference. A comparison of the cumulative RTD between the model and prototype for the τ =4 h test showed a difference in baffle factor of 2.7 % and in dispersion index of 2.3 %. In Figure 4.10, the difference between the RTD of two tests at the different τ is not readily apparent. However, the difference between the two tests is more clearly shown in the cumulative residence time distribution curve in Figure 4.11. Therefore, the results above showed a strong dependence on the flow development time for the lowest flow rate in the model and some improvement in the dispersion index for intermediate and maximum flow rates.

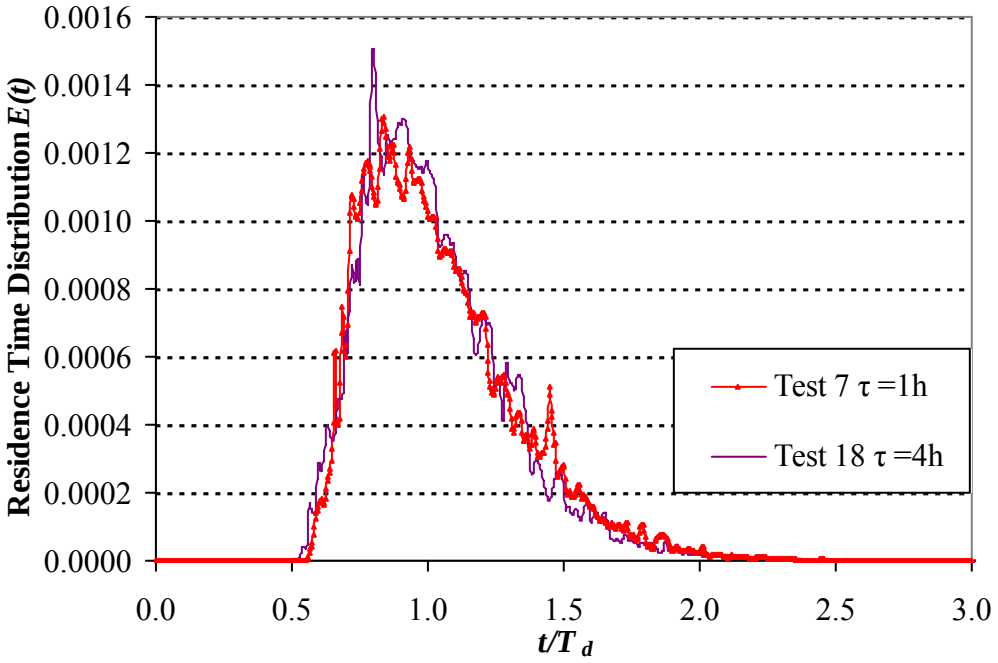

Figure 4.10 Residence Time Distribution for 2.87 L/s flow rate (390 ML/d in prototype) for various flow development times.

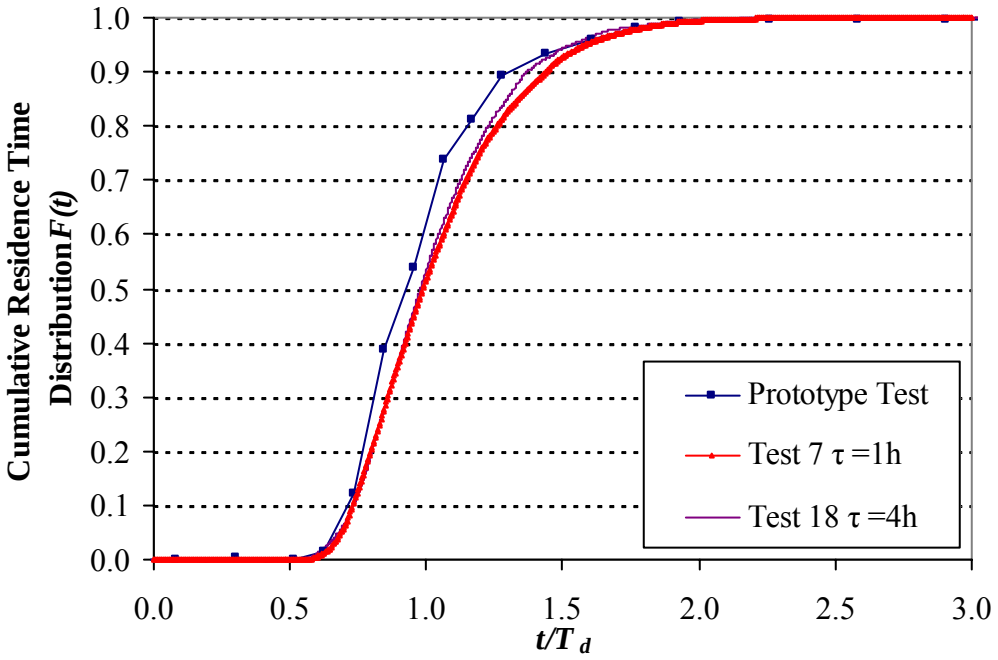

Figure 4.11 Cumulative Residence Time Distribution for 2.87 L/s flow rate (390 ML/d in prototype) for various flow development time.

To investigate the effect of the columns in the model on the flow development time, a series of tests with varied τ were carried out for the "with columns" conditions of the model. Tests were carried out at the minimum flow for the same development times as tested for the without columns condition (τ = 1, 3.5, 7, 10.5, and 14 h). In Figure 4.12, it is seen the residence time distribution curve has little relative change with flow development time when compared to the without columns condition (Figure 4.5). Figure 4.13 shows the cumulative residence time distribution function (RTD) produced for the same experiments. The baffle factors observed in the physical model in the "with columns" condition are closer to the prototype tracer study results compared to the baffle factor "without columns" condition at the same flow development time (τ = 1, 3.5 and 7 h). Analysis of the results showed the biggest difference of the baffle factor from the cumulative RTD curve in these experiments was 9.1 % and the dispersion index differed only 7.6 % between τ = 1 and 14 h. Table 4.2 summarizes the percentage differences in baffle factor and dispersion index results between the model and prototype for both the "with" and "without columns" condition for the model for varied τ. Note that the model results are averages when there are repeated tests.

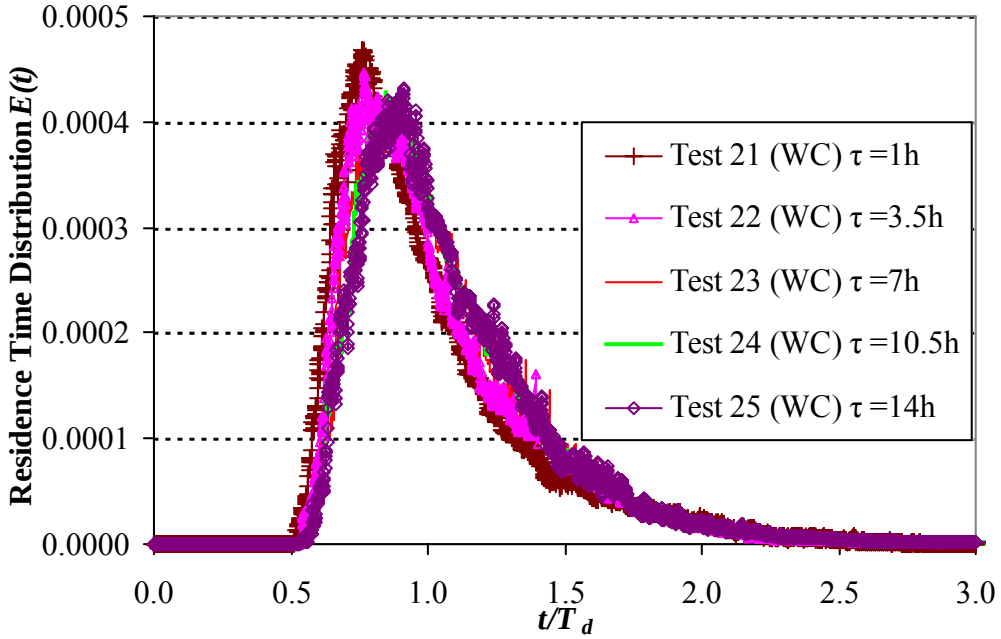

Figure 4.12 Residence Time Distribution for 0.85 L/s flow rate (115 ML/d in prototype) with columns for various flow development time.

Table 4.2 Difference of baffle factor and dispersion index without columns and with columns compared to the prototype for the minimum flow

Flow development time (τ hours)	% Difference of values between "without columns" tests and prototype		% Difference of values between "with columns" tests and prototype	
	Baffle factor	Dispersion Index	Baffle factor	Dispersion Index
1	42.7	50.0	9.4	23.9
3.5	13.1	12.0	5.8	19.6
7	5.6	9.1	2.9	15.0
10.5	0.2	2.1	0.8	14.8
14	0.1	3.8	0.4	15.2

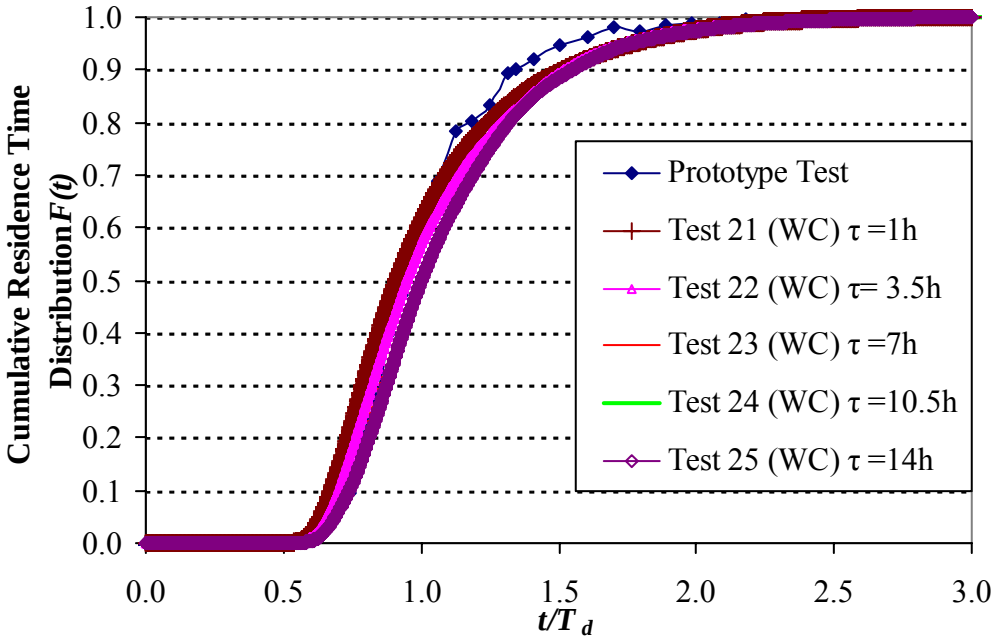

Figure 4.13 Cumulative Residence Time Distribution for 0.85 L/s flow rate (115 ML/d in prototype) with columns for various flow development time.

The variation of the baffle factor and dispersion index with the time allowed for flow development for the "with columns" condition is shown in Figure 4.14. The same tendency towards asymptotical values occurred as for the "without columns" condition (Figure 4.7). It is seen that the physical model baffle factor and dispersion index asymptotically approach the prototype value and seem to reach a stable value still after

only about 10.5 h of flow development at the minimum flow rate. The increased time for flow development did not greatly improve the baffle factor and dispersion index over the 14 h test. The baffle factor is the same and the dispersion index has a 0.4 % difference between τ =10.5 and 14 h. Again the increasing baffle factor is related to a decreasing dispersion index with increasing flow development time. The baffle factors observed in the physical model with columns condition are closer to the prototype tracer study results compared to the baffle factor without columns condition at τ =1, 3.5 and 7 h. However, more dispersion occurs in the "with columns" condition, with a difference of 15 % compared with a difference of 3.8 % under no columns conditions when τ = 14 h.

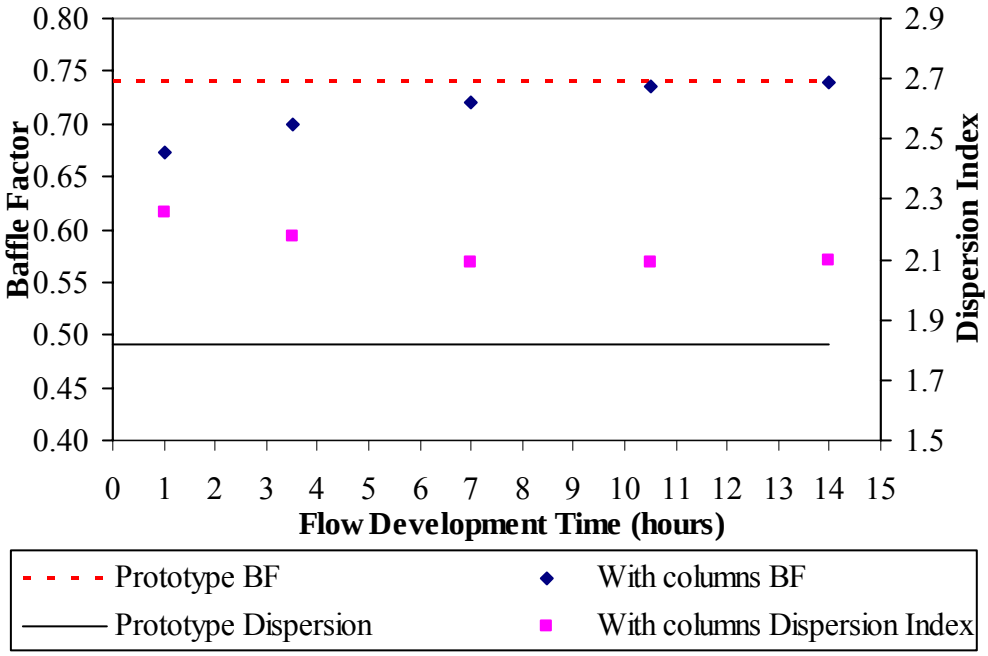

Figure 4.14 Baffle factor and Dispersion index for minimum flow rate (0.85 L/s in model, 115 ML/d in prototype) tests with column condition.

In Figure 4.15, the residence time distribution curves at the flow rate of 2.06 L/s (280 ML/d in prototype) for a model with columns shows that two tests conducted with the development time τ =1 and 5 h fall on top of each other. Figure 4.16 shows that the flow development time had no effect on the cumulative residence time distribution and therefore baffle factor and the dispersion index. The baffle factor and dispersion index between the two tests were different only by 1 %. For the test conducted 5 h after

initiation of flow through the model, the baffle factor and dispersion index between the model and prototype were 4 % and 12 % difference respectively.

Further testing was then conducted at the maximum flow rate of 2.87 L/s (390 ML/d in prototype). Slug tracer tests were conducted after 1 and 4 h of flow development. Figure 4.17 gives residence time distribution curves for these tests. Again the results fall on the same curve. From the cumulative residence time distributions shown in Figure 4.18, it was found that the baffle factor was constant at 0.73. The dispersion indices for the tests were 2.14 and 2.13 with the increase in τ from 1 to 4 h. Prototype measurements had a baffle factor of 0.71 and dispersion index of 1.83 at the maximum flow rate. Compared to the results for Q=2.87 L/s after 4 h of flow development under the without columns condition, the baffle factor was the same, but there was a 13.9 % increase in dispersion index when columns were placed in the clearwell. There was 8.6 % increase in dispersion index between without column and with columns after 1 h of initial flow development. The later part of the cumulative residence time distributions curve for the

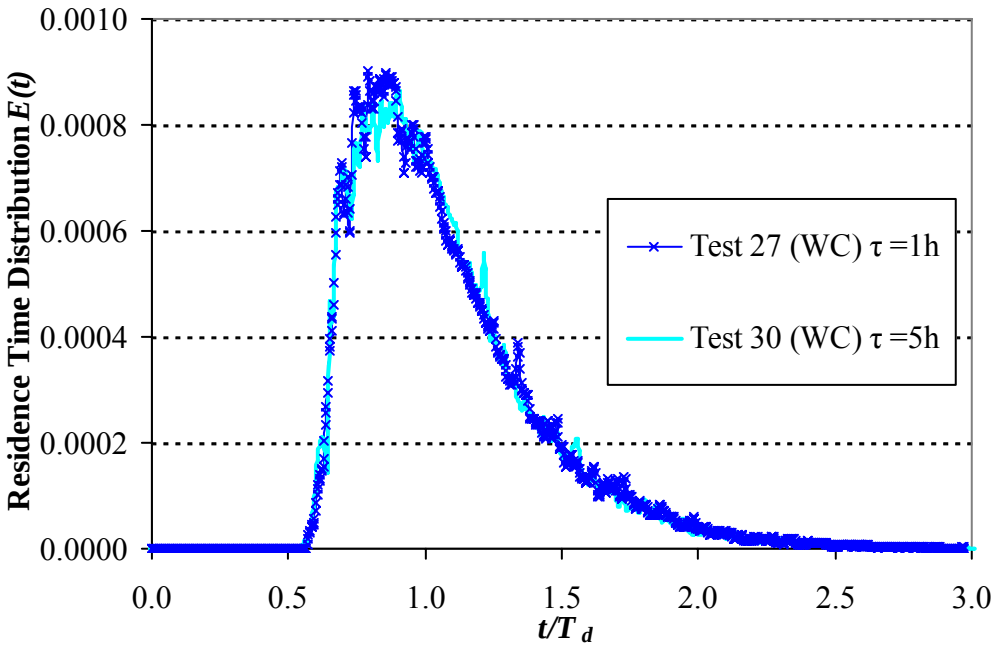

Figure 4.15 Residence Time Distribution for 2.06 L/s flow rate (280 ML/d in prototype) with columns for various flow development time.

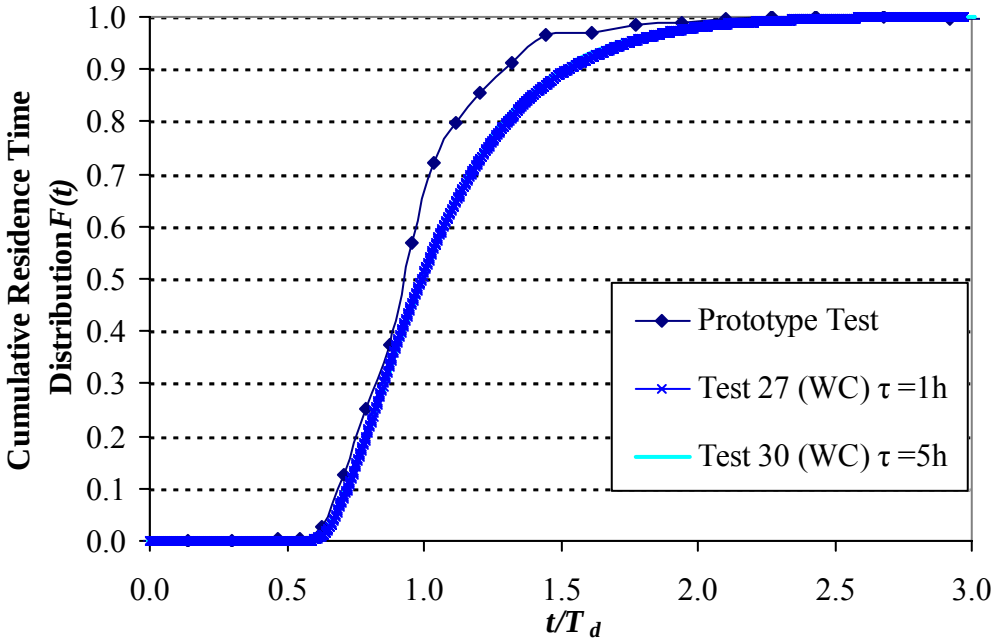

Figure 4.16 Cumulative Residence Time Distribution for 2.06 L/s flow rate (280 ML/d in prototype) with columns for various flow development time.

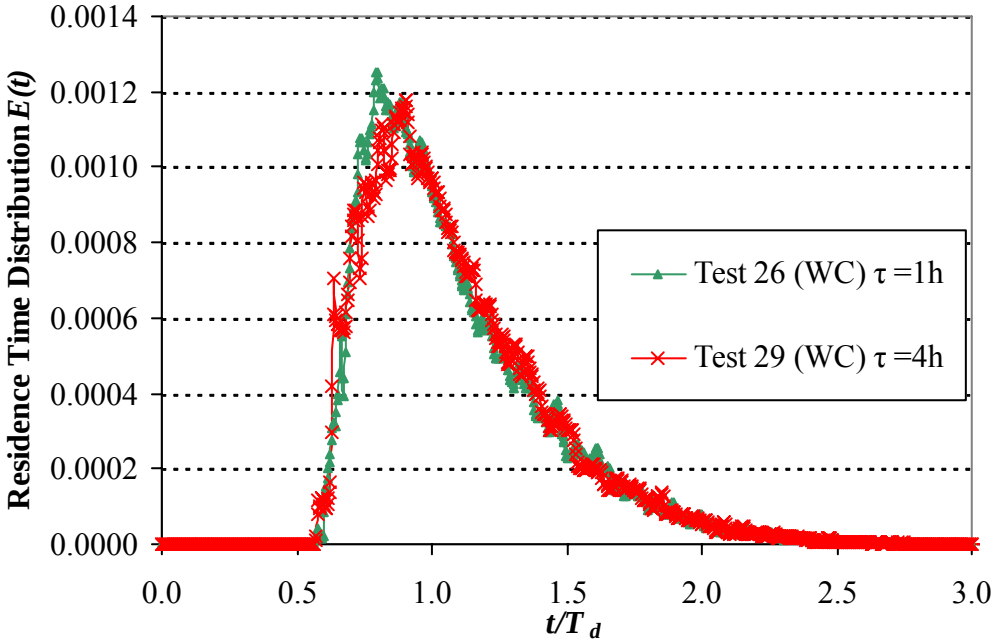

Figure 4.17 Residence Time Distribution for 2.87 L/s flow rate (390 ML/d in prototype) with columns for various flow development time.

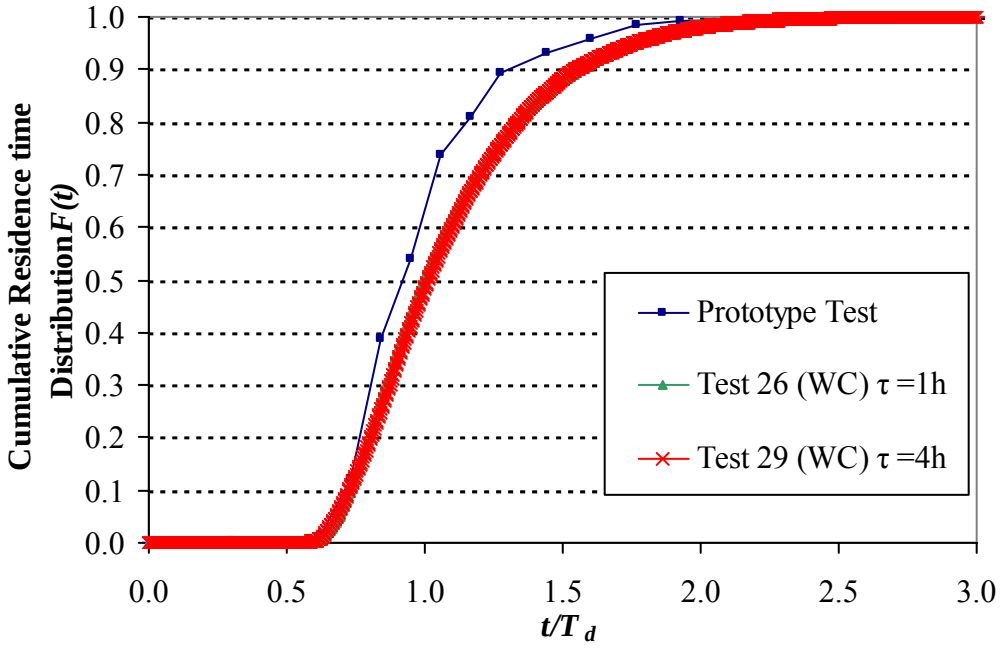

Figure 4.18 Cumulative Residence Time Distribution for 2.87 L/s flow rate (390 ML/d in prototype) with columns for various flow development time.

"with column" condition in the model does not follow the prototype residence time distribution as well as the model for the "without columns" condition (see Figure 4.11).

In order to help explain how the time allowed for flow development affected the tracer test results, the images from the visualization tests were analyzed to determine if there were any changes in dead space in the clearwell with the flow development. In addition, an alternative analysis to determine reservoir dead space that used the tracer test results was carried out using the procedure described by Rebhun and Argaman (1965) discussed in Chapter 2. In this procedure, a log transformation of the cumulative residence time distribution is used to characterize the clearwell into three fractions representing plug flow volume (*p*), mixed reactor volume (*m*) and dead zone volume (*d*). The results of this analysis are presented in Table 4.1.

Composite images showing the entire clearwell from the flow visualization tests were prepared for the Q=0.85 L/s without columns condition for flow development times of τ = 1, 7 and 14 h and these are shown in Figure 4.19 (a, b, c). Note the dashed line in

the following composite figure means the injection location of potassium permanganate dye. It is seen that the percentage area of dead space, based on a visual determination of zones of separation in a plan view of the model, decreased from 50 % to 39 % for the lowest flow rate with the increase in flow development time from 1 to 14 h. In comparison, dead space fraction calculated by the method of Rehbun and Argunam (1965) showed a decrease from 54.9 to 43.9 %. The decrease in dead space fraction explains the significant increase in baffle factor with τ at the lowest flow. This appears to be a result of better distribution of momentum through the model flow at longer times.

The composite images prepared for the minimum flow rate tests under the "with columns" condition for flow development time τ= 1, 7 and 14 h respectively, are shown in Figure 4.20 (a, b, c). It was seen that the percentage area dead space, based on a visual determination of zones of separation in a plan view of the model, decreased from 43 % to 41 % for the lowest flow rate with the increase in flow development time from 1 to 14 h. In comparison, dead space fraction calculated by the method of Rehbun and Argunam (1965) showed a decrease from 40.6 to 39.6 %. Less change of dead zone space is consistent with the changes in baffle factor with the flow development time between the two model conditions (Table 4.3). This shows that the effect of the flow development time on the reduction of dead space under the "with column" condition is less than under the "without columns" condition.

Flow visualization tests were also conducted in the scale model for flows rates (2.06 and 2.87 L/s) for the condition with and without columns present. The calculations to estimate the dead zone proportion of clearwell based upon the flow visualization tests indicate no significant change in dead zone area between the with columns and without columns conditions for the reservoir, as seen by the results given in Table 4.3. It should be noted that the accuracy of this visual analysis is estimated to be ± several percent at best.

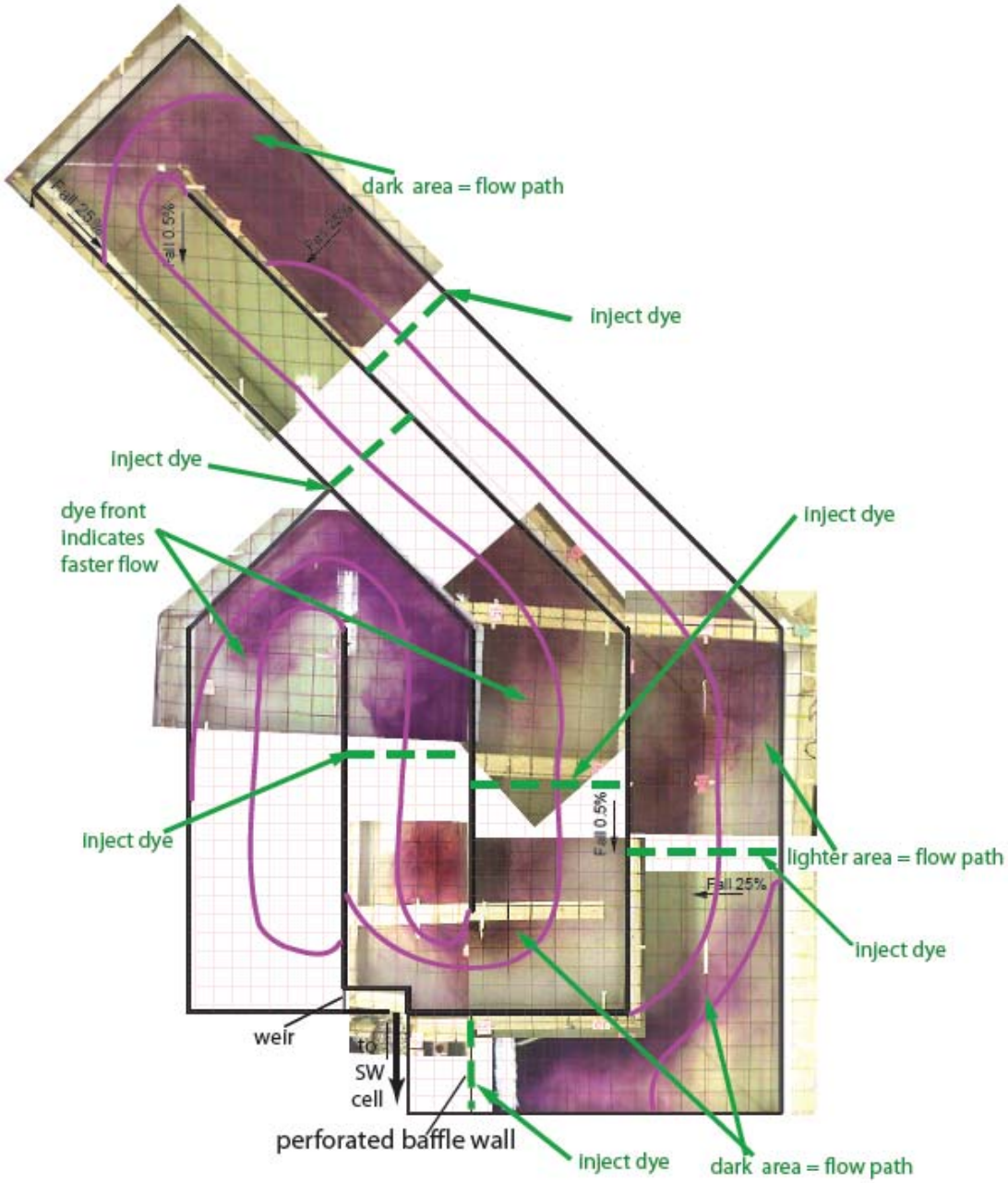

(a)

Figure 4.19 Flow pattern for minimum flow rate (0.85 L/s) without columns (a) for τ =1 h ,(b) for τ =7 h, (c) for τ =14 h.

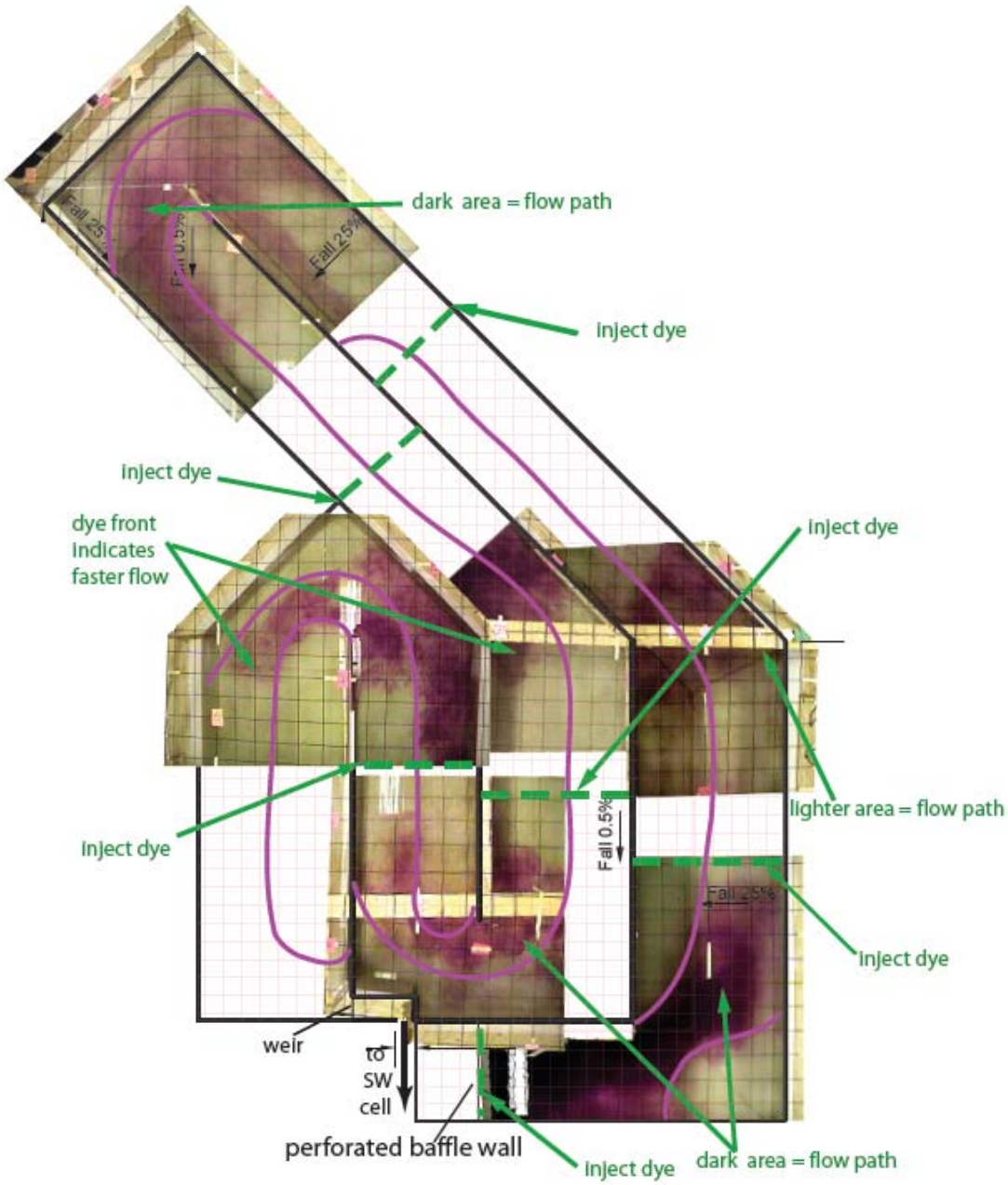

(b)
Figure 4.19 Cont'd

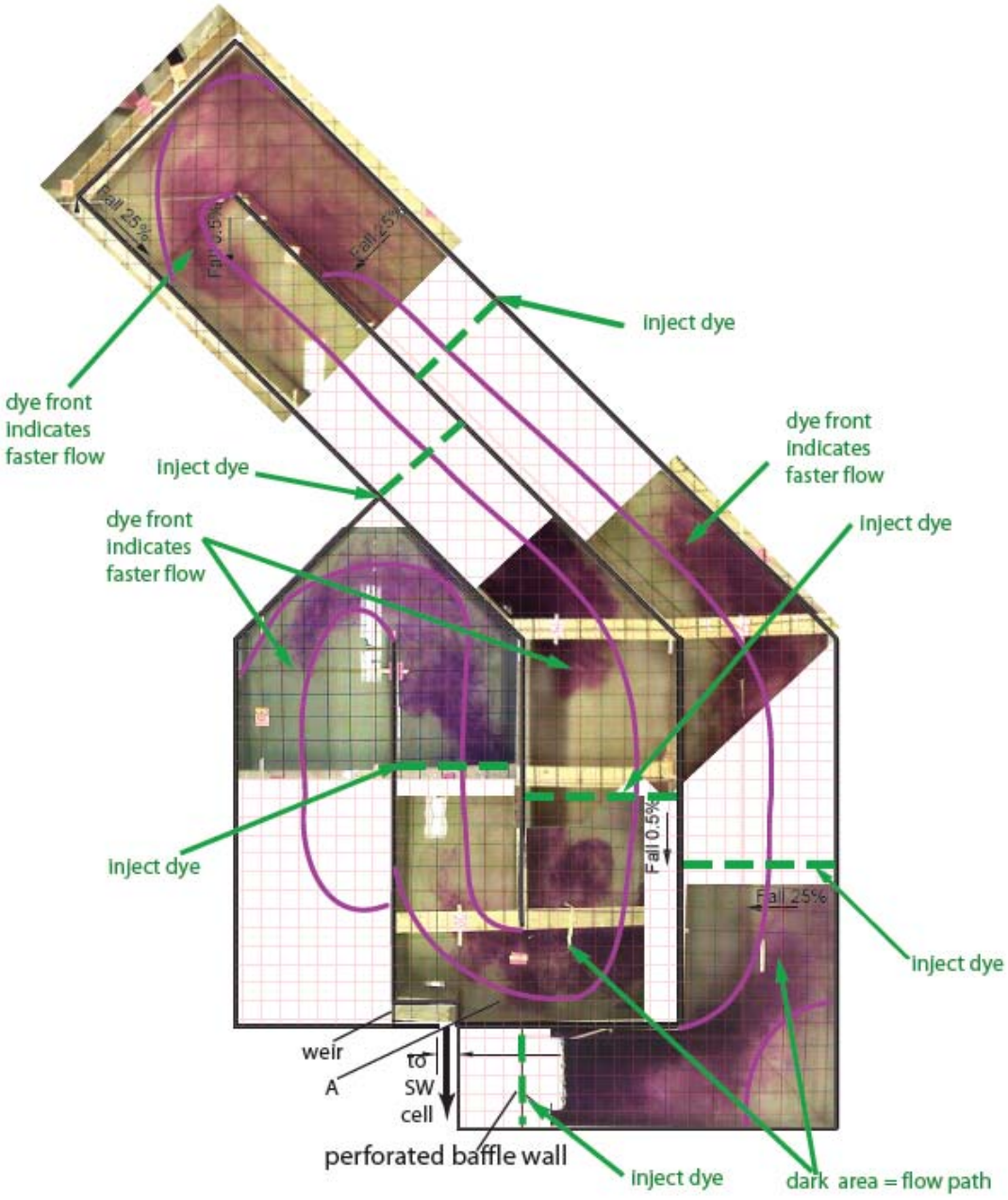

(c)
Figure 4.19 Cont'd

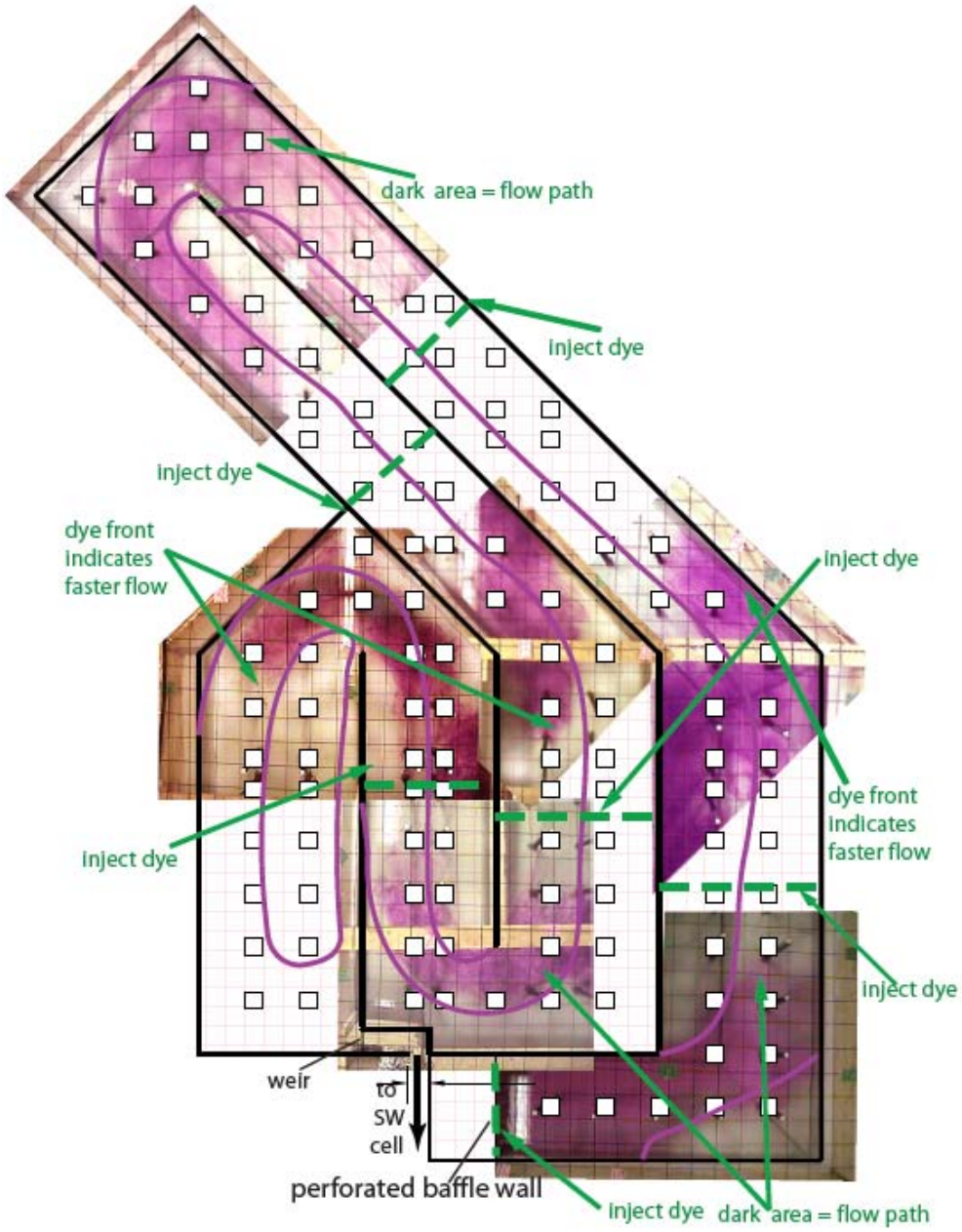

(a)

Figure 4.20 Flow pattern for minimum flow rate (0.85 L/s) with columns (a) for τ =1 h (b) for τ=7 h (c) for τ =14 h.

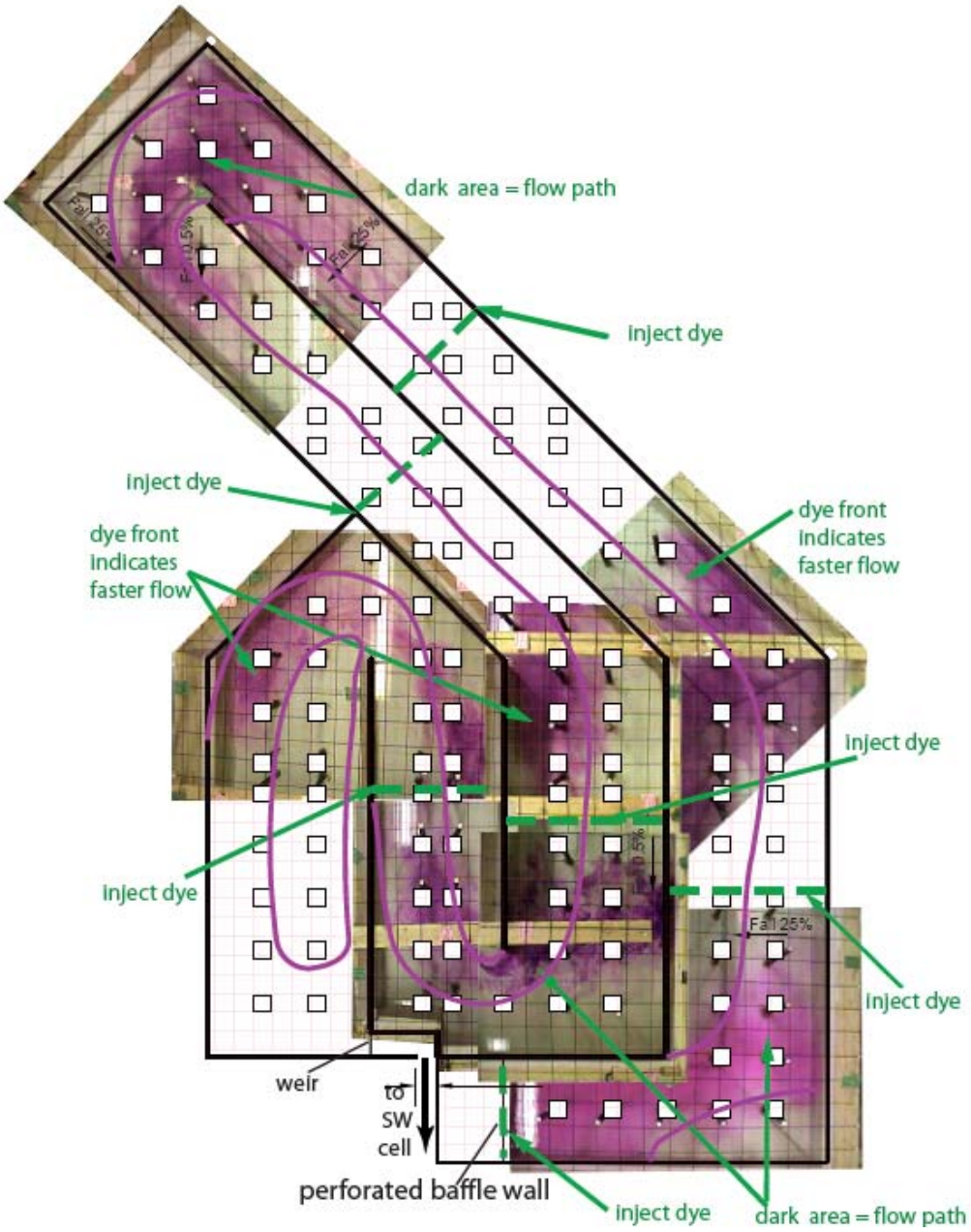

(b)

Figure 4.20 Cont'd

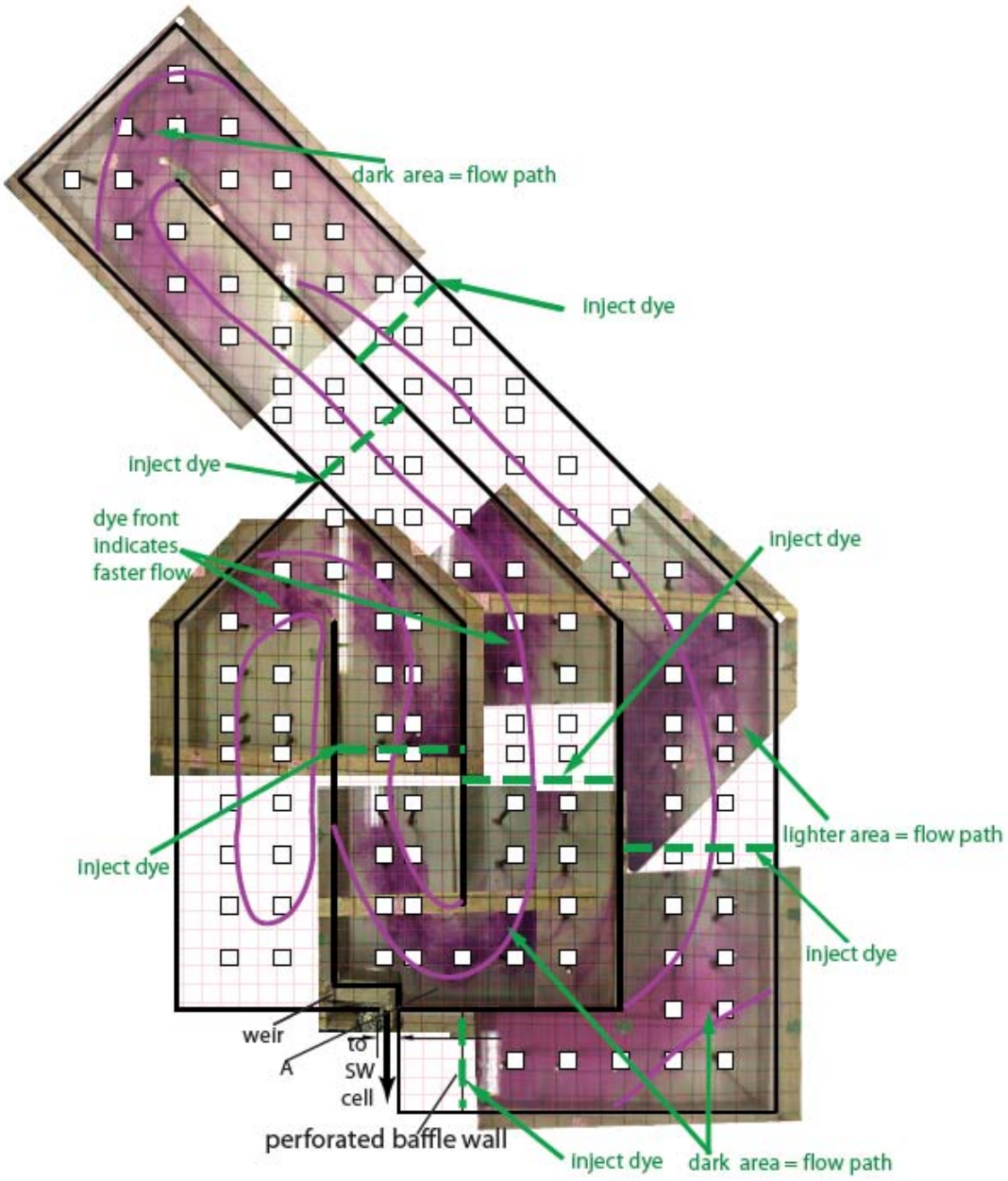

(c)
Figure 4.20 Cont'd

Table 4.3 Dead zone proportion of clearwell from visualization tests in the scale model tests

Flow (L/s)	τ (hour)	From flow visualization		Rehbun and Argunam (1965)	
		Dead space no columns (% of area)	Dead space with columns (% of area)	Dead space no columns (% of area)	Dead space with columns (% of area)
0.85	1	50	42	54.9	40.6
	7	44	41	44.5	41.7
	14	39	40	43.9	39.6
2.06	1	37	36	40.3	39.6
	5	38	38	42.6	40.8
2.87	1	33	36	38.6	36.3
	4	34	35	39.2	37.8

4.3.3. Effect of columns

It was shown above that the baffle factor at the lowest flow rate for the "with columns" condition was closer to the prototype value at τ = 1, 3.5 and 7 h compared with the "without columns" condition. For intermediate flow and maximum flow, the baffle factors at the shorter development times did not vary greatly from prototype values. Therefore, considering only the baffle factor, the columns did not have significant effect on the required flow development time for these cases.

Considering now only "fully developed flow", Table 4.4 gives the baffle factor and dispersion index results for the scale model with and without columns and the associated values from the prototype tracer tests. Note that the model results for Q=0.85 L/s are the average results for the tests that were considered fully developed (i.e. for times of τ = 10.5, 14 and 30 h). As the results show, there is little difference in the baffle factor between with and without condition for fully developed flow. However, the dispersion index for the "without columns" case is closer to the prototype value than for the "with columns" case.

A potential explanation for the poorer modelling results when columns were present in the scale model is that the wake area behind the column may hold some tracer within it. This would cause tracer to be "emitted" into the bulk of the flow over a

Table 4.4 Baffle factor and Morril dispersion index results for the tracer tests and prototype test

Test type	Flow rate	No Columns		With Columns	
		Baffle Factor	Dispersion Index	Baffle Factor	Dispersion Index
Prototype	115 ML/d	-	-	0.74	1.82
	280 ML/d	-	-	0.69	1.88
	390 ML/d	-	-	0.71	1.83
Scale model tracer tests	0.85 L/s	0.74	1.88	0.74	2.10
	2.06 L/s	0.75	1.91	0.72	2.11
	2.87 L/s	0.73	1.87	0.73	2.13

longer time in the test. The Reynolds number of column of scale model is range from 59-197, the wake behind the column is laminar. However, the Reynolds number of column of prototype clearwell is range from 4800-16280. This would cause the residence distribution curve to have more skew and hence there would be a higher dispersion index for the test.

4.4. River2DMix Modelling Results

4.4.1. Calibration Results

As mentioned in Chapter 3, River2DMix was used for simulating the flow and residence time distribution in the scale model of the clearwell. It was run with and without the columns in the clearwell and the results was compared to the measurements taken in the fully developed flow in the scale model. The first step using River2DMix is to calibrate it. Also noted in Chapter 3, the eddy viscosity coefficient used for determining the turbulent shear stresses in the model is composed of three parts: a constant ε_1, a bed shear generated term ε_2, and a transverse shear generated term ε_3. During the calibration, $\varepsilon_1 = 0$, $\varepsilon_2 = 0.2$, and $\varepsilon_3 = 0.1$ were chosen as the initial value (Albers and Maksymetz 2004). The model was calibrated using the scale model tracer test data for the minimum and maximum flow. To do this, the simulation results were compared to the cumulative residence time produced in the scale model. Mohamed et al.

(2008) recommended the statistical parameters to assess the computational model performance on the basis of an entire set of data that is outputted as a curve (such as the cumulative residence time distribution). For the present work, to measure the goodness-of-fit of the computational model to the scale model results, the root mean squared error (*RMSE*) was used, which is defined as

$$RMSE = \sqrt{\frac{1}{N}\sum_{i=1}^{N}\left(O_i - P_i\right)^2} \tag{4.4}$$

where P_i and O_i are respectively the computational and physical model values at time i, and N is the number of data points. As noted in Chapter 3, the cumulative residence time distributions produced in the computational and physical models were compared between the start of the tracer test and the time T_{99}. The best calibration coefficients for the simulations are those that give the lowest *RMSE*. Tables 4.5-4.8 show results of the calibration procedure for the two different flows simulated and two different model conditions (with/without columns). Note that ε_1 was not calibrated because it usually takes a zero value (Steffler and Blackburn 2002).

From Table 4.5, it is seen for minimum flow rate and without columns condition, the calibration coefficients that minimized the *RMSE* were ε_2 = 0.15 and ε_3 = 0.084. From Table 4.7, for the maximum flow rate and "without columns" condition, the coefficients that provided the best fit to the data were ε_2 = 0.15 and ε_3 = 0.1. Thus, it is seen that the calibration coefficients do not strongly depend on the flow rate.

Table 4.6 shows the calibration coefficients that minimized the *RMSE* were ε_2= 0.15 and ε_3 = 0.036 for minimum flow rate and the "with columns condition". From Table 4.8, the coefficients that provided the best fit to the data were ε_2 = 0.15 and ε_3 = 0.04 for maximum flow rate and "with columns condition". This shows again that the calibration coefficients do not strongly depend on the flow rate and also that the columns decrease ε_3.

Table 4.5 Calibration coefficients and resulting difference in baffle factor and dispersion index between simulation and physical model for Q = 0.85 L/s for the "without columns" condition

No.	Baffle Factor difference between simulation and physical model	Dispersion Index difference between simulation and physical model	RMSE	Hydrodynamics		Mixing	
				ε_2	ε_3	ε_2	ε_3
(1)	2.7%	9.2%	0.020	0.2	0.1	0.2	0.1
(2)	2.0%	7.9%	0.018	0.15	0.1	0.15	0.1
(3)	0.5%	5.6%	0.015	0.15	0.1	0.15	0.075
(4)	-1.4%	2.0%	0.014	0.15	0.075	0.15	0.075
(5)	-6.4%	7.7%	0.027	0.15	0.05	0.15	0.05
(6)	-5.4%	5.6%	0.025	0.2	0.05	0.2	0.05
(7)*	0.0%	-4.7%	0.013	0.15	0.084	0.15	0.084

Table 4.6 Calibration coefficients and resulting difference in baffle factor and dispersion index between simulation and physical model for Q = 0.85 L/s for the "with columns" condition

No.	Baffle Factor difference between simulation and physical model	Dispersion Index difference between simulation and physical model	RMSE	Hydrodynamics		Mixing	
				ε_2	ε_3	ε_2	ε_3
(1)	10.8%	18.6%	0.049	0.15	0.075	0.15	0.075
(2)	-5.4%	2.5%	0.029	0.15	0.03	0.15	0.03
(3)*	-1.6%	1.4%	0.007	0.15	0.036	0.15	0.036
(4)	17.2%	25.0%	0.07	0.15	0.1	0.15	0.1
(5)	-17.7%	25.3%	0.069	0.15	0.01	0.15	0.01
(6)	-8.1%	7.1%	0.031	0.15	0.025	0.15	0.025

Table 4.7 Calibration coefficients and difference in baffle factor and dispersion index between simulation and physical model for Q = 2.87 L/s for the "without columns" condition

No.	Baffle Factor difference between simulation and physical model	Dispersion Index difference between simulation and physical model	RMSE	Hydrodynamics		Mixing	
				ε_2	ε_3	ε_2	ε_3
(1)	1.4%	1.7%	0.007	0.2	0.1	0.2	0.1
(2)*	0.1%	0.2%	0.006	0.15	0.1	0.15	0.1
(3)	-4.1%	8.5%	0.019	0.15	0.075	0.15	0.075
(4)	-2.7%	6.3%	0.015	0.15	0.08	0.15	0.08
(5)	-9.6%	19.9%	0.036	0.15	0.05	0.15	0.05
(6)	3.2%	5.0%	0.013	0.15	0.12	0.15	0.12

Table 4.8 Calibration coefficients and difference in baffle factor and dispersion index between simulation and physical model for Q = 2.87 L/s for the "with columns" condition

No.	Baffle Factor difference between simulation and physical model	Dispersion Index difference between simulation and physical model	RMSE	Hydrodynamics		Mixing	
				ε_2	ε_3	ε_2	ε_3
(1)	19.6%	20.9%	0.071	0.15	0.1	0.15	0.1
(2)	0.0%	1.9%	0.007	0.15	0.0375	0.15	0.0375
(3)	-4.1%	9.4%	0.018	0.15	0.03	0.15	0.03
(4)	-7.7%	14.7%	0.027	0.15	0.025	0.15	0.025
(5)	8.0%	8.5%	0.033	0.15	0.06	0.15	0.06
(6)*	0.0%	0.46%	0.003	0.15	0.04	0.15	0.04

4.4.2. Comparison of Simulation and Scale Model Results

Figure 4.21 shows the cumulative residence distribution curves F(t) based on the physical hydraulic model and final calibrated computational model for the flow of 0.85 L/s and the without columns condition. The baffle factor determined from the simulation was the same as the scale model value of 0.74. The dispersion index was 1.79 in the simulation and 1.88 in the physical model with a 4.7 % difference. A comparison of the simulation and prototype results showed no difference in baffle factor and a difference in dispersion of 1.5 %.

Figure 4.22 shows the simulation results for the velocity field when looking in plan at the Glenmore clearwell for Q = 0.85 L/s and the "without columns" model condition. It is seen at the inlet the velocity is uniform across the width of the channel. Zones shown as regions of recirculation and those where velocities are very small are considered dead zones and are generally coloured blue. In Figure 4.22, the dead zones are located in all corners of the clearwell. Also, for each 180 degree turn of the flow direction, a recirculation zone is

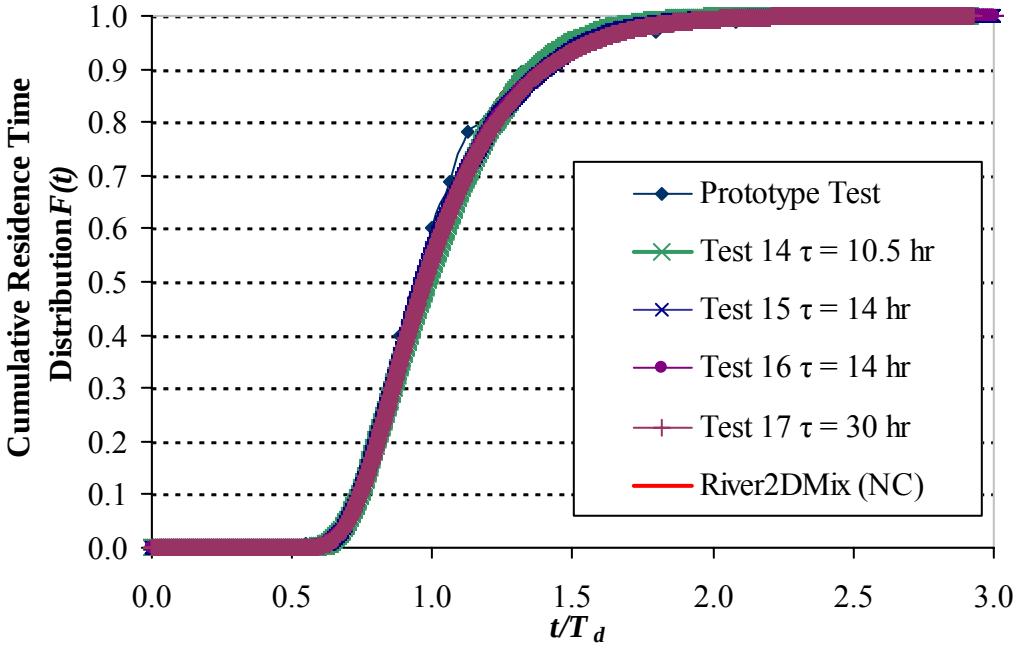

Figure 4.21 Comparison of the Cumulative Residence Time of the full-scale test to the simulated breakthrough curves and hydraulic model tracer test results for the without columns condition for the flow rate 0.85 L/s.

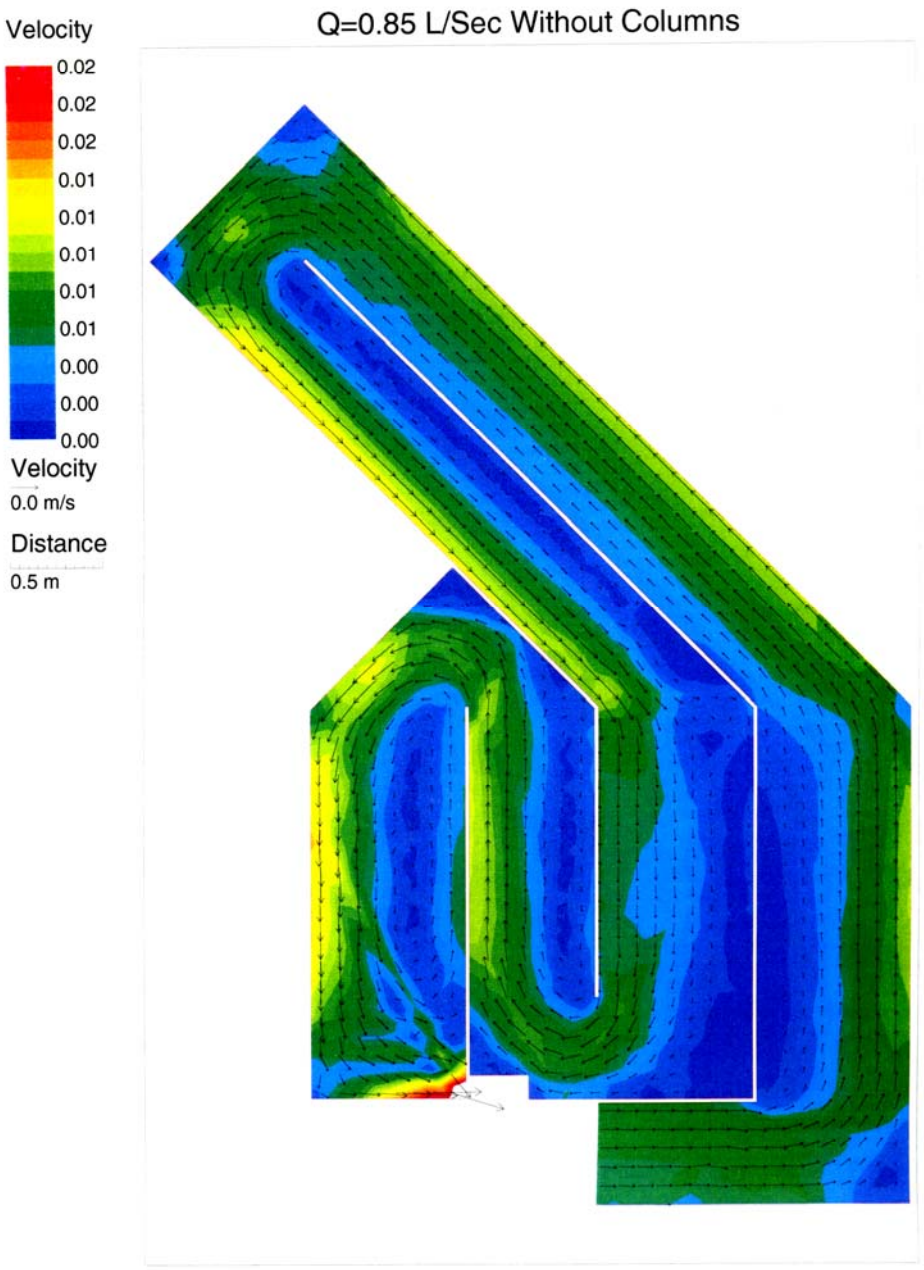

Figure 4.22 Velocity field produced by River2DMix for the 0.85 L/s flow simulation of the physical scale model without columns.

.

created at the inside of channel starting at the upstream edge of the wall. This compares well with what was found in Figure 4.19c, which gives the results of the flow visualization in the physical model. The main difference between the simulated and measured flow patterns are that the scale model had a much larger dead zone within the section labelled as point A in Figure 4.19c.

When simulating the flow of 2.06 L/s for the without columns condition, the same values of ε_2 and ε_3 were used as the maximum flow rate (ε_2 = 0.15 and ε_3 = 0.1). This was because the flow rate Q = 2.06 L/s is closer to the maximum flow rate than the minimum flow rate of Q=0.85 L/s. Figure 4.23 shows the cumulative residence distribution curves based for the physical and computation models for the flow of 2.06 L/s for the "without columns" condition. The baffle factor determined from the simulation was 0.73 as compared to the scale model value of 0.75, which gives a 2.7 % difference then between the simulation and scale model. The dispersion index was 1.85 in the simulation and 1.91 in physical model, which gives a 3.2 % difference in values.

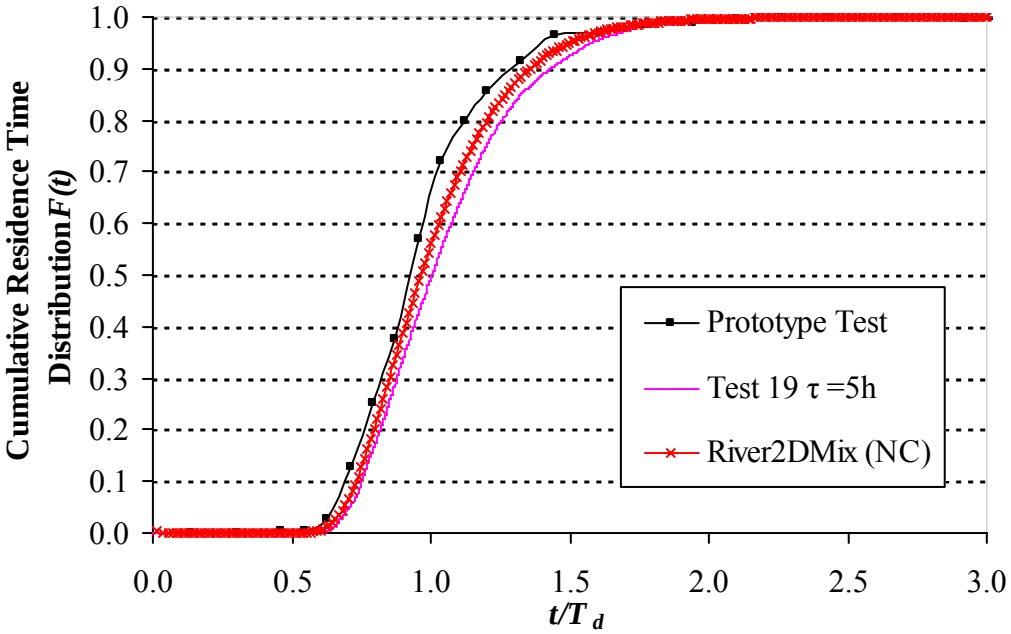

Figure 4.23 Comparison of the Cumulative Residence Time Distribution of the full-scale test to the simulated breakthrough curves and hydraulic model tracer test results for the without columns condition for the flow rate 2.06 L/s.

Meanwhile, a comparison of the cumulative RTD between the simulation and prototype showed a difference in baffle factor of 5.8 % and difference in dispersion index of 1.6 %.

Figure 4.24 shows the simulated velocity field at the flow rate Q=2.06 L/s for the "without columns" condition in the model. Again, the flow visualization (Figure 4.25) showed similar results in comparison with the predictions obtained using River2DMix. Both of them showed a large stagnant zone behind the baffle wall and small stagnant zones in the upstream and downstream corners of the channel. The same issue existed for this flow as for the minimum flow rate. The simulation did not predict the stagnant zone shown in the region given by point A in Figure 4.25.

Figure 4.26 shows the cumulative residence distribution curves F(t) based on the hydraulic model and final calibrated computational model for the flow of 2.87 L/s and the "without columns" condition. The baffle factor determined from the simulation was the same as the scale model value of 0.73. Also the dispersion index determined from the simulation was same as the physical model value of 1.87. Meanwhile, a comparison of the cumulative RTD between the simulation and prototype results showed the difference in baffle factor of 2.9 % and difference in dispersion index of 2.4 %.

Figure 4.27 shows the simulated velocity field at the flow rate Q=2.87 L/s for the "without columns" condition in the model. In Figure 4.27, there are dead zones in all corners of the clearwell. Also, a recirculation zone is located at the 180-degree turn of the flow direction when starting at the upstream edge of the wall. The simulated flow pattern showed similar results as the measured flow pattern (Figure 4.28), except again that the extent dead zone at point A is smaller in the simulated flow pattern (Figure 4.27).

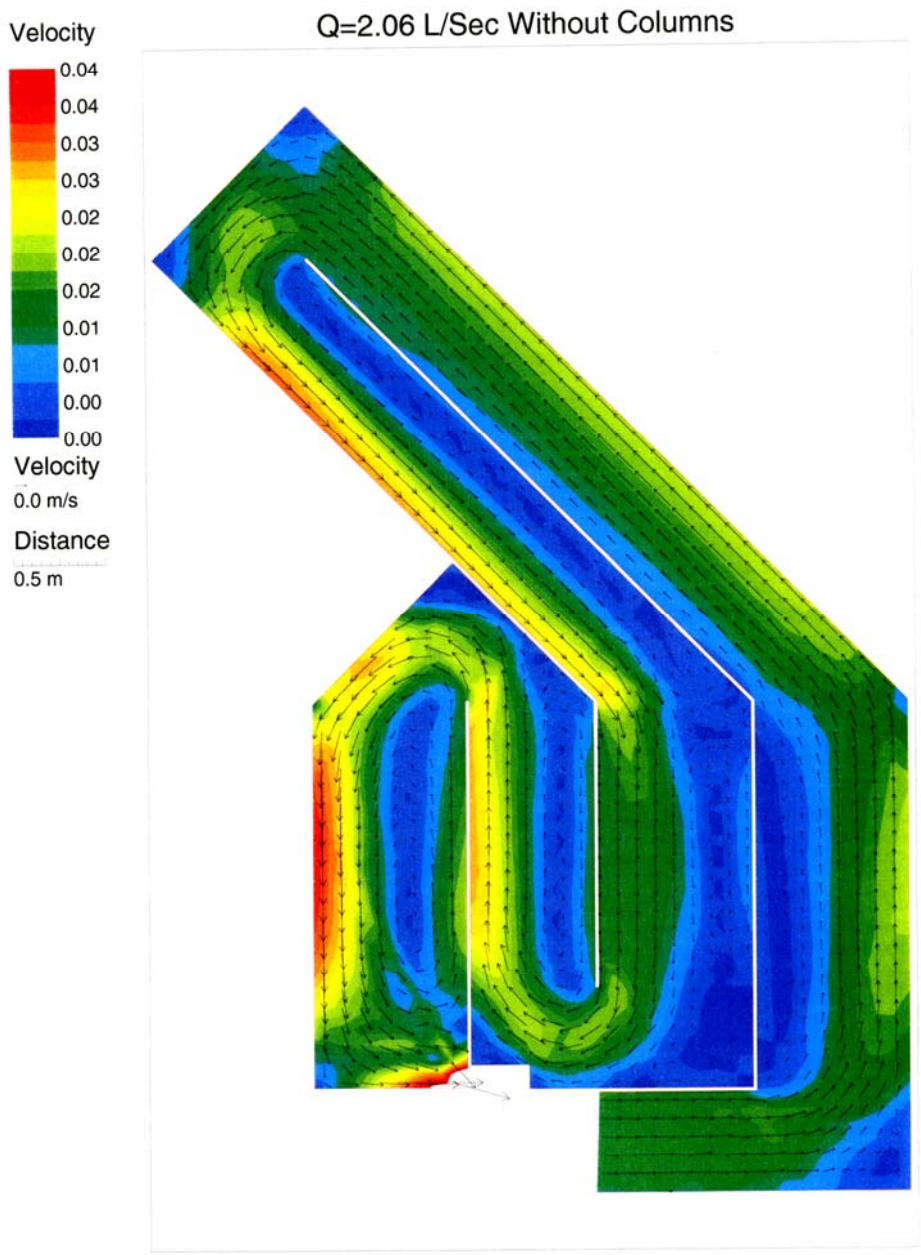

Figure 4.24 Velocity field produced by River2DMix for the 2.06 L/s flow simulation of the physical scale model without columns.

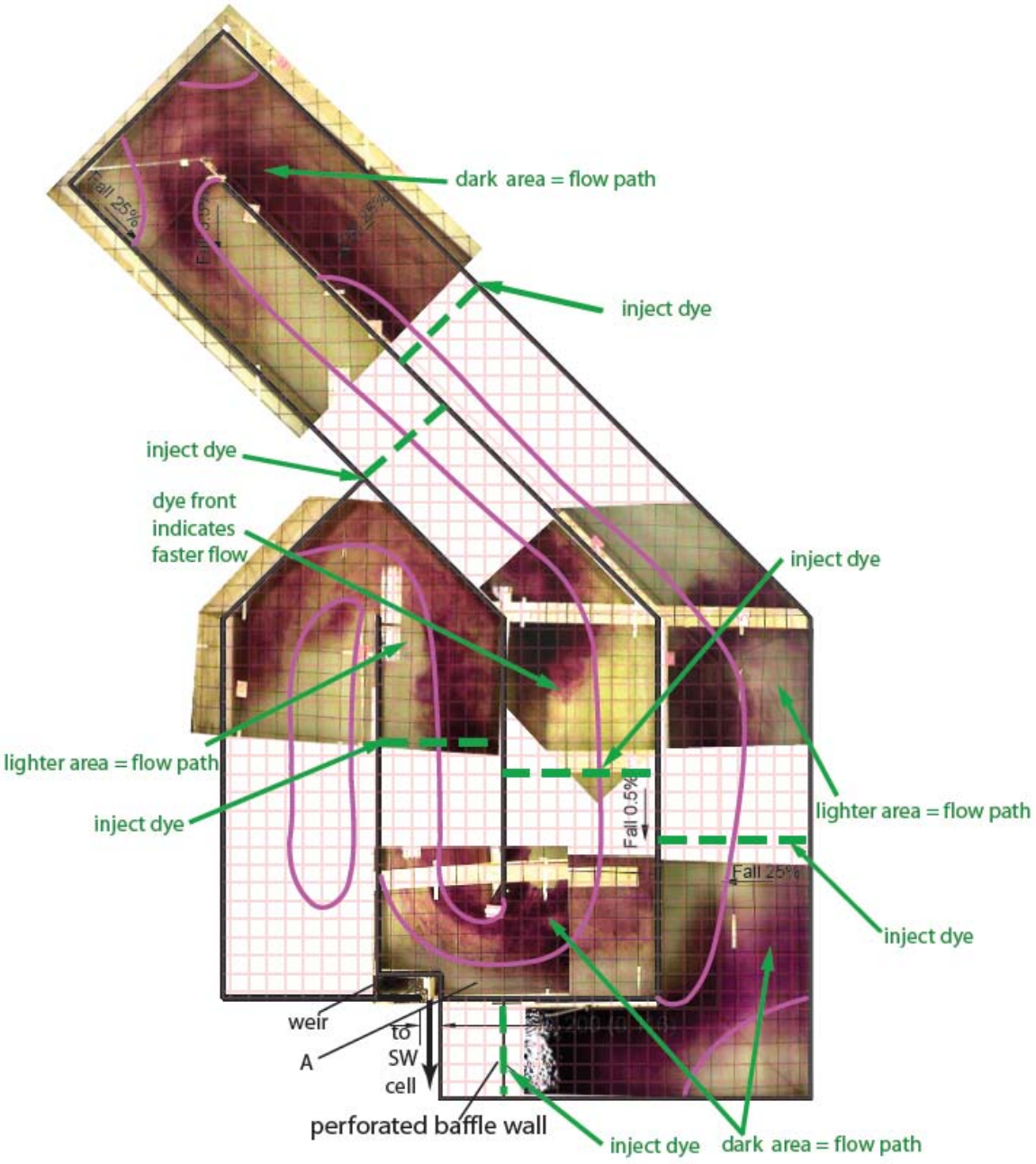

Figure 4.25 Flow pattern in scale model for flow rate Q=2.06 L/s without columns for τ =5 h (fully developed flow).

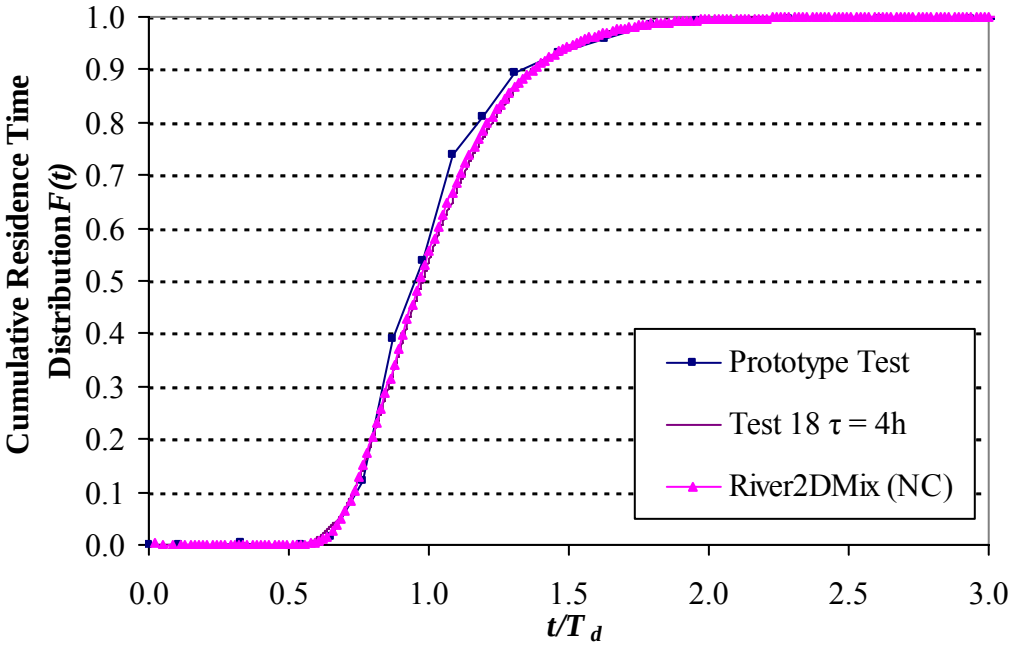

Figure 4.26 Comparison of the Cumulative Residence Time Distribution of the full-scale test to the simulated breakthrough curves and hydraulic model tracer test results for the without columns condition for the flow rate 2.87 L/s.

Figure 4.29 shows the cumulative residence distribution curves F(t) based on the hydraulic model and final calibrated computational model for the flows of 0.85 L/s and the "with columns" condition. The baffle factor determined from the simulation was 0.73 and 0.74 in the physical model with a 1.6% difference. Also, the dispersion index was 2.13 in the simulation and 2.10 in physical model with a 1.4 % difference. Meanwhile, a comparison of the cumulative RTD between the simulation and prototype showed difference in baffle factor of 1.6 % and difference in dispersion index of 16.9 %.

Figure 4.30 shows the simulation results for the velocity field of flow rate Q=0.85 L/s and the "with columns" model condition. In Figure 4.30, the dead zones are seen in all corners of the clearwell. In comparison to the "without columns" condition simulation (Figure 4.22), the flow pattern is similar between the two different cases. However, for the "with columns" case, there are more slow velocity zones for the first half of the flow length than for the "without columns" case. In comparison of the "with column" results to the hydraulic model, the main difference between the simulated and measured flow

patterns were again that the scale model had a much larger dead zone within the section labelled as point A in Figure 4.20c, which was also seen for the "without columns" case.

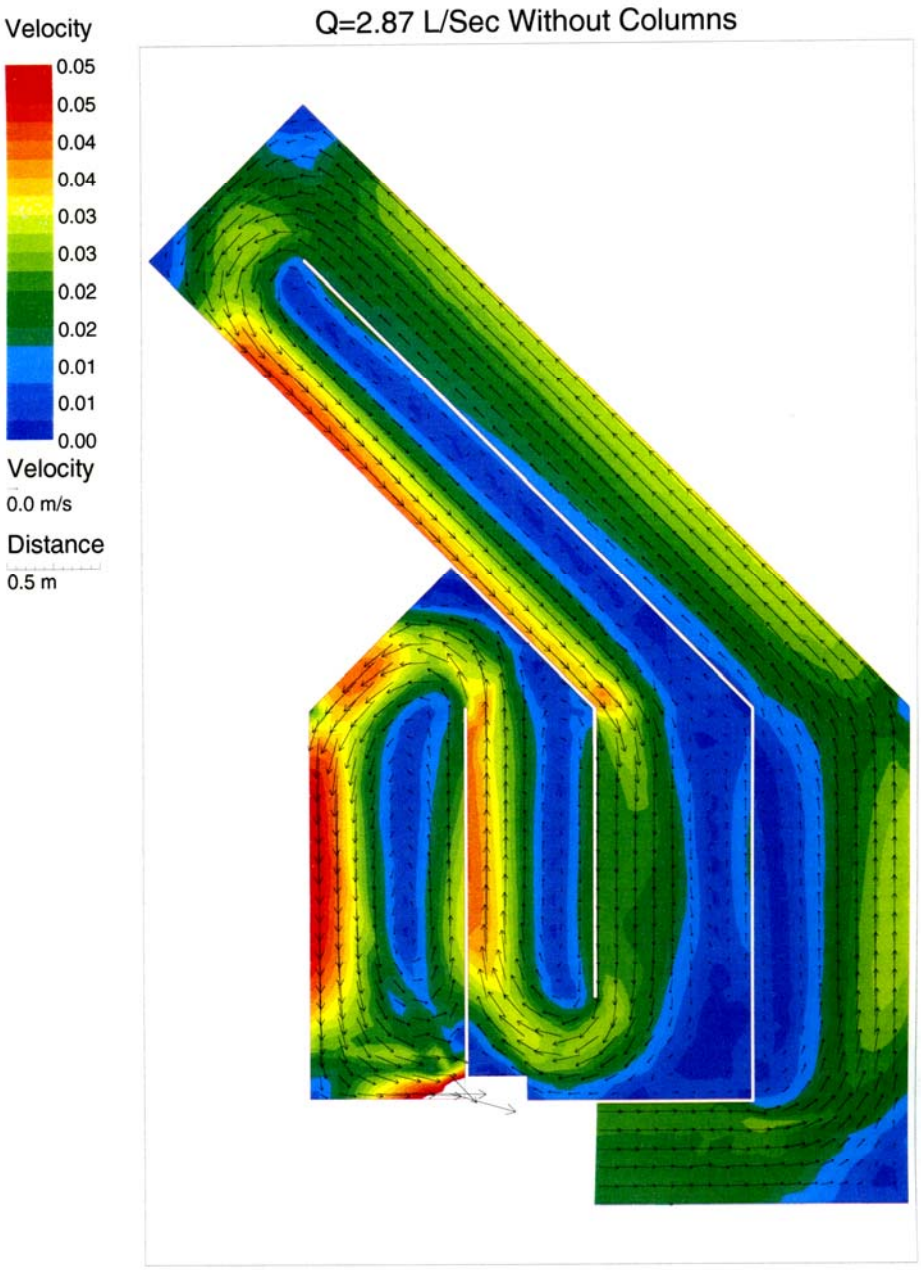

Figure 4.27 Velocity field produced by River2DMix for the 2.87 L/s flow simulation of the physical scale model without columns.

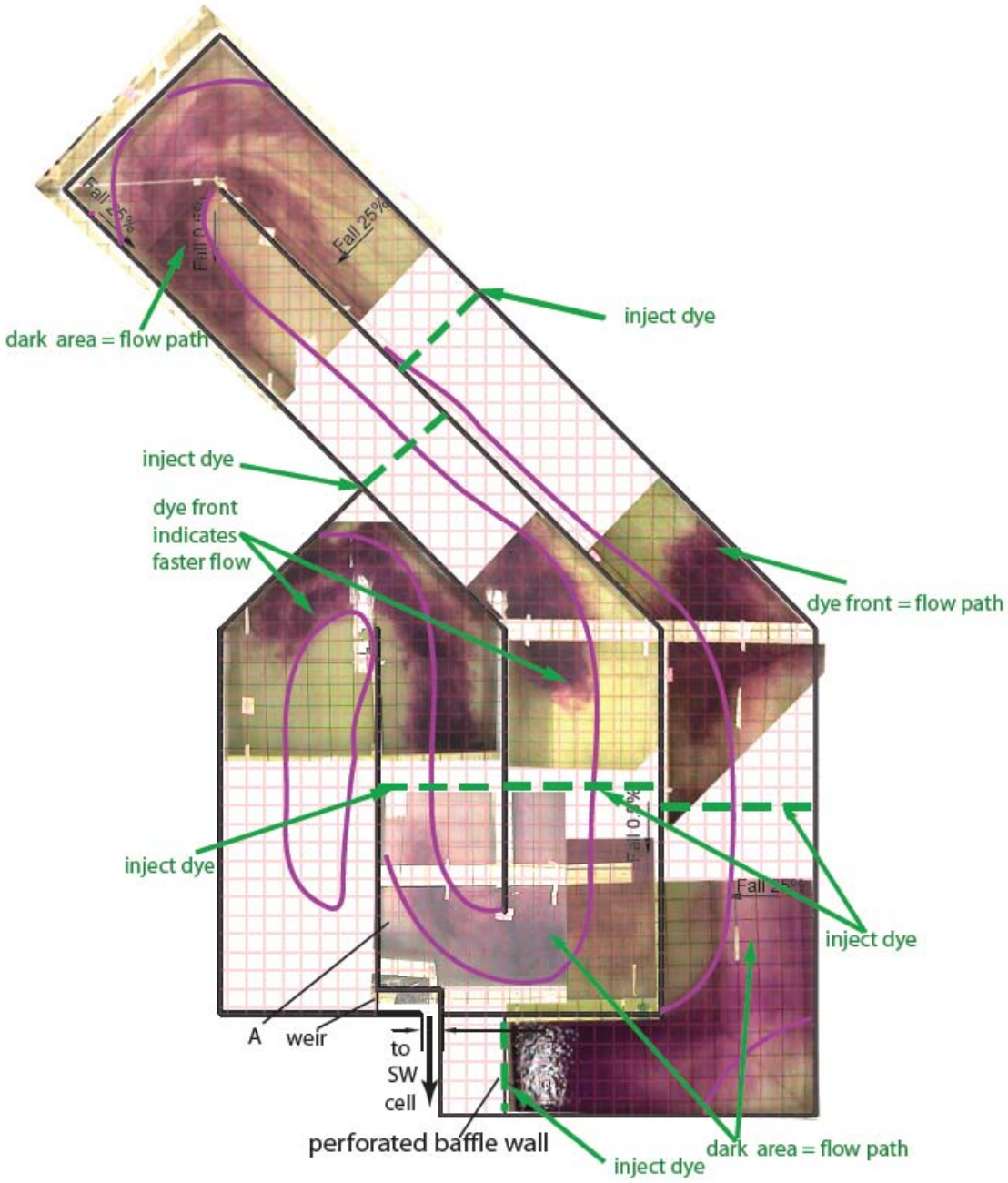

Figure 4.28 Flow pattern in scale model for flow rate Q=2.87 L/s without columns for τ =4 h (fully developed flow).

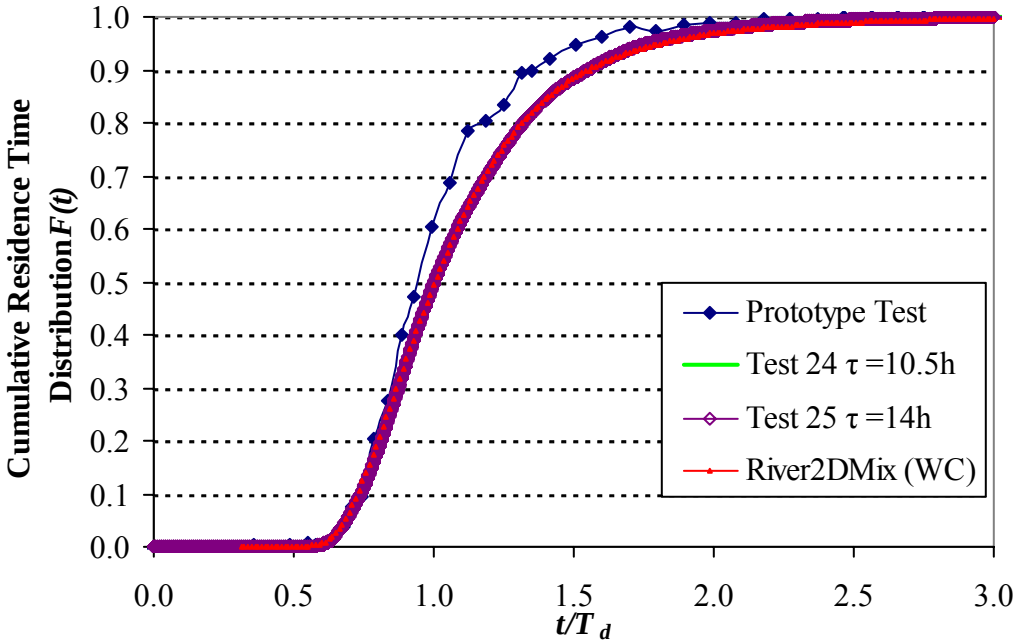

Figure 4.29 Comparison of the Cumulative Residence Time Distribution of the full-scale test to the simulated breakthrough curves and hydraulic model tracer test results for the with columns condition for the flow rate 0.85 L/s.

When simulating the flow of 2.06 L/s and the "with columns" condition, the same value of ε_2 and ε_3 were used as the maximum flow rate (ε_2 = 0.15 and ε_3 = 0.04). Figure 4.31 shows the cumulative residence distribution curves F(t) based on the physical and computational models for the flows of 2.06 L/s for the "with columns" condition. The baffle factor determined from the simulation was 0.70 as compared to the scale model value of 0.72, which gives a 2.78 % difference. The dispersion index was 2.17 in the simulation and 2.11 in physical model, which gives a 2.84 % difference in values. Meanwhile, a comparison of the cumulative RTD between the simulation and prototype showed difference in baffle factor of 1.4 % and difference in dispersion index of 15.2 %.

Figure 4.32 shows the simulated velocity field at the flow rate Q=2.06 L/s for the "with column" condition in the model. The flow visualization (Figure 4.32) showed similar results in comparison with the predictions obtained using River2DMix. Both of them showed a large stagnant zone behind the baffle wall and small stagnant zones in the

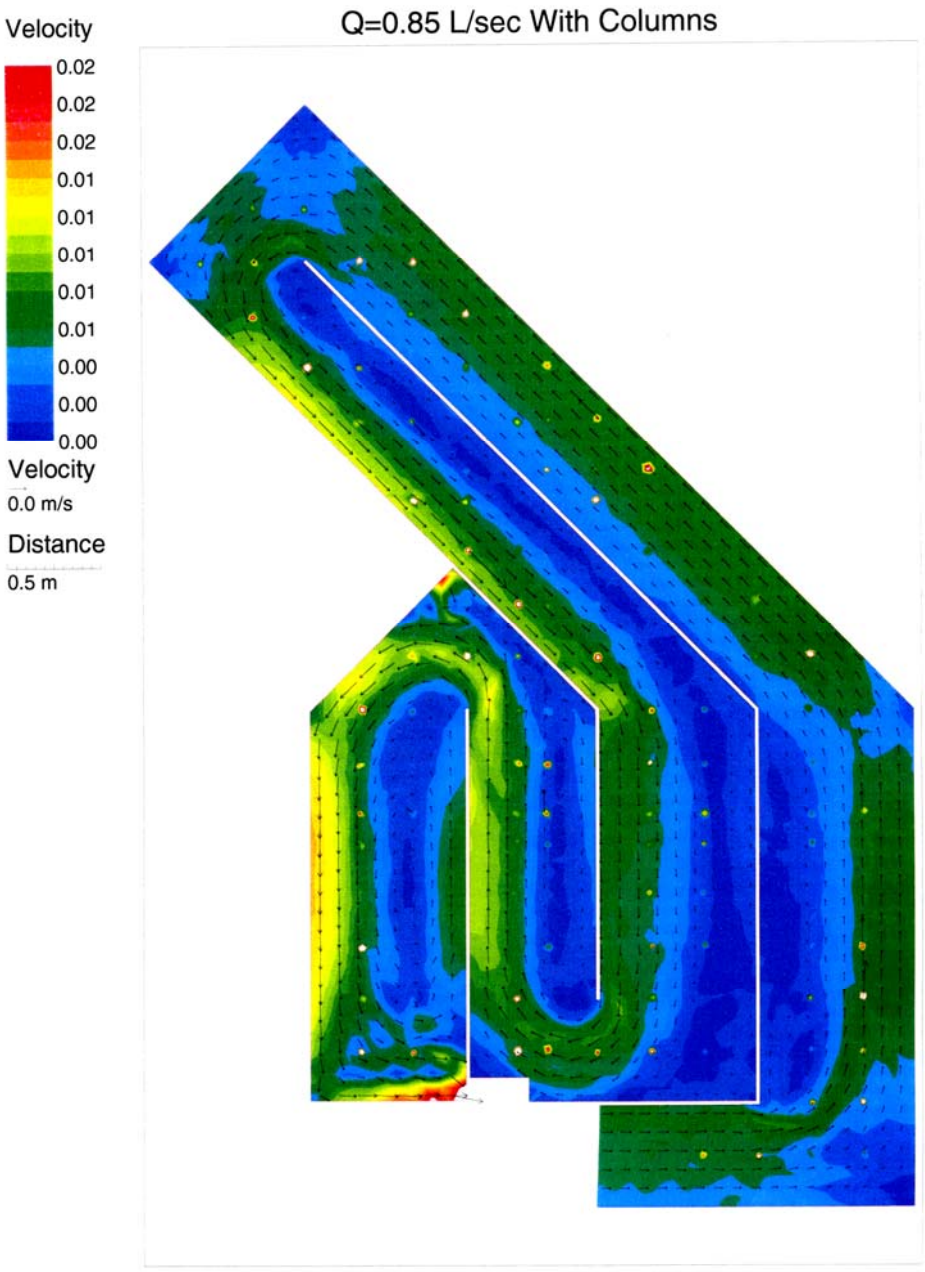

Figure 4.30 Velocity field produced by River2DMix for the 0.85 L/s flow simulation of the physical scale model with columns.

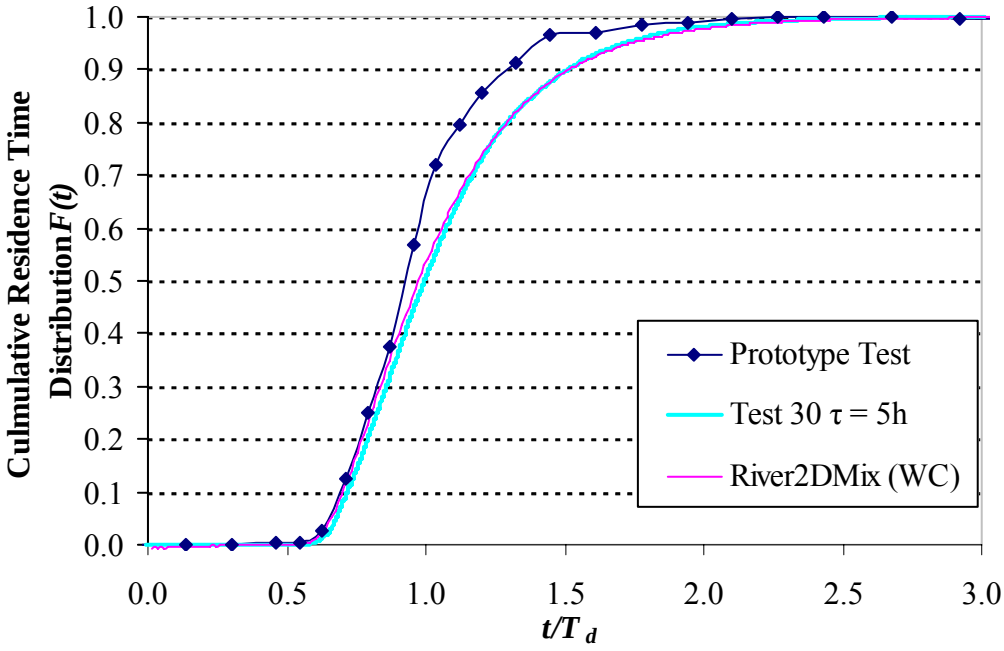

Figure 4.31 Comparison of the Cumulative Residence Time Distribution of the full-scale test to the simulated breakthrough curves and hydraulic model tracer test results for the with columns condition for the flow rate 2.06 L/s.

upstream and downstream corners of the channel. The same issue existed for this flow as for the minimum flow rate (Q = 0.85 L/s). The simulation did not predict the stagnant zone shown in the region given by point A in Figure 4.33.

Figure 4.34 shows the cumulative residence distribution curves F(t) based on the hydraulic model and final calibrated computational model for the flows of 2.87 L/s and the "with columns" condition. The baffle factor determined from the simulation was 0.73, which is the same as the value found in the scale model. The dispersion index was 2.14 in simulation and 2.13 in physical model with a 0.46 % difference. Meanwhile, a comparison of the cumulative RTD between the simulation and prototype showed a difference in baffle factor of 2.8 % difference and in dispersion of 16.9 %.

Figure 4.35 shows the simulated velocity field at the flow rate Q=2.87 L/s for the "with column" condition in the model. Again, the flow visualization (Figure 4.36) showed similar results in comparison with the predictions obtained using River2DMix. It was found that the separation of the flow initiates at the baffles' toes. Then, each of the

three 180-degree turns within the clearwell generated a recirculation region behind the baffle wall. There are stagnant zones almost equal to the entire length of baffle wall and some localized stagnant zones around the corners. Again, the simulation did not predict the stagnant zone shown in the region given by point A in Figure 4.36.

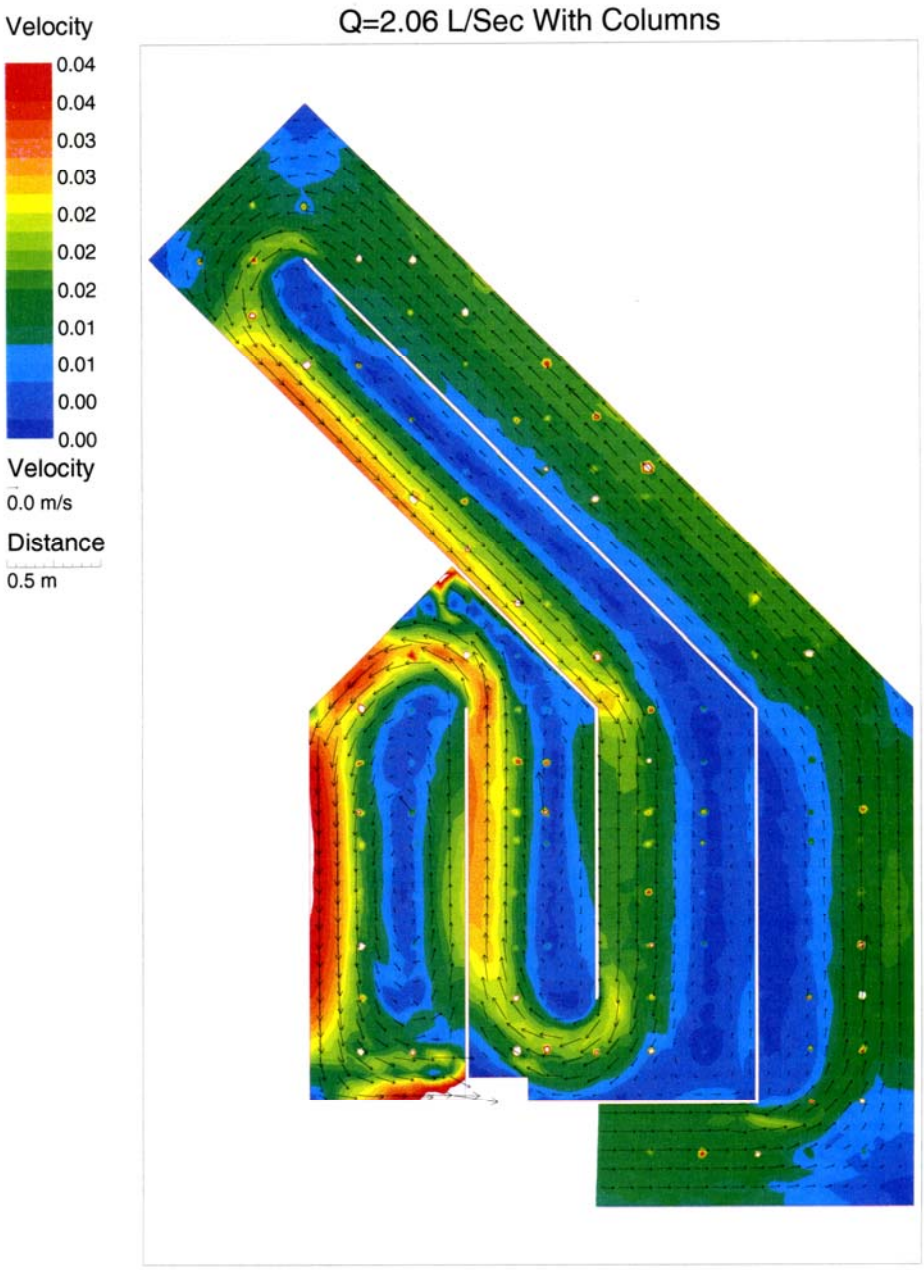

Figure 4.32 Velocity field produced by River2DMix for the 2.06 L/s flow simulation of the physical scale model with columns.

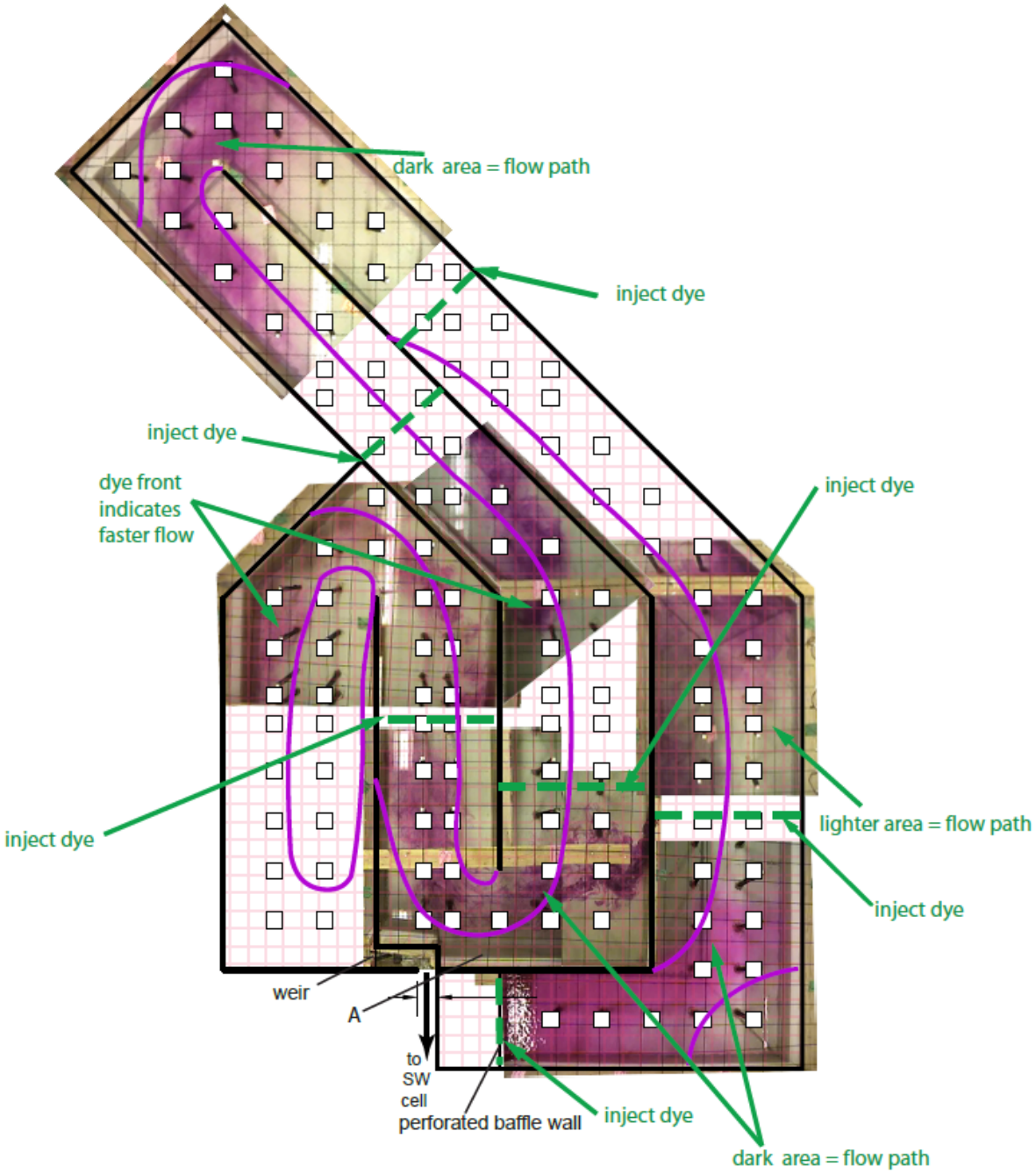

Figure 4.33 Flow pattern in scale model for flow rate Q=2.06 L/s with columns for τ =5 h (fully developed flow).

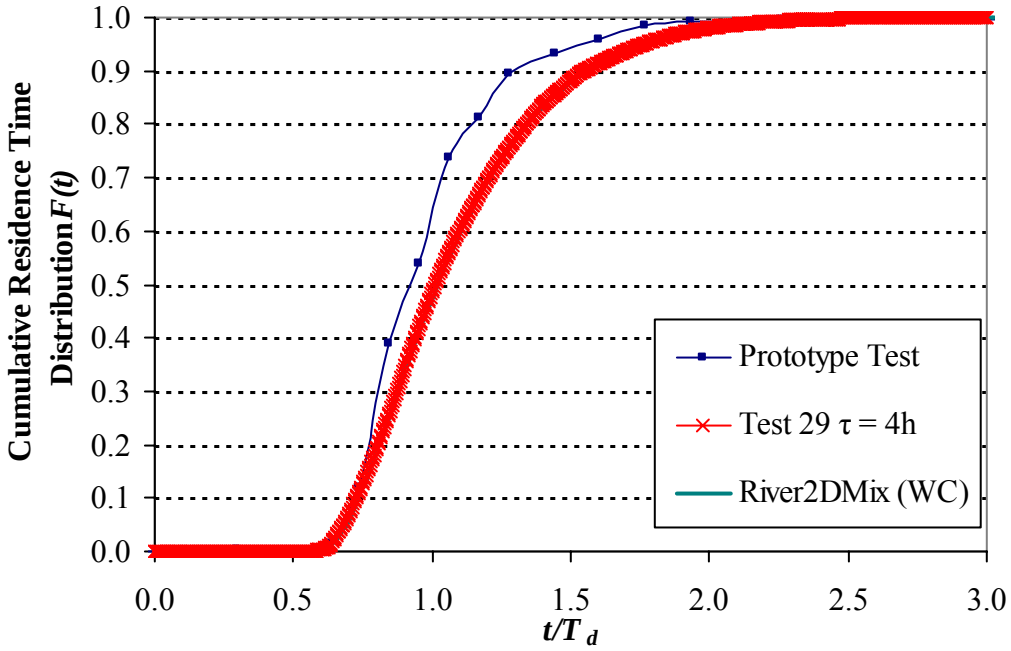

Figure 4.34 Comparison of the Cumulative Residence Time Distribution of the full-scale test to the simulated breakthrough curves and hydraulic model tracer test results for the with columns condition for the flow rate 2.87 L/s.

In summary, it was found that River2DMix adequately simulated the residence time distribution and flow pattern for the scale model of the Glenmore clearwell. There was little difference between measured and predicted (simulated) baffle factors and dispersion indices both for the scale model and the prototype. River2DMix was able to predict the location of recirculation zones within the clearwell, although River2DMix significantly underestimates the size of the separated zone seen in the model at the particular point in the flow path.

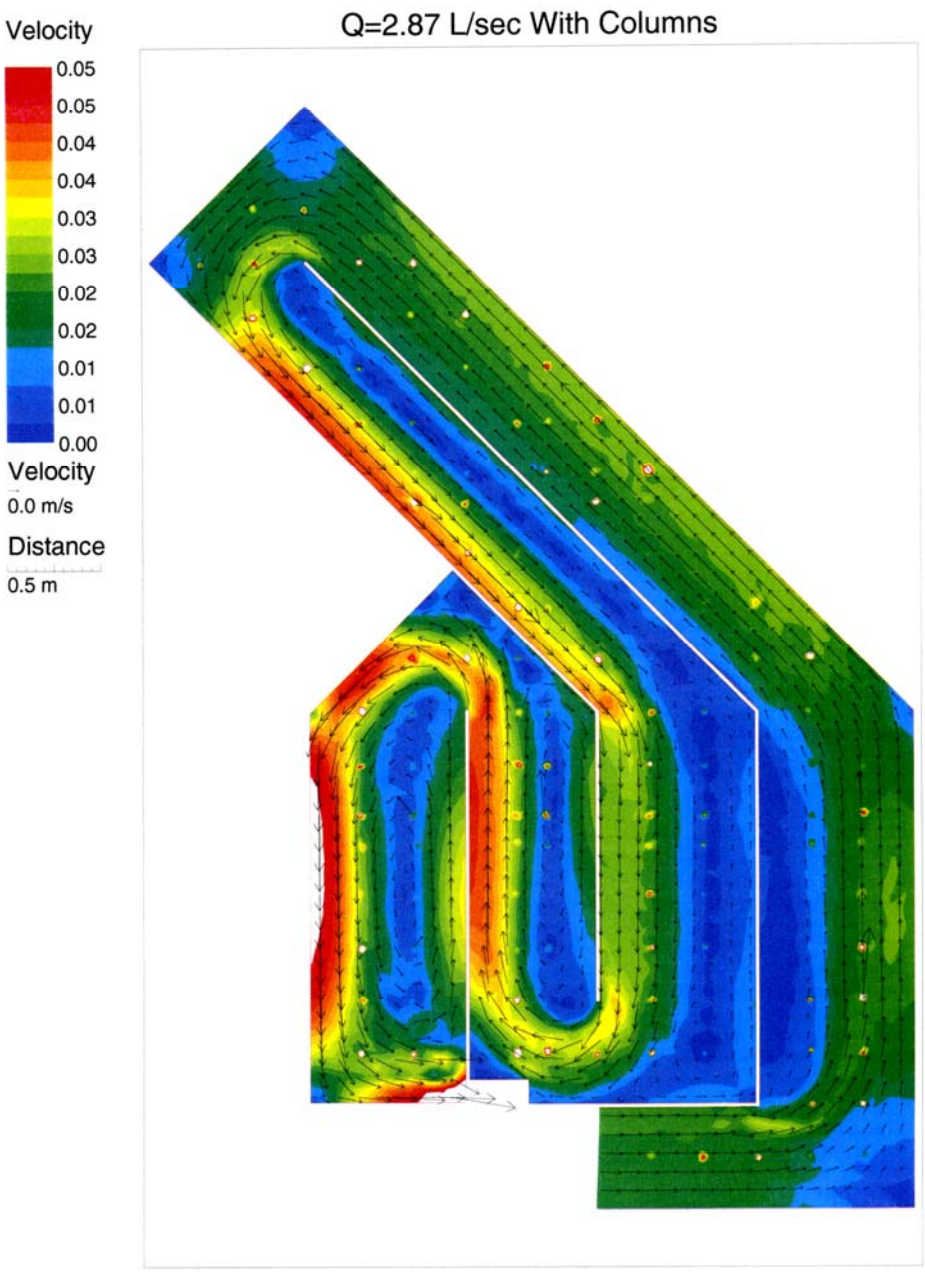

Figure 4.35 Velocity field produced by River2DMix for the 2.87 L/s flow simulation of the physical scale model with columns.

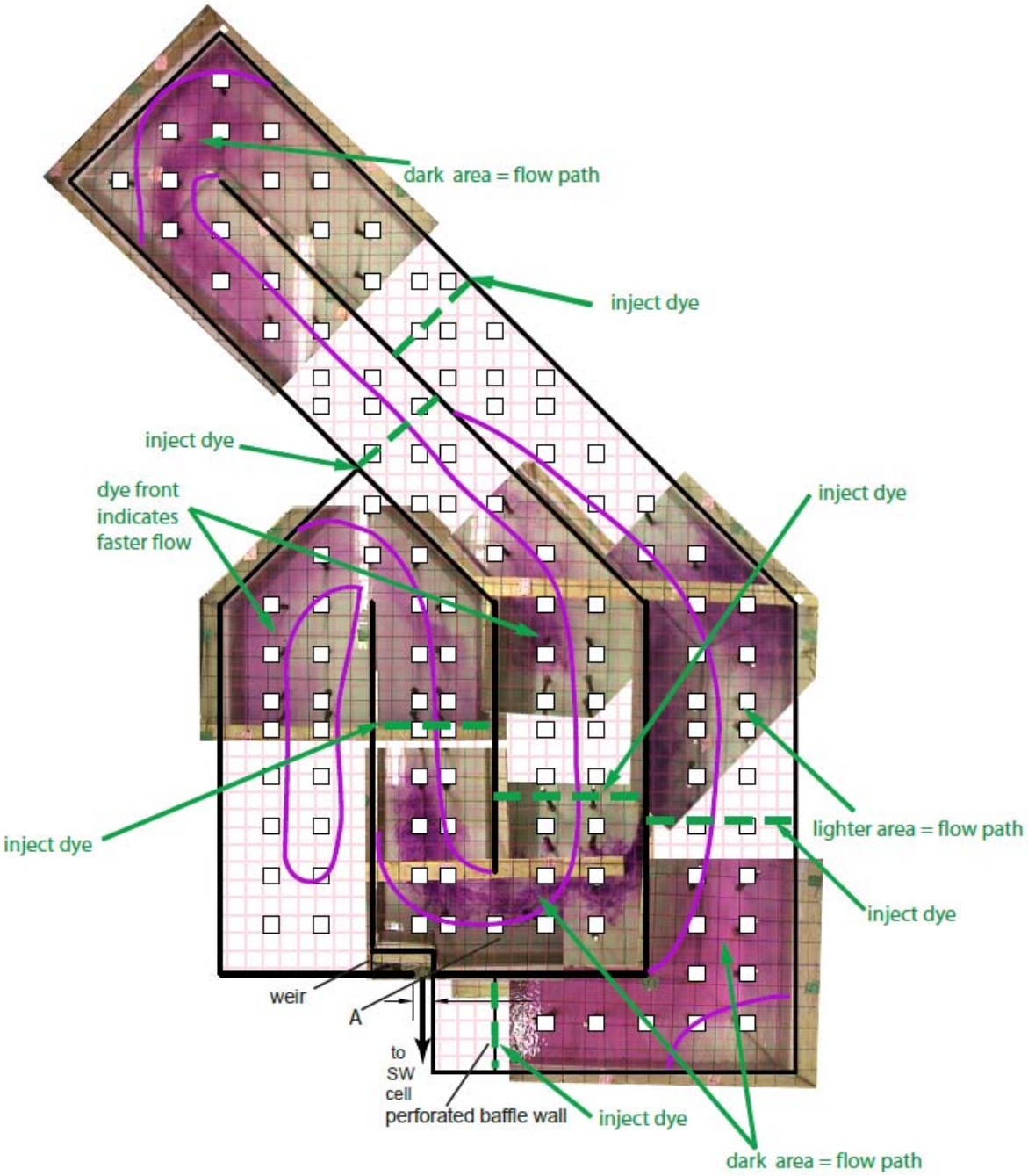

Figure 4.36 Flow pattern in scale model for flow rate Q=2.87 L/s with columns for τ =4 h (fully developed flow).

4.5. Analysis of Errors

The analysis of the errors in the mass recovery is described below. The calculations used to estimate the errors are according to the method defined by Topping (1979). There are three syringes used as holder for Rhodamine (WT) solution with concentration of 175 ppm. Each has the theoretical capacity of 140 mL. During tests, there were air bubbles in the syringe when withdrawing the 175 ppm solution from the plastic bottle which contained the solution. To compensate for the volume of air bubbles, the bottom of core of syringe was to a point a little higher than the 140 mL scale marked on the syringe, which results an estimated error of 3.9 % when the 175 ppm solution was measured by the syringe. When making up the 175 ppm solution, there are pipettes used for measuring the solution and volumetric flasks used for the dilution. The estimated error for pipettes is range from 0.08 to 0.8 %, and for volumetric flask is range from 0.08 to 0.1%. A theoretical mass N_0 is expressed as the product of C_0V_s, where C_0 is the makeup 175 ppm solution and V_s is the theoretical volume of syringes. When C_0 and V_s have fractional errors 0.2 % and 11.7 % respectively, the total estimated error is 11.9 % in physical model tracer tests in the worst condition. The above estimated error for the total mass inputted into the clearwell also result in the mass recovery in most tests with higher error.

The flow rate into the physical model of clearwell was checked by the volumetric method. The estimated error for flow measurement is ± 2.1 % for worst case over the range of the flow rate. The fluorometer manufacturer's error is ± 1 % of the full scale. Various precautions were taken to eliminate the errors in the concentration readings while carrying the tracer test. By applying the above estimates of uncertainty for the ΔN (the mass of tracer leaving the physical model of the clearwell in time interval Δt), the maximum error for the residence time distribution E(t) is ± 10 % and for the cumulative residence time distribution F(t) is ± 10 %.

CHAPTER 5: CONCLUSIONS AND RECOMMENDATIONS

5.1 Conclusions and Recommendations

The objectives of the work were to study the affect of flow rate on the flow behavior and the resulting residence time distributions in the Calgary Glenmore NE Clearwell, to evaluate the influence of columns on the flow behavior, and to investigate whether River2DMix could simulate the flow behavior and residence time distribution curves seen in the scale physical model (with and without columns in the model). After some initial testing, it also became evident that a certain flow development time was needed in order to achieve steady state results in the hydraulic model and this was also investigated.

At the low flow tested, the flow development time significantly impacted the residence time distribution of the scale model of the clearwell for without column case. At a flow development time τ =1 h, there was 42.7 % difference in baffle factor between the physical model and the prototype value. At τ =10.5, 14 and 30 h, there were 0.2 %, 0.1 % and 0.2 % differences in baffle factor between the physical model and the prototype value, respectively. At τ =1 h, there was a 50.0 % difference in Morril dispersion index between the physical model and the prototype value. However, at τ =10.5, 14 and 30 h, there were 2.1 %, 3.8 % and 3.8 % differences in Morill dispersion between the physical model and the prototype values, respectively. It was seen that it required approximately 10.5 hours of flow development time before a tracer test was initiated in the model at the lowest flow rate tested to achieve steady results in baffle factor and dispersion index and also results that closely matched prototype values. This low flow rate testing used a low Reynolds number for the flow in the reservoir of R_r = 2011.

For the "with columns" condition for the model at the lowest flow rate tested, at τ =1 h, there was 9.4 % difference in baffle factor between the physical model and the prototype value. At τ =10.5 and 14 h, there were 0.8 % and 0.4 % differences in baffle factor between the physical model and the prototype value respectively. At τ =1 h, there

was a 23.9 % difference in Morril dispersion index between the physical model and the prototype value. At τ =10.5 and14 h, there are 14.8 % and 15.2 % difference in Morril dispersion index between the physical model and the prototype value respectively. It is thus seen that the flow was closer to prototype conditions at earlier flow development times for the with columns case than for that without column. However, the baffle factor and dispersion index still reached steady values only after 10.5 h of testing. It is also seen that there was more of a departure of the dispersion index from prototype values at steady state for the "with columns" condition.

For intermediate flow rate tested, there was only improvement in the Morril dispersion index, not the baffle factor, with increased flow development time. For the "without columns" condition, at τ =1 h, there was a 4.2 % difference in baffle factor and a 13.8 % difference in Morril dispersion index between the physical model and the prototype value. At τ =5 h, there was an 8.6 % difference in baffle factor and a 1.5 % in Morril dispersion index between the physical model and the prototype value. For the "with columns" model condition, both the baffle factor and the Morril dispersion index between the two tests τ =1 and 5 h were different only by 1.0 %. It appeared the flow development time had no effect on the baffle factor and the dispersion index for the with columns case.

For the highest flow rate tested, at τ =1 h, there was a 2.8 % difference in baffle factor and a 7.9 % difference in Morril dispersion index between the physical model and the prototype value. At τ =4 h, there was a 2.7 % difference in baffle factor and a 2.3 % difference in Morril dispersion index between the physical model and the prototype value. Again, it appeared at this flow rate that the flow development time had an impact on the Morril dispersion index but not the baffle factor. For the with columns case, the baffle factor was constant at 0.73 and the dispersion indices for the tests were 2.14 and 2.13 with the increase of τ = 1 to 4 h. Again, the flow development time had no effect on the baffles factor and the dispersion index in the highest flow rate for the with columns model condition.

The above work shows that in hydraulic model studies of clearwells, results should be checked to ensure the flow is fully developed for tracer tests by running a few tests at different flow development times. It also indicates that baffle factors expected for normal operating conditions may be lower upon startup of the clearwell than anticipated, for example, in the case of start-up of the clearwell after maintenance.

To evaluate the influence of columns on flow behavior within the clearwell and on the resulting residence time distribution curves, a comparison was made between the "without columns" and 'with columns" condition at the full range of flow rates for the fully developed flow condition. There was little difference in the baffle factor between with and without columns model conditions for fully developed flow. However, the dispersion index for the "without columns" case is closer to the prototype value than for the "with columns" case. For minimum flow rate, there was the same baffle factor and 11.7 % difference of Morril dispersion index between the "without column" and "with column". For intermediate flow rate, there are 4.0 % difference of baffle factor and 10.5 % difference of Morril dispersion index between the "without column" and "with column" condition. For maximum flow rate, there are same baffle factor and 13.9 % difference of Morril dispersion index between the "without column" and "with column" condition. The potential reason could be that the wake differences behind the square column probably changed dispersion index of the scale model. In terms of the Reynolds number of column (Table 3.1), the wakes behind the square column in the scale model of clearwell are laminar compared to the turbulence wake behind the square column in the prototype clearwell.

The dispersion index for the "without columns" case is closer to the prototype value than for the "with columns" case, so it is indicated that it is likely not necessary to model the structure columns in the clearwell when building the physical model of clearwell as long as a check to see whether the flow is fully developed is undertaken. However, it was seen that the columns increased the percentage mixing in the flow by a few percent (2 to 3 %) over the without columns case for fully developed flow and that this increased mixing was taken from the dead space portion of the flow.

To investigate whether River2DMix could simulate the flow behavior and residence time distribution curves seen in the scale physical model (with and without columns in the model), a comparison was made between the simulation, physical model (for fully developed flow) and prototype test results. For minimum flow rate, there was the same baffle factor and 4.7 % difference of Morril dispersion index between the simulation and scale model for "without column" condition. There was a 1.6 % difference of baffle factor and a 1.4 % difference of the Morril dispersion index between the simulation and scale model for "with column" condition. For intermediate flow rate, there are 2.7 % difference of baffle factor and 3.2 % difference of Morril dispersion index between the simulation and scale model for "without column" condition. There was a 2.8 % difference of baffle factor and 2.8 % difference of the Morril dispersion index between the simulation and scale model for "with column" condition. For maximum flow rate, there were the same baffle factor and Morril dispersion index between the simulation and scale model for "without column" condition. There were the same baffle factor and 0.46 % difference of the Morril dispersion index between the simulation and scale model for "with column" condition. Hence, River2DMix simulation of the scale model flow conditions support the trends in baffle factor and dispersion index effects observed in the scale model tracer test results.

Comparison between the simulated velocity field from the River2DMix and the visualization test results showed that the measured and simulated flow patterns are similar. There was a large stagnant zone behind the baffle wall and small stagnant zones in the upstream and downstream corners of the channel. However, the scale model had a large dead zone for one section with a 180 degree turn in the flow. In general, River2DMix can simulate the flow behavior and residence time distribution curves seen in the scale physical model with and without columns for this clearwell over a range of flows. Even though, in modeling at the smaller scale, both the physical and computation models showed increased dispersion as compared to results from tracer studies in the full-scale reservoir. It appears that a two-dimensional model such as River2Dmix can provide good results in the case where the flow is not expected to have large vertical variation in horizontal velocity. Generally, the River2DMix software package does not need the

more computational time than 3-D model. And it is also give the reasonable and good result when applied with the 2-D flow condition like effluent discharges into rivers, water storage reservoir, and disinfection contact chamber.

5.2 Future Research

The following recommendations should be considered for future research:

- There were differences in required flow development time for tracer study results to reach steady state between the flow rates tested. At the low flow, allowing for a longer flow development time seemed to compensate for a relatively low Reynolds number for the flow (and less turbulent mixing). It shows that the can be transient conditions in the clearwell that have to be assessed. The flow development concept should be pursued in future studies.

- For the Glenmore Clearwell itself, the hydraulic efficiency of NE cell of Glenmore clearwell over flow range is within the superior baffle condition (more than 0.7). It is noted that this clearwell has a high proportion of plug flow. However, the distribution of disinfectant across the clearwell is also important and there are some recirculating areas in this flow. Future designers should consider taking steps aimed at reducing the separating at the toe of baffle near the inside of a turn in the flow such as the vane or intra-diffusion wall at down stream the turn.

- It was found that the two-dimensional depth-averaged computational model River2DMix could predict the flow pattern seen in the hydraulic model in the Glenmore clearwell well. However, this is a flow situation where the flow could be expected to be approximately two-dimensional depth-averaged flow. Additional work must also be conducted to test whether such a model can adequately simulate different potential modifications to the clearwell to improve flow conditions such as finger baffles or screens. A two-dimensional depth-averaged model will likely not simulate the flow in the clearwell where the inlet is circular and small compared to the overall depth of flow. In such a case, a three-dimensional computational model

would be required at least near the inlet. Limits for the use of the depth-averaged model need to be addressed.

- More work needs to be done to give a range of calibration coefficients that will be appropriate for modeling clearwells using River2DMix, as velocity measurements and prototype tracer study results are often not available for developing such a model.

REFERENCES

AEP (Alberta Environmental Protection). 1988. Standards and guidelines for municipal water supply, wastewater, and storm drainage facilities. Standards and Guidelines Branch, Environmental Assessment Division Environmental Service, Alberta Environmental Protection, Edmonton, Alberta, Canada.

Albers, C. and Maksymetz, B. 2004. Computational modeling of reservoir baffle factor. 56th conference of the Western Canada Water and Wasterwater Association, 17-20 October 2005, Calgary, Alberta, pp.1-13.

Albers, C., Maksymetz, B., and Mazurek, K. 2005a. Flow through and mixing in potable water reservoirs-making the black box transparent, 57th Annual conference of the Western Canada Water and Wastewater Association, 16-19 October 2005, Saskatoon, Saskatchewan, pp. 1-10 (on CD).

Albers, C., Maksymetz, B., and Mazurek, K. 2005b. Mixing in municipal reservoirs- the column connection. 17th CSCE Canadian Hydrotechnical Conference, 17-19 August 2005, Edmonton, Alberta, pp. 1-9 (on CD).

American Society of Civil Engineers, ASCE. 2000. Hydraulic modeling: concepts and practice. ASCE manuals and Reports on Engineering Practice No.97. Task committee on Hydraulic Modeling, R. Ettema, chair and editor, R. Arndt, P. Roberts, T. Wahl. ASCE, Virginia, U.S.A.

American Water Works Association, AWWA. 1999. Water quality and treatment: a handbook of community water supplies, 5th Edition, McGraw-Hill Inc., U.S.A.

Baawain, M.S., El-Din, M.G., and Smith, D.W. 2006. Computational fluid dynamics application in modeling and improving the performance of a storage reservoir used as a contact chamber for microorganism inactivation. Journal of Environmental Engineering and Science, **5**(2): 151-162.

Bishop, M.M., Morgan, J.M., Cornwell, B., and Jamison, D.K. 1993. Improving the disinfection detention time of a water plant clearwell. Journal of American Water Works Association, **85**(3): 68-75.

Boulous, P.F., Grayman, W.M., Bowcock, R.W., Clapp, J.W., Rossman, L.A., Clark, R.M., Deininger, R.A., and Dhingra, A.K. 1996. Hydraulic mixing and free chlorine residual in reservoirs. Journal of American Water Works Association, **88**(7): 47-59**.**

Clark, R.M., Abdesaken, F., Boulos, P., and Mau, R. 1996. Mixing in distribution system storage tanks: its effect on water quality. Journal of Environmental Engineering, **122**(9), 814-821.

Crittenden, J.C., Trussell, R.R., Hand, D.W., and Tchobanoglous, G. 2005. Water Treatment Principles and Design (2nd Edition). New Jersey: John Wiley and Sons, Inc.

Crozes, G.F., Hagstrom, J.P., Clark, M.M., Ducoste, J., and Burns, C. 1999. Improving clearwell design for CT compliance. American Water Works Association Research Foundation, Denver, Colorado, USA.

Daiguji, H. and Kobayashi, S. 1981. Numerical solution for the time-dependent two-dimensional viscous flows past obstacle. 2nd report: A stationary obstacle in a uniform flow. Bulletin of the Japan Society Mechanical Engineers. **24**(195): 1550-1556.

Edge, T., Byrne, J.M., Johnson, R., and Robertson, W. 2003. Waterborne pathogens. publication of National Water Research Institute (NWRI), Environment Canada, Burlington, Ontario, Canada. http://www.nwri.ca/threatsfull/ch1-1-e.html. Last accessed date: 24/06/07.

Falconer, A., and Lu, S.Q. 1988. Modeling solute transport using QUICK scheme. Journal of Environmental Engineering, **114**(2): 3-19.

Falconer, A., and Tebbutt, N. Y., 1986. A theoretical and hydraulic model study a chlorine contact tank. Proceedings of the Institution of Civil Engineers, Part 2, **81**(6): 255-276.

Falconer, A., and Ismail, A.I.B.M. 1997. Numerical modeling of tracer transport in a contact tank. Environment International, **23**(6): 763-773.

Fisher, H.B., List, J.E., Imberger, J., and Brooks, N.H. 1979. Mixing in inland and coastal waters. Academic Press, Inc., London, Ltd.

Fogler, H.S. 1992. Elements of Reaction Engineering. 2nd edition, Prentice-Hall, Upper Saddle River, New Jersey, USA.

Grayman, W.M., Deiniger, R.A., Green, A., Boulous, P, F., Bowcock, R.W., and Godwin, C.C. 1996. Water quality and mixing models for tanks and reservoirs. Journal of American Water Works Association, **88**(7): 60-73.

Grayman, W.M., Rossman, L.A., Deininger, R.A., Smith, C.D., Arnold, C.N., and Smith, J.F. 2004. Mixing and aging of water in distribution system storage facilities. Journal of American Water Works Association, **96**(9): 70-80.

Hannoun, I.A., and Boulous, P.F. 1997. Optimizing distribution storage water quality: a hydrodynamic approach. Applied Mathematical Modelling, **21**(8): 495-502.

Hannoun, I.A., and Boulous, P.F., and List, J. 1998. Using hydraulic modeling to optimize contact time. Journal of American Water Works Association, **90**(8): 77-87.

Hannoun, I.A., Bowman, K., and Lamoreaux, D. 2003. Computational fluid dynamics: optimizing water quality in clearwells, tanks, and distribution storage reservoirs. World Water and Environmental Resources Congress 2003 and Related Symposia Proceedings of the Congress, 3393-3401: June 23-26, 2003, Philadelphia, Pennsylvania, U.S.A.

Hart, F. L., and Gupta, S.K. 1978. Hydraulic analysis of model treatment units. Journal of Environmental Engineering division**,** American Society of Civil Engineers, **104**(4):785-798.

Hart, F.L. 1979. Improved hydraulic performance of chlorine contact chamber, Journal of Water Pollution Control Federation, **51**(12):2868-2875.

Hart, F. L., and Vogiatzis, Z. 1982. Performance of modified chlorine contact chamber. Journal of Environmental Engineering division**,** American Society of Civil Engineers**, 108**(3):549-561.

Health Canada. 2006. Guidelines for Canadian drinking water quality: guideline technical document. http://www.hc-sc.gc.ca/ewh-semt/alt_formats/hecs-sesc/pdf/pubs/water-eau/microbio-eng.pdf, Publication of Federal-Provincial-Territorial Committee on Drinking Water, Ottawa, Ontario, Canada.

Hudson, H. E. 1975. Residence times in pre-treatment. Journal of American Water Works Association, **67**(1): 45-52.

Hurting, K.I. 2003. Hydraulic modelling of storage tanks in water distribution systems, M.A.Sc., thesis, Department of Civil and Environmental Engineering, University of Alberta. Edmonton, Alberta, Canada.

Jain, S.C. 2001. Open-Channel Flow, 1st Ed., Wiley, New York.

Johnson, P. Graham, N. Dawson, M. and Barker, J. 1998. Determining the optimal theoretical residence time distribution chlorine contact tanks. Journal of Water Supply: Research and Technology - Aqua, **47**(5): 209-214.

Joost, R., Chowdhury, Z.K., aand Francis, T. 1990. Plant-scale tracer studies: an assessment of actual detention times for primary disinfection. Proceeding of the 1990 Annual Conference, American Water Works Association, 17-21 June 1990, Cincinnati, Ohio, U.S.A, pp. 1583-1600.

Krogstad, P., Antonia, R.A., Browne, L.W. 1992. Comparison between rough- and smooth- wall turbulent boundary layers. Journal of Fluid Machanic. **245**, pp: 599-617.

Kothandaraman, V., and Evans, R.L. 1972. Hydraulic model studies of chlorine contact tanks. Journal of Water Pollution Control Federation, **44**(4): 625-633.

Kumar, S.R., Sharma, A., and Agrawal, A. 2008. Simulation of flow around a row of square cylinders. Journal of Fluid Mechanics, **606**(7):369-397.

Levenspiel, O., 1972. Chemical reaction engineering. New York: John Wiley and Sons.

Li, H. 2008. Two staggered finite circular cylinders in cross-flow. M.A.Sc Thesis, Department of Mechanical Engineering, University of Saskatchewan, Saskatoon, Saskatchewan, Canada.

Liem, L.E., Stanley, S.J., and Smith, D.W., 1999. Residence time distribution analysis as related to the effective contact time. Canadian Journal of Civil Engineering, **26**(2):135-144.

Louie, D.S., and Fohrman, M.S. 1968. Hydraulic model studies of chlorine mixing and contact chamber. Journal of the Water Pollution Control Federation, **40**(2):174-184.

Lyn, D.A., Einav, S. Rodi, W. and Park, J.H., 1995. A laser-Doppler velocimetry study of ensemble-averaged characteristics of the turbulent near wake of a square cylinder. Journal of Fluid Mechanics, **304**: 285-319.

Maksymetz, B. 1998. Development of real-time disinfection evaluation (CT) program at a large conventional water treatment plant. 50th Annual Conference of the Western Canada Water and Wastewater Association, 25-28 October 1998, Calgary, Alberta, pp. 1-20.

Maksymetz, B. 2003. Design and implementation of online real-time disinfection performance (CT) monitoring systems. 2003 Annual Conference and Exhibition of the American Water Works Association, 15-19 June 2003, Los Angeles, California, USA, pp. 1-20.

Marske, D.M. and Boyle, J.D. 1973. Chlorine contact chamber design-A field evaluation. Water and Sewage Works, **1973**(1): 70-77.

McCorquodale, J.A., and Machina, D.W. 2002. Final report on hydraulic model studies of the village of Wheatley waterworks reservoirs. Lafontaine, Cowie, Buratto and Associates Limited, Windsor, Ontario, Canada.

Mitha, S.A., and Mohsen, M.F. 1990. Scale effect on dispersion in chlorine contact chambers. Canadian Journal of Civil Engineering, **17**(2): 156-165.

Nour, M., Smith, D., EI-Din, M., and Prepas, E. 2008. Effect of watershed subdivision on water-phase phosphorus modelling: An artificial neural network modelling application. Journal of Environmental Engineering and Sciences, **7**: S95-S108.

Okajima, A., 1982. Strouhal numbers of rectangular cylinders. Journal of Fluid Mechanics (UK), **123**: 379-398.

Reddy, S., Russell, J., Narasimhan, R., and Burns, C. 1999. Improving clearwell design using computational fluid dynamics. Proceedings of the 29th Annual Water Resources Planning and Management Conference, 6-9 June 1999, Tempe, Arizona, USA, pp. 1-9.

Rebhun, M., and Argaman, Y., 1965. Evaluation of hydraulic efficiency of sedimentation Basins. Journal of Sanitary Engineering Division, Proceeding, American Society of Civil Engineers**, 88**, SA5: 37-45.

Rajaratnam, N. and Flint-Peterson, L. 1989, Low Reynolds number circular turbulent jets. Proceedings-Institution of Civil engineers, Part 2: Research and Theory, **87**: 299-305.

Roy, B., Mazurek, K.A., McCorquodale, J.A., and Machina, D.W. 2002. Hydraulic model study of the village of wheatley waterworks reservoir. Proceedings of the 2002 Joint CSCE/EWRI of ASCE Environmental Engineering Conference, 21-24 July 2002, Niagara, Ontario, pp. 1-14 (on CD).

Socolofshy, S.A., and Jirka, G.H. 2002. Environmental fluid mechanics, part I: mass transfer and diffusion. Engineering Lectures 2nd, University of Karlsruhe, Germany.

Steffler, P., and Blackburn, J. 2002. River2D two-dimensional depth averaged model of river hydrodynamics and fish habitat (Introduction to depth averaged modeling and user's manual). Department of Civil and Environmental Engineering, University of Alberta, Edmonton, Alberta.

Stovin, V.R., and Saul, A.J. 1998. A computational fluid dynamics (CFD) particle tracking approach to efficiency prediction. Water Science and Technology, **37**(1): 285-293.

Ta, C.T., and Brignal, W.J. 1998. Application of computational fluid dynamics technique to storage reservoir studies. Water Science and Technology, **37**(2): 219-226.

Taras, M. J. 1956. Estimation of flow-through time by the continuous – dose method. Journal of American Water Works Association, **June**: 700-713.

Teefy, S.M., and Singer, P.C. 1990. Performance and analysis of tracer tests to determine compliance of a disinfection scheme with SWTR. Journal of American Water Works Association, **12**: 88-98.

Templeton, M.R., Hofmann, R., and Andrews, R.C. 2006. Case study comparisons of computational fluid dynamics (CFD) modeling versus tracer testing for determining clearwell residence times in drinking water treatment. Journal of Environmental Engineering and Science, **5**(6): 529-536.

Thirumurthis, D., 1969. A break-through in the tracer studies of sedimentations tanks. Journal of Water Pollution Control Federation. **41**(11), Part 2: 405-418.

Topping, J., 1972. Errors of observation and their treatment, 4th Edition. The Institute of Physics, London, UK.

Turki, S. Abbassi, H. and Nasrallah, S.B., 2003. Effect of the blockage ratio on the flow in a channel with a built-in square cylinder. Computational Mechanics, **33**(1):22-29.

Turner Designs, 1993. Model 10-AU-005 Field fluorometer user's manual: part number 10-AU-075, Turner Designs, Inc. Sunnyvale, Canada.

USEPA. 1989. Guidance Manual for compliance with the filtration and disinfection requirements for public water systems using surface water sources. Publication of Environmental Protection Agency, Washington, DC, USA.

Wang, H., and Falconer, R.A. 1998a. Numerical modeling of flow in chlorine disinfection tanks. Journal of Hydraulic Engineering, **124**(9): 918-930.

Wang, H., and Falconer, R.A. 1998b. Simulating disinfection processes in chlorine contact tanks using various turbulence models and high-order accurate difference schemes. Water Resource, **32**(5): 1529-1543.

Wang, H., Shao, X. and Falconer, R.A. 2003. Flow and transport simulation models for prediction of chlorine contact tank flow-through curves. Water Environment Research, **75**(5): 455-471.

Williamson, C.H.K. 1996. Vortex dynamics in the cylinder wake. Annual Review Fluid Mechanics, **28**: 477-539.

Wilson, J.F., Cobb, E.D., and Kilpatrick, F.A. 1986. Fluormetric procedures for dye tracing, techniques for water-resources investigations of the United States Geological Survey. Chapter A12, Book 3- Applications of Hydraulics, U. S. geological Survey, Denver, Colorado, USA.

Wolf, D., and Resnick, W. 1963. Residence time distribution in real system. Journal of Industrial and Engineering Chemical Fundamentals, **2**(4):28-293.

Zdravkovich, M. M. 1997. Flow around circular cylinders: a comprehensive guide through flow phenomena, experiments, application, Vol. 2. Oxford, New York: Oxford University Press.